

# AUPIMO: Redefining Anomaly Localization Benchmarks with High Speed and Low Tolerance

Joao P. C. Bertoldo<sup>1</sup>  
jpcb Bertoldo@minesparis.psl.eu

Dick Ameln<sup>2</sup>  
dick.ameln@intel.com

Ashwin Vaidya<sup>2</sup>  
ashwin.vaidya@intel.com

Samet Akçay<sup>2</sup>  
samet.akcay@intel.com

<sup>1</sup> Mines Paris, PSL University,  
Centre for mathematical  
morphology (CMM),  
77300 Fontainebleau, France

<sup>2</sup> Intel

## Abstract

Recent advances in anomaly localization research have seen AUROC and AUPRO scores on public benchmark datasets like MVTec and VisA converge towards perfect recall. However, high AUROC and AUPRO scores do not always reflect qualitative performance, which limits the validity of these metrics. We argue that the lack of an adequate and domain-specific metric restrains progression of the field, and we revisit the evaluation procedure in anomaly localization. In response, we propose the Area Under the Per-Image Overlap (AUPIMO) as a recall metric that introduces two major distinctions. First, it employs a validation scheme based solely on normal images, which avoids biasing the evaluation towards known anomalies. Second, recall scores are assigned *per image*, which is fast to compute and enables more comprehensive analyses (*e.g.* cross-image performance variance and statistical tests). Our experiments (27 datasets, 8 models) show that the stricter task imposed by AUPIMO redefines anomaly localization benchmarks: current algorithms are not suitable for all datasets, problem-specific model choice is advisable, and MVTec AD and VisA have *not* been near-solved. Available on GitHub<sup>1</sup>.

## 1 Introduction

Anomaly Detection (AD) is a machine learning task based on *normal* patterns, meaning they are not of special interest at inference time. As such, the model must identify deviations from the patterns observed in the training set, *i.e.* *anomalies*. Within this domain, Visual Anomaly Detection focuses on image or video-related applications, including both the detection of anomalies in images (answering the question, “Does this image contain an anomalous structure?”) and the more precise task of anomaly localization or segmentation, where the goal is to determine if specific pixels belong to an anomaly. Our emphasis is on anomaly localiza-

<sup>1</sup>Official implementation: [github.com/jpcb Bertoldo/aupimo](https://github.com/jpcb Bertoldo/aupimo). Integrated in anomalib [github.com/openvinotoolkit/anomalib](https://github.com/openvinotoolkit/anomalib). This research was conducted during Google Summer of Code 2023 (GSoc 2023) with the anomalib team from Intel’s OpenVINO Toolkit.

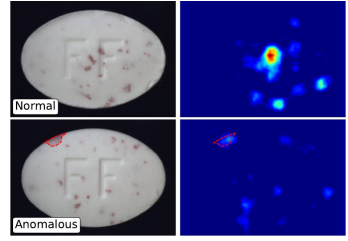
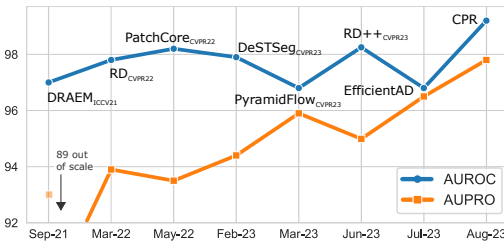


Figure 1: Left: performance on MVTec AD over time, approaching a near 100% performance plateau. Right: images from the dataset Pill (left column) and their inferred anomaly maps (right column; higher values mean anomalous; JET colormap) from the best performing model in this dataset (EfficientAD; see Appendix D), with 98.7% AUROC and 96.7% AUPRO. The normal image (top) has higher anomaly scores than the anomaly (bottom).

tion in image applications (other modalities are out of the scope of this paper, but extensions of our work are possible and briefly discussed in Sec. 6).

Anomaly localization research has achieved significant progress, partly thanks to the increased availability of suitable datasets [9, 8, 12, 13, 28]. In particular, MVTec Anomaly Detection (MVTec AD) [9] and Visual Anomaly (VisA) [28] comprise (together) 27 datasets (22 object and 5 texture-oriented) with high-resolution images and pixel-level annotations.

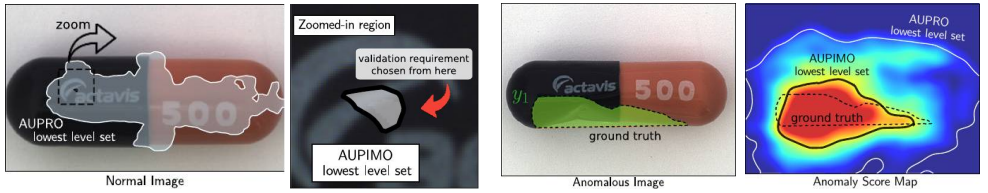
AUROC [11] and AUPRO [6] – respectively, the Area Under the Curve (AUC) of the Receiver Operating Characteristic (ROC) and Per-Region Overlap (PRO) curves (see Sec. 3.1) – have been used to evaluate anomaly localization, but it has been observed that the extreme class imbalance at pixel level inflates the scores produced by these metrics<sup>2</sup> [14, 13]. As a result, the performance numbers on MVTec AD and VisA reported in the literature are converging towards 100% (Fig. 1, left), giving the impression that these datasets have been solved. Meanwhile, even the top performing models often fail to localize anomalous regions in some of the more challenging samples from these datasets while raising many False Positives (FPs) (*i.e.* a normal pattern wrongly flagged as anomalous in Fig. 1, right).

We argue that the anomaly localization literature urges a metric well-suited to its unique characteristic: the positive (anomalous) class is unknown beforehand and may have an unlimited number of modes. While anomalous samples (even of different types) are available in public datasets, the goal of an AD model is to detect *any* type of anomaly. Our work emphasizes on this unsupervised nature of the problem to build a performance metric that does *not* depend on anomalies available at hand to avoid a bias towards known anomalies.

In response, we present the **Area Under the Per-Image Overlap (AUPIMO)** curve (Sec. 3.2). It relies on a clear separation of normal and anomalous images for, respectively, validation and evaluation of models – thus avoiding class imbalance-related issues. Its strict validation requirement sets a more challenging task in-line with the latest advances in the field. Our work provides means to comprehensively compare models with image-specific evaluation scores and, along with the standard procedure proposed in Sec. 4, tackles cross-paper comparison issues. In summary, our work presents the following contributions:

1. A validation-evaluation framework based on strict low tolerance for FPs on normal images only, which avoids conditioning the model behavior on known anomalies, thus providing a recall measure consistent with AD’s unsupervised nature (Sec. 3.3);

<sup>2</sup>The term “metric” is used as a synonym for “performance measure” in this paper. It does *not* refer to the mathematical concept of distance in a metric space.



(a) AUPIMO’s integration bound is chosen so false positive regions in normal images are small. Zoomed-in region: the lowest (*i.e.* largest) level set seen by AUPIMO in a normal image is insignificant compared to the structure of the image (more examples in Appendix A). AUPRO’s equivalent is larger as it is chosen to yield recall-achievable results (*i.e.* based on the anomalies).

(b) Left: anomalous image and its ground truth annotation mask (green region means anomalous). Right: anomaly map (JET colormap; blue/red means lower/higher anomaly score). The upper bound level sets are the lowest level sets seen by each metric. Their areas under the curve (AUCs) correspond to the average recall of the level sets above them (*i.e.* inside these contours).

Figure 2: AUPRO and AUPIMO’s upper bounds visualized as level sets from the anomaly score maps. Solid contours are level sets at thresholds yielding the maximum FPR in AUPRO (white) and AUPIMO (black). Images from the dataset MVTEC AD/ Capsule.

2. Per-image recall scoring, enabling the analysis of cross-image performance variance and high-speed execution at high resolution both on CPU and GPU (Sec. 5).
3. Empirical evidence suggesting that MVTEC AD and VisA datasets have *not* been near-solved and that problem-specific model choice is advisable (Sec. 5).

## 2 Related Work

AUROC is a threshold-independent metric for binary classifiers [10], and it is widely used to assess anomaly localization, treating it as a pixel-level binary classification. However, it has recently been argued that, in real-world applications, full or partial localization of anomalous regions is more relevant than pixel accuracy [4, 27]. Furthermore, it has been shown that AUROC is not suitable for anomaly localization datasets due to the extreme class imbalance [19, 23], prompting the exploration of other evaluation metrics in the field [4, 19, 27].

Bergmann et al. [9] proposed a ROC-inspired curve called Per-Region Overlap (PRO). At each binarization threshold, it measures the region-scoped recall averaged across all anomalous regions available in the test set. Notably, AUPRO excludes thresholds yielding False Positive Rate (FPR) values above 30% in the computation of the area under the PRO curve to force the metric to operate over a range of meaningful thresholds.

Recent studies have proposed metrics that index the thresholds based on recall instead of FPR. Rafiei et al. [24] observed that the high pixel-level class imbalance in MVTEC AD and similar anomaly localization datasets challenges the effectiveness of AUROC and AUPRO for model comparison. They concluded that the area under the Precision-Recall (PR) curve is a more suitable metric for AD as it is conditioned on the positive class (anomalous). Alternatively, other authors [11, 28] have used the  $F_1$ -max score, which is the best achievable  $F_1$  (harmonic mean of recall and precision), implying an anomaly score threshold choice. Zhang et al. [27] proposed the Instance Average Precision (IAP), a modified version of the PR curve where recall is defined at the region-level, counting a region as detected if at least half of its pixels are correctly detected. This alternative recall metric is further used as a

Table 1: Notation.

Symbol	Description	Symbol	Description
$M, j$	Number and index of pixels in an image	$\mathbf{a} \in \mathbb{R}_+^M$	Anomaly score map
$\neg, \wedge$	Pointwise logical negation/AND	$\mathbf{y} \in \{0, 1\}^M$	Ground truth (GT) mask
$ \cdot $	Cardinality of a set or number of 1s in a mask	$\mathbf{r} \in \{0, 1\}^M$	Region mask
$\mathbf{a} \geq t$	Binarization of $\mathbf{a}$ by $t$	$t \in \mathbb{R}_+$	Threshold
$L, U$	Integration lower/upper bounds	$\mathcal{A}, \mathcal{Y}, \mathcal{R}$	Sets of $\mathbf{a}$ , $\mathbf{y}$ , and $\mathbf{r}$

validation requirement (threshold choice) and the pixel-level precision is used to compare models (precision-at- $k\%$ -recall).

AUPIMO uses a validation criterium based only on normal images to avoid a bias towards detectable anomalies. As detailed in Sec. 3, we advocate in favor of normal-only validation to build an evaluation score in line with AD’s unsupervised nature, while using recall only to rate models. Finally, AUPIMO uses image-scoped metrics, preserving the structured information from the images and making its computation significantly faster (Fig. 5a).

### 3 Metrics

We define a framework to compare AUROC and AUPRO (Sec. 3.1), introduce our new metric (Sec. 3.2), and discuss its properties (Sec. 3.3). Key notation is listed in Tab. 1.

Our goal is to compare a model’s output  $\mathbf{a}$  (an anomaly score map; higher means more likely to be anomalous) with its ground truth mask  $\mathbf{y}$  (0 and 1 labels indicate “normal” and “anomalous” respectively), illustrated in Fig. 2b. We define  $\mathbf{r}$  as a region in  $\mathbf{y}$  such that instances do not overlap (maximally connected components). All metrics are *pixel-wise* (one score/annotation per pixel), not *image-wise* (one score/annotation per image) since our focus is to measure whether a model can detect anomalous structures *within an image*. We define the False Positive Rate (FPR) and True Positive Rate (TPR), *i.e.* recall, across three scopes: **set** (all pixels in all images confounded; subscript s), **per-image** (all pixels in an image; subscript i), and **per-region** (pixels in a single anomalous region; subscript r):

$$F_s : t \mapsto \frac{\sum_{\mathbf{y} \in \mathcal{Y}} |(\mathbf{a} \geq t) \wedge (\neg \mathbf{y})|}{\sum_{\mathbf{y} \in \mathcal{Y}} |\neg \mathbf{y}|} \quad T_s : t \mapsto \frac{\sum_{\mathbf{y} \in \mathcal{Y}} |(\mathbf{a} \geq t) \wedge \mathbf{y}|}{\sum_{\mathbf{y} \in \mathcal{Y}} |\mathbf{y}|} \quad (1)$$

$$F_i : t \mapsto |(\mathbf{a} \geq t) \wedge (\neg \mathbf{y})| / |\neg \mathbf{y}| \quad T_i : t \mapsto |(\mathbf{a} \geq t) \wedge \mathbf{y}| / |\mathbf{y}| \quad (2)$$

$$T_r : t \mapsto |(\mathbf{a} \geq t) \wedge \mathbf{r}| / |\mathbf{r}| \quad . \quad (3)$$

Instances at each scope ( $\mathbf{r}$ ,  $\mathbf{y}$ , and  $\mathbf{a}$ ) are omitted in the notation for brevity.

#### 3.1 Precursors: AUROC and AUPRO

The ROC and PRO curves (Fig. 3a) can be defined as

$$\text{ROC} : t \mapsto (F_s(t), T_s(t)) \quad \text{and} \quad \text{PRO} : t \mapsto (F_s(t), \overline{T_r}(t)) \quad , \quad (4)$$

where  $\overline{T_r} : t \mapsto \frac{1}{|\mathcal{R}|} \sum_{\mathbf{r} \in \mathcal{R}} T_r^{\mathbf{r}}(t)$  is the average Region TPR;  $T_r^{\mathbf{r}}$  refers to the  $T_r$  applied to the instance  $\mathbf{r}$  and  $\mathcal{R}$  is the set of all  $\mathbf{r}$  from all  $\mathbf{y} \in \mathcal{Y}$ . Both curves trace the trade-off between False Positives (FPs) and True Positive (TP)s across all potential binarization thresholds.



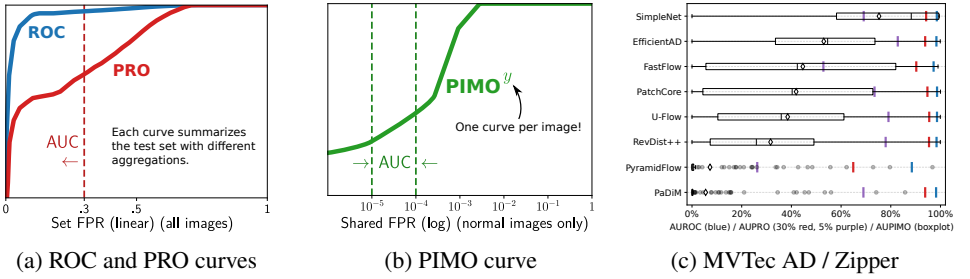


Figure 3: (a, b) ROC, PRO, and PIMO curves. The y-axes are TPR metrics: ROC uses the set TPR (all anomalous pixels from all images confounded); PRO uses the region-scoped TPR averaged across all regions from all images; PIMO uses the image-scoped TPR keeping one curve per anomalous image (no cross-instance averaging). The x-axes are FPR metrics shared by all instances (*i.e.* anom. regions for PRO and anom. images for PIMO), which indexes the binarization thresholds. ROC and PRO use the set FPR (all normal pixels from all images confounded) in linear scale. PIMO uses the image-scoped FPR averaged across normal images only in log scale. The curves are summarized by their (normalized) area under the curve (AUC), with different integration ranges: AUROC in  $[0, 1]$ , AUPRO in  $[0, 0.3]^3$ , and AUPIMO in  $[10^{-5}, 10^{-4}]$ . (c) Benchmark on dataset MVTec AD / Zipper shows how their AUCs differ.

Both use the Set FPR as the x-axis, but different recall measures as the y-axis, reflecting distinct Region TPR aggregation strategies. PRO calculates the arithmetic average (equal weight to each region). ROC uses the Set TPR, which is equivalent to averaging the Region TPRs with region size weighting. Their respective AUCs, AUROC and AUPRO, summarize the curves into a single score:

$$\text{AUROC} = \int_0^1 T_s(F_s^{-1}(z)) dz \quad \text{and} \quad \text{AUPRO} = \frac{1}{U} \int_0^U \overline{T_r}(F_s^{-1}(z)) dz, \quad (5)$$

where  $F_s^{-1}$  is the inverse of  $F_s$ . In practice, they are computed using the trapezoidal rule with discrete curves given by a sequence of anomaly score thresholds.

AUPRO is restricted to thresholds such that  $F_s(t) \in [0, U]$  (*i.e.* to the left of the vertical line in Fig. 3a), where  $U$  is the upper bound FPR. This means that AUPRO only accounts for recall values obtained from level sets higher than (*i.e.* inside) the white level set in the anomaly score map in Fig. 2. The default value of  $U = 30\%^3$  is based on the intuition that at such FPR levels the segmentation contours of the anomalies are no longer meaningful [9], so that should be the “worst case”. From this perspective, the FPR restriction in AUPRO acts as a model validation – an implicit requirement since a partial threshold choice is imposed.

## 3.2 Our Approach: AUPIMO

PRO measures region-scoped recall at each binarization threshold, which are indexed by an FPR metric (the x-axis) shared by all region instances. We generalize this idea and employ the term *Shared FPR* ( $F_{sh}$ ) to refer to “any FP measure shared by all anomalous instances.” In our approach, the Set FPR used as x-axis by ROC and PRO is replaced by the average

<sup>3</sup>We also considered a AUPRO with  $U = 5\%$  (noted AUPRO<sub>5%</sub>) in our experiments for the sake of making the metric more challenging.

Image FPR on normal images only:  $F_{sh} : t \mapsto \frac{1}{|\mathcal{Y}^0|} \sum_{\mathbf{y} \in \mathcal{Y}^0} F_i^{\mathbf{y}}(t)$ , where  $\mathcal{Y}^0 \subset \mathcal{Y}$  contains only and all normal images in  $\mathcal{Y}$ , and  $F_i^{\mathbf{y}}$  refers to  $F_i$  computed on instance  $\mathbf{y}$ . This design choice is a major counterpoint with previous approaches, and its implications are discussed in Sec. 3.3. The **Per-Image Overlap (PIMO)** curve (Fig. 3b) and its AUC are defined as

$$\text{PIMO}^{\mathbf{y}} : t \mapsto (\log(F_{sh}(t)), T_i(t)) \quad \text{and} \quad \text{AUPIMO}^{\mathbf{y}} = \int_{\log(L)}^{\log(U)} \frac{T_i(F_{sh}^{-1}(z))}{\log(U/L)} d\log(z) \quad , \quad (6)$$

where the integration bounds have default values  $L = 10^{-5}$  and  $U = 10^{-4}$ . To have a better resolution at low FPR levels, the x-axis is in log-scale, and the term  $1/\log(U/L)$  normalizes the integral's score to  $[0, 1]$ . Contrasting with AUROC and AUPRO, which define a single score for the entire test set, we keep one score per image (superscript  $\mathbf{y}$ ).

### 3.3 AUPIMO's properties

AUPIMO significantly diverges from its predecessors by: (1) considering only normal instances for validation and using a stricter requirement (integration range in the x-axis), (2) evaluating metrics at the image scope, and (3) calculating individual scores for each image. This section discusses the implications and advantages of these design choices.

**Bias-free validation** AUROC is a threshold-independent metric, which limits its usage in real-world applications that require threshold selection for inference. AUPRO addresses this by imposing an FPR restriction, which selects a range of valid thresholds, thus carrying an implicit model validation based on the Set FPR. AUPIMO uses a similar strategy, but – to produce a bias-free score – we propose that the validation metric (x-axis of the curve) should only use normal images, while anomalous images are only used for evaluation.

AD is often viewed as a binary classification problem, yet this simplification is misleading. While the normal class is well-defined by the training set, the anomalous class is, by definition, unknown, unbounded, thus inherently multi-modal. Public datasets (*e.g.* MVTec AD and VisA) provide various types of anomalies, but the objective in AD is to detect *any* type of anomaly. As the positive class in AD can have an unlimited number of modes, we argue that an evaluation metric in benchmarks should avoid conditioning the model behavior (*i.e.* creating a bias, *e.g.* selecting a threshold range) based on *known* anomalies.

The x-axis in AUPIMO ( $F_{sh}$ ) is built only from normal images, which can be reasonably assumed from the same distribution as the training set. In this framework, the variance of the normal class coming from acquisition conditions, sensor noise, *etc.* is accounted for in the validation metric ( $F_{sh}$ ). By ensuring that these variations are not falsely detected, the model's capacity to detect anomalies is isolated from the normal class's variability. This essential change avoids biasing the evaluation metric towards available anomalies, which is consistent with the unsupervised nature of AD. Note that an alternative AUPRO could be defined in the same way, but AUPIMO carries additional advantages discussed below.

**Anomaly-dependent metrics** The Area Under the Precision-Recall (AUPR) and its variant Instance Average Precision (IAP) [27] use recall measures on the x-axis and precision on the y-axis. Similar to the AUCs defined in Sec. 3.1 and Sec. 3.2, they express the average of the y-axis over a range of thresholds, which are indexed by the x-axis. Using the recall as x-axis biases the metric in favor of detectable anomalies, making the metric sensitive to the distribution of known anomalies. The threshold at the integration lower bound is the maxi-

imum full-recall threshold, making them sensitive to hard anomalies<sup>4</sup> – while not revealing them. Conversely, easy anomalies can be over-represented because low-recall thresholds are covered – *i.e.* unnecessarily high thresholds are accounted for.

The  $F_1$ -max score and IAP further choose, respectively, optimal and minimum thresholds based on the recall. Similarly, AUPRO validates models using anomalous images as well because it restricts the Set FPR (Eq. (1)), which encompasses all test images (thus the normal-annotated pixels in anomalous images). While such threshold choices are useful for practical applications, we argue that benchmarks should prefer bias-free metrics so that model comparison is more consistent across different datasets and applications.

Finally, AUPIMO’s validation is insensitive to imprecisions in the anomaly annotations – *i.e.* when only loose bounding box annotations are available. Other model conditioning criteria – as in  $F_1$ -max and IAP in particular – carry pixel-level imprecision but AUPIMO is not affected because normal images are only annotated at the image level.

**Low tolerance** From an application perspective, anomalies are expected to contain information deserving the user’s attention. A high FPR can lead to user frustration and diminish trust in the model. To tighten evaluation, we restrict the FPR range in AUPIMO to be between  $10^{-5}$  and  $10^{-4}$  for datasets like MVTec AD and VisA. At such levels, the FP regions in normal images are small compared to the structures seen in the images (see Fig. 2 and Appendix A). An AUPIMO score can be interpreted as the “*average segmentation recall in an anomalous image given that the model (nearly) does not yield FP regions in normal images*”. These default values were chosen to establish a challenging task in-line with recent advances in research, but they can be adapted to application-specific needs.

**AUPRO vs. AUPIMO** Fig. 2 shows a visual comparison between AUPRO and AUPIMO. The upper bound in AUPRO is chosen from a precision-inspired criterion (“beyond that point the anomaly segmentations are no longer useful”), so the FP regions on normal images can be large. In contrast, AUPIMO chooses a more conservative upper bound. The model conditioning in AUPIMO ensures that FP regions in normal images are insignificant. As a result, its recall on the anomalous region (on the right in Fig. 2b) is lower than AUPRO’s – which is expected.

**Image-scoped metrics** Note that the set-scoped metrics in AUROC and AUPRO are ill-suited for images because information within each image is disregarded (all pixels are confounded). AUPIMO avoids this problem by only using image-scoped metrics (*i.e.* ratios of pixels within each image). Image-scoped measures account for image structure, are fast to compute (Fig. 5a), and are robust to noisy annotations (see Fig. 5b).

**Image-specific scores** Since each curve/score refers to an image file, it is easy to index scores to instances<sup>5</sup>. Achieving the same with region-based scores would require more meta-data, and finding connected regions is implementation-sensitive. For instance, Anomalib’s [10] CPU and GPU-based implementations are from `opencv-python` [10] and `kornia` [12], and the AUPRO scores slightly differ. Per-image scores enable fine-grained analyses otherwise impossible with AUROC and AUPRO. Score distributions (*e.g.* Fig. 3c) – instead of single-valued scores – provide insight into performance variance, which we exploit to select representative samples for qualitative analysis in Appendix D. Finally, it also enables the use of statistical tests, which we showcase in an ablation study in Appendix C.1.

<sup>4</sup>Reminder: lower threshold means higher recall, so the anomalies with lowest anomaly score are the hardest.

<sup>5</sup>A standard format is proposed in Appendix D and implemented in our repository.

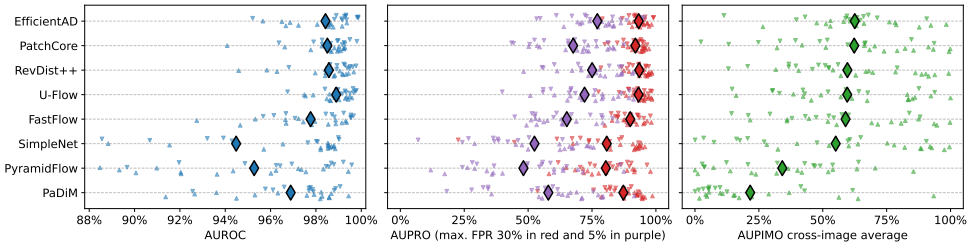


Figure 4: Dataset-wise comparison. Each triangle is a set-scoped score (AUROC, AUPRO, and  $\text{AUPRO}_{5\%}$ ) or a cross-image statistic (average AUPIMO) from a dataset in MVTec AD ( $\Delta$ ) or VisA ( $\nabla$ ). Diamonds are cross-dataset averages (all confounded). Plots have different x-axis scales. AUPIMO reveals that all models have a large cross-problem variance, meaning that none of the models is robust to all problems.

## 4 Experimental Setup

We benchmark the datasets from MVTec AD and VisA with State-of-the-Art (SOTA) models to compare the performances reported in terms of AUROC, AUPRO, and AUPIMO. We also report AUPRO with  $U = 5\%$  ( $\text{AUPRO}_{5\%}$ ) for the sake of comparing with a more challenging alternative of that metric.

We reproduce a selection of models: PaDiM [8] from ICPR 2021, PatchCore [22] from CVPR 2022, SimpleNet [15], PyramidFlow<sup>6</sup>[14], and RevDist++ [25] from CVPR 2023, along with the recently published models UFlow [24], FastFlow [26], and EfficientAD [0]. Our aim is to ensure a comprehensive evaluation with a set of different algorithm families. This selection includes methods based on memory bank (PatchCore), reconstruction (SimpleNet), student-teacher framework (RevDist++, EfficientAD), probability density modelling (PaDiM), and normalizing flows (FastFlow, PyramidFlow, UFlow).

All models were trained with  $256 \times 256$  images (downsampled with bilinear interpolation, no center crop), and with the hyperparameters reported in the original papers. We used the official implementations or Anomalib [0]. The implementations of AUROC and AUPRO are from Anomalib [0]. Details provided in Appendix D.

Cross-paper comparisons in the anomaly localization literature often have conflicting evaluation procedures. We aim to tackle this issue by proposing our evaluation guidelines as a standard: (1) compute test set metrics at the annotations’ full resolution with bilinear interpolation for resizing the anomaly score maps if necessary; (2) do *not* apply crop to the input images; (3) publish per-image scores<sup>5</sup>; (4) (ideally) report the score distribution (*e.g.* boxplots as in Fig. 3c). Details in Appendix D.

## 5 Results

In this section we comment on the results of a single dataset (Fig. 3c), present a summary across all datasets (Fig. 4), and compare AUROC, AUPRO, and AUPIMO in terms of the execution time and robustness to noisy annotation. Due to the space constraints, additional

<sup>6</sup>Our AUPRO results significantly differ from PyramidFlow’s paper. Their implementation has higher scores because it does not apply the maximum FPR (30%) as proposed by [0] <https://github.com/gasharper/PyramidFlow> (commit 6977d5a), see function `compute_pro_score_fast` in the file `util.py`.

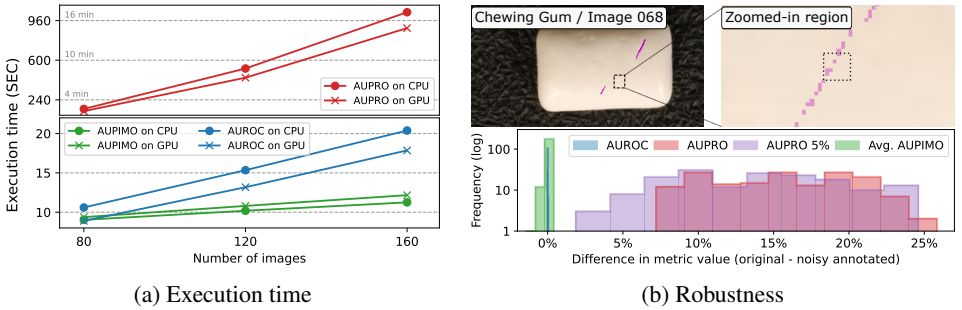


Figure 5: (a) Execution time of metrics on MVTec AD / Screw dataset (image resolution of  $1024 \times 1024$ ; average times over 3 runs). (b, top) An anomalous sample from the dataset VisA / Chewing Gum superimposed with its annotation (pink) shows meaningless, tiny (even 1-pixel) regions (the mask has *not* been downsampled). (b, bottom) Robustness to noisy annotation. Histograms show the distribution of the difference between the scores without and with the synthetic mistakes (closer to zero is better).

results are available in Appendix C and the benchmarks from all datasets in MVTec AD and VisA are documented in Appendix D.

**Benchmark on MVTec AD / Zipper** Fig. 3c illustrates two common observations in our benchmarks. First, it shows how AUROC and AUPRO fail to reveal differences between models (e.g. differences of 0.1% and 0.4% between the two best models). While AUPRO<sub>5%</sub> amplifies the differences, AUPIMO’s strict validation causes the best model to stand out more clearly. Note that AUPRO<sub>5%</sub> and AUPIMO show different rankings, which might be attributed to how they weight small anomalies differently. Second, image-specific performance often has large variance and the best models have left-skewed AUPIMO distributions – c.f. the best models per dataset in Appendix D.3. In Fig. 3c for example, several models have worst and best-case samples at 0% and 100% AUPIMO respectively. Fortunately, AUPIMO provides the means to investigate this by programatically identifying specific instances or anomaly types not well-detected by a model.

**Cross-dataset analysis** Fig. 4 reveals two key insights regarding the SOTA in anomaly localization. First, the benchmark datasets from MVTec AD and VisA still have room for improvement. While AUPRO<sub>5%</sub>’s (purple) stricter validation is more challenging, AUPIMO (green) reveals that even the best models have failure cases when constrained to low FP tolerance. We argue that setting such a challenging standard will push the next generation of models to achieve a more trustworthy task: high anomaly recall with near-zero false positives. Second, none of the models consistently achieves reasonable performance across all datasets. For example, despite PatchCore’s high performance in many problems, it performs poorly on VisA / Macaroni 2 (details in Appendix D.3). Meanwhile, EfficientAD has a reasonable performance on this dataset, thus the dataset is not unsolvable with the current models. This provides a useful insight for practitioners: problem-specific model choice is highly advised because a model’s failure in one dataset does not imply failure in another one.

**Execution time** Having computationally efficient metrics is essential to enable fast iterations and not create computational bottlenecks in research and development. Fig. 5a shows that AUROC and AUPIMO have comparable execution time, but AUPRO is significantly slower both on CPU and GPU. The main reason is that AUPRO requires connected com-

ponent analysis, while AUROC and AUPIMO do not. AUPIMO’s implementation relies on simple operations, enabling the use of `numba` [13] to further accelerate the computation (reported execution times include the just-in-time compilation). The GPU used was an NVIDIA GeForce RTX 3090 and the CPU was an Intel Core i9-10980XE. Note that the chosen model does not influence the execution time because the anomaly score maps are precomputed.

**Robustness** In real-world use-cases, high-quality annotation is hard to acquire or even to define. Fig. 5b shows an example of a ground truth mask where noisy regions can be seen. We found this issue to be prevalent in VisA (more examples in Appendix B). In the PRO curve, these tiny regions have the same weight as the actual anomalous regions. In contrast, AUPIMO is more robust to this issue due to their limited contribution to the overall image score. Fig. 5b demonstrates this in an experiment with artificially added noise. Random mistakes mimicking statistics from VisA are added to the datasets in MVTec AD. We generate one noisy mask for each anomalous mask by adding randomly shaped anomalous regions to it. The number and size of the noisy regions are randomly sampled with probabilities matching the statistics of the VisA dataset (average frequencies from Tab. 2 in Appendix B).

## 6 Conclusion

We introduced AUPIMO: a novel recall metric tailored for anomaly localization addressing the limitations of its predecessors (AUROC and AUPRO) and formalizing a validation-evaluation framework. As a guiding principle, it was proposed that the validation step should only depend on normal images to avoid biasing the model behaviour towards known anomalies, thus making the metric consistent with the unsupervised nature of AD. Finally, a stringent false positive restriction is proposed to establish a more challenging task on contemporary benchmark datasets and expose differences between models.

AUPIMO is built with image-scoped metrics and enables simple assignment of image-specific scores. As demonstrated, these design choices offer advantages in terms of computational efficiency (see Fig. 5a), fine-grained performance analysis (see Fig. 3c and Appendix C.1), and resilience against noisy annotation (see Fig. 5b).

Evaluating eight recent models on 27 datasets with AUPIMO revealed a significant insights about the SOTA in anomaly localization. We show evidence that problem-specific model selection is highly advised, raising further questions for future research. Namely, can one identify dataset traits causing a model to succeed or fail? Or conversely, which model features should one look for to succeed on a specific problem?

**Limitations** In this paper we focused on (2D) image anomaly localization, but AUPIMO can be easily adapted to 3D imaging (*e.g.* X-ray tomography), 3D point clouds (*e.g.* LiDAR), and video-based applications (a proof of concept is shown in Appendix C.3). Other domains like times series would require more careful adaptation, which is left for future work. As a recall metric, the notion of segmentation quality is not covered by AUPIMO, but Appendix C.4 briefly discusses alternatives based on the same validation-evaluation principle.

## 7 Acknowledgements

This research was conducted during Google Summer of Code 2023 (GSoC 2023) with the anomalib team from Intel’s OpenVINO Toolkit. We would like to thank the OpenVINO team

for their support and feedback during the project. We would like to thank Matías Tailanian for having collaborated by training the UFlow models and providing the evaluation results for the benchmark.

## References

- [1] Samet Akcay, Dick Ameln, Ashwin Vaidya, Barath Lakshmanan, Nilesh Ahuja, and Utku Genc. Anomalib: A Deep Learning Library for Anomaly Detection. In *ICIP*, pages 1706–1710, 2022.
- [2] Kilian Batzner, Lars Heckler, and Rebecca König. EfficientAD: Accurate Visual Anomaly Detection at Millisecond-Level Latencies, 2023.
- [3] Alessio Benavoli, Giorgio Corani, and Francesca Mangili. Should We Really Use Post-Hoc Tests Based on Mean-Ranks? *Journal of Machine Learning Research*, 17(5):1–10, 2016.
- [4] Paul Bergmann, Michael Fauser, David Sattlegger, and Carsten Steger. MVTec AD – A Comprehensive Real-World Dataset for Unsupervised Anomaly Detection. In *CVPR*, pages 9592–9600, 2019.
- [5] Paul Bergmann, Kilian Batzner, Michael Fauser, David Sattlegger, and Carsten Steger. The MVTec Anomaly Detection Dataset: A Comprehensive Real-World Dataset for Unsupervised Anomaly Detection. *IJCV*, 129(4):1038–1059, 2021.
- [6] Jakob Božič, Domen Tabernik, and Danijel Skočaj. Mixed supervision for surface-defect detection: From weakly to fully supervised learning. *Computers in Industry*, 129:103459, 2021.
- [7] G. Bradski. The OpenCV Library. *Dr. Dobb's Journal of Software Tools*, 2000.
- [8] Thomas Defard, Aleksandr Setkov, Angelique Loesch, and Romaric Audigier. PaDiM: A Patch Distribution Modeling Framework for Anomaly Detection and Localization. In *ICPR*, pages 475–489, 2021.
- [9] Janez Demšar. Statistical Comparisons of Classifiers over Multiple Data Sets. *Journal of Machine Learning Research*, 7(1):1–30, 2006.
- [10] Tom Fawcett. An introduction to ROC analysis. *Pattern Recognition Letters*, 27(8): 861–874, 2006.
- [11] Jongheon Jeong, Yang Zou, Taewan Kim, Dongqing Zhang, Avinash Ravichandran, and Onkar Dabeer. WinCLIP: Zero-/few-shot anomaly classification and segmentation. In *CVPR*, pages 19606–19616, 2023.
- [12] Renato A. Krohling, Guilherme J. M. Esgario, and José A. Ventura. BRACOL - A Brazilian Arabica Coffee Leaf images dataset to identification and quantification of coffee diseases and pests, 2019.
- [13] Siu Kwan Lam, Antoine Pitrou, and Stanley Seibert. Numba: a LLVM-based Python JIT compiler. In *Proceedings of the Second Workshop on the LLVM Compiler Infrastructure in HPC*, pages 1–6, 2015.



- [14] Jiarui Lei, Xiaobo Hu, Yue Wang, and Dong Liu. PyramidFlow: High-Resolution Defect Contrastive Localization Using Pyramid Normalizing Flow. In *CVPR*, pages 14143–14152, 2023.
- [15] Zhikang Liu, Yiming Zhou, Yuansheng Xu, and Zilei Wang. SimpleNet: A Simple Network for Image Anomaly Detection and Localization. In *CVPR*, pages 20402–20411, 2023.
- [16] Vijay Mahadevan, Weixin Li, Viral Bhalodia, and Nuno Vasconcelos. Anomaly detection in crowded scenes. In *CVPR*, pages 1975–1981, 2010.
- [17] Pankaj Mishra, Riccardo Verk, Daniele Fornasier, Claudio Piciarelli, and Gian Luca Foresti. VT-ADL: A Vision Transformer Network for Image Anomaly Detection and Localization. In *2021 IEEE 30th International Symposium on Industrial Electronics (ISIE)*, pages 01–06, 2021.
- [18] Mantini Pranav, Li Zhenggang, and Shah Shishir K. A day on campus - an anomaly detection dataset for events in a single camera. In *ACCV*, 2020.
- [19] Mehdi Rafiei, Toby P. Breckon, and Alexandros Iosifidis. On Pixel-level Performance Assessment in Anomaly Detection, 2023. URL <http://arxiv.org/abs/2310.16435>.
- [20] Bharathkumar Ramachandra and Michael J. Jones. Street scene: A new dataset and evaluation protocol for video anomaly detection. In *Proceedings of the IEEE/CVF Winter Conference on Applications of Computer Vision (WACV)*, pages 2558–2567, 2020.
- [21] Edgar Riba, Dmytro Mishkin, Daniel Ponsa, Ethan Rublee, and Gary Bradski. Kornia: an Open Source Differentiable Computer Vision Library for PyTorch. In *Proceedings of the IEEE/CVF Winter Conference on Applications of Computer Vision (WACV)*, pages 3674–3683, 2020.
- [22] Karsten Roth, Latha Pemula, Joaquin Zepeda, Bernhard Schölkopf, Thomas Brox, and Peter Gehler. Towards Total Recall in Industrial Anomaly Detection. In *CVPR*, pages 14318–14328, 2022.
- [23] Takaya Saito and Marc Rehmsmeier. The Precision-Recall Plot Is More Informative than the ROC Plot When Evaluating Binary Classifiers on Imbalanced Datasets. *PLOS ONE*, 10(3):e0118432, 2015.
- [24] Matías Tailanian, Álvaro Pardo, and Pablo Musé. U-Flow: A U-shaped Normalizing Flow for Anomaly Detection with Unsupervised Threshold, 2023. URL <http://arxiv.org/abs/2211.12353>.
- [25] Tran Dinh Tien, Anh Tuan Nguyen, Nguyen Hoang Tran, Ta Duc Huy, Soan T. M. Duong, Chanh D. Tr Nguyen, and Steven Q. H. Truong. Revisiting Reverse Distillation for Anomaly Detection. In *CVPR*, pages 24511–24520, 2023.
- [26] Jiawei Yu, Ye Zheng, Xiang Wang, Wei Li, Yushuang Wu, Rui Zhao, and Liwei Wu. FastFlow: Unsupervised Anomaly Detection and Localization via 2D Normalizing Flows, 2021. URL <http://arxiv.org/abs/2111.07677>.

- 
- [27] Xuan Zhang, Shiyu Li, Xi Li, Ping Huang, Jiulong Shan, and Ting Chen. Destseg: Segmentation guided denoising student-teacher for anomaly detection. In *CVPR*, pages 3914–3923, 2023.
- [28] Yang Zou, Jongheon Jeong, Latha Pemula, Dongqing Zhang, and Onkar Dabeer. Spot-the-difference self-supervised pre-training for anomaly detection and segmentation. In *ECCV*, pages 392–408, 2022.

## A False positives on normal images

We argue that, in Anomaly Detection (AD), the negative class (normal) is the only well-defined class, and that FPR is a meaningful metric to validate models. The positive class (anomalous) is *not* a well-defined concept because it covers the entire complement of the normal class. As such, it is impossible to cover all types and variations. Based on this principle, we argue that it is problematic to use anomalous samples for model validation (not to be confused with model *evaluation*). For this reason, we propose the validation to depend solely on normal instances, thus based on FPs.

For the sake of complementing the discussion, we present an alternative to the (pixel-wise, image-scoped) FPR used in AUPIMO. Counting the number of regions falsely detected as anomalous can be used as meaningful metric to validate (*i.e.* constrain) models. However, such metric is not used in AUPIMO because it is inconvenient to compute, so we propose the FPR as a proxy. Finally, we present visual examples of FP masks at different levels of FPR to provide an intuition of what it represents in practice.

### A.1 Rate vs. number of regions

In this section the relation between two (pixel-wise, image-scoped) metrics is analyzed (both measured on normal images at different binarization thresholds of anomaly score maps):

1. False Positive Rate (FPR): the ratio between the number of FP pixels and the total number of pixels;
2. Number of False Positive Regions (NumFPRReg): the number of maximally connected FP regions.

To be trusted in real-world applications, an anomaly localization model is expected to find image structures worth the user’s attention. Raising false detections eventually diminishes the user’s interest, so it should happen as rarely as possible. One could assume, for instance, that users eventually investigate detected anomalies manually – or even programatically. From this perspective, we argue that the Number of False Positive Regions (NumFPRReg) is an informative metric in practice because it directly relates to how often a user would investigate FPs, so it is a good estimator of the human cost for using the model (*i.e.* how often one’s time is wasted). A good estimate of the expected NumFPRReg would allow a user to set a threshold based on its operational cost.

However, computing NumFPRReg requires connected component analysis, which has two major drawbacks. First, it is slow to compute, especially on the CPU. Second, some implementations use an iterative process that may not converge in some cases. For instance, the implementation in `kornia` [14] (see `kornia.contrib.connected_components`). The FPR, on the other hand, is fast to compute and, as we show next, can be used as a proxy for the NumFPRReg at low FP levels.

**Experiment** Anomaly score maps from our experiments were randomly sampled from the set of normal images, upsampled with bilinear interpolation to the same resolution as the original annotation masks, binarized with a series of thresholds, and the NumFPRReg and the FPR were computed for each binary mask. All models and datasets were confounded on purpose because we seek to understand the relationship between FPR and NumFPRReg *in general*, not

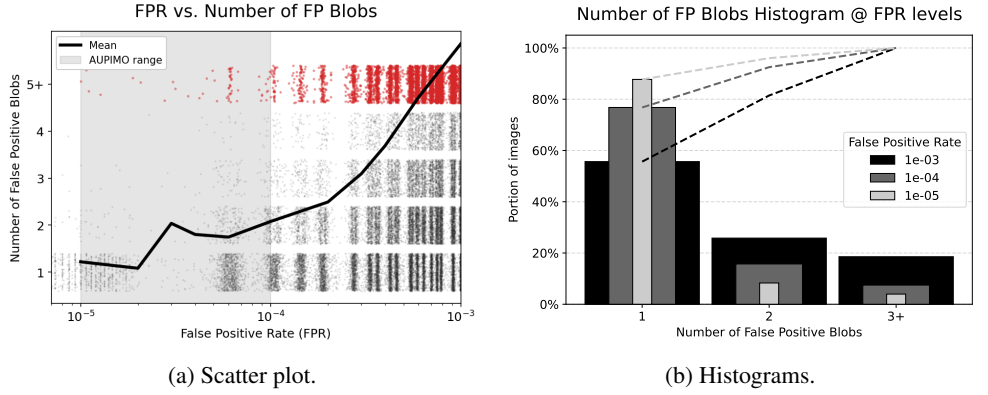


Figure 6: False Positivity. How Image False Positive Rate (ImFPR) relates to the Number of False Positive Regions (NumFPRReg).

for a specific model or dataset. Thresholds were chosen such that a series of logarithmically-spaced FPR levels from  $10^{-5}$  to  $10^{-3}$  are covered. A random multiplying factor  $\in [0.9, 1.1]$  was added to each target FPR value in this range (like a jitter). Assumptions:

1. Each threshold is interpreted as an operational threshold set to automatically obtain binary masks from an AD model;
2. Both metrics are computed at the image scope (*i.e.* ratio of pixels and number of regions in each image);
3. In an real-life scenario, the expected values of these metrics would be estimated to describe a model's behavior to control its operational cost.

Fig. 6a shows a scatter plot of FPR (X-axis, in logarithmic scale) vs. NumFPRReg (Y-axis). NumFPRReg was clipped to the maximum value of 5 and jitter was added to avoid overlapping points. A mean line is displayed in black. The Y-axis values of the mean line are computed as the average NumFPRReg in the bins centered around the pre-set FPR levels.

Fig. 6b shows histograms (counts are numbers of images) of NumFPRReg at three FPR levels:  $10^{-5}$ ,  $10^{-4}$ , and  $10^{-3}$ . At each level  $L$ , all the points from the scatter in the range  $[L/2, 2L]$  are accounted to have a sufficient number of samples. The histograms are normalized to sum to 1. The dashed lines show the sum of the bars' values from left to right.

**Results** Fig. 6 shows that the FPR can effectively be used as a proxy for the number of FP regions:

1. FPR and NumFPRReg correlate positively;
2. The majority of images have  $\leq 2$  regions (more than 90% at FPR  $10^{-4}$  and nearly 100% at FPR  $10^{-5}$ );
3. Inside AUPIMO's integration range, the average NumFPRReg tends to 1, so the FPR generally equals the relative size of the single FP region in the mask.

In summary, at AUPIMO's default integration range, the FPR tends to translate to the maximum relative size of FP regions in normal images because they tend to have a single FP region.

As a practical implication, AUPIMO’s bounds can be leveraged to filter out model predictions. For instance, one can ignore detected regions with areas smaller than AUPIMO’s lower bound. Notice in that MVTec AD’s datasets do not have anomalies with relative size smaller than  $10^{-5}$ , and very few as small as  $10^{-4}$  (see Appendix B).

## A.2 Visual intuition of FP levels

We intend to build an intuition of what Image FPR ( $F_i$ ) levels visually represent on normal images. The Image FPR on normal images is the relative area covered by an FP mask. As shown in the previous section, with AUPIMO’s low levels of FPR, it further tends to translate to the size of a single FP region.

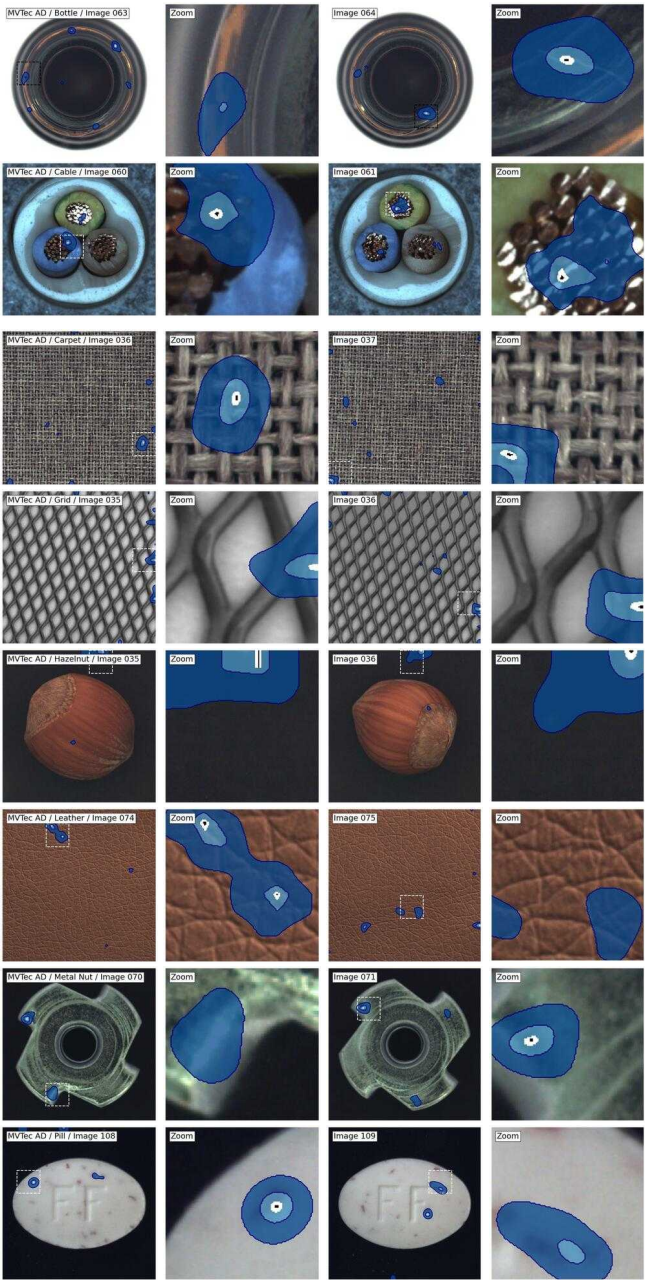
Fig. 7 shows examples of normal images from all the datasets in MVTec AD and VisA superposed by FP masks. Each dataset is in a row with three samples from the test set. Each image is presented with a zoom on the right (the zoomed area is highlighted in the original image with a dashed rectangle). Each color corresponds to a predicted mask at a given ImFPR level. Color code:

1. Darker blue is  $F_i = 10^{-2}$ ;
2. Lighter blue is  $F_i = 10^{-3}$ ;
3. White is  $F_i = 10^{-4}$ ;
4. Black is  $F_i = 10^{-5}$ .

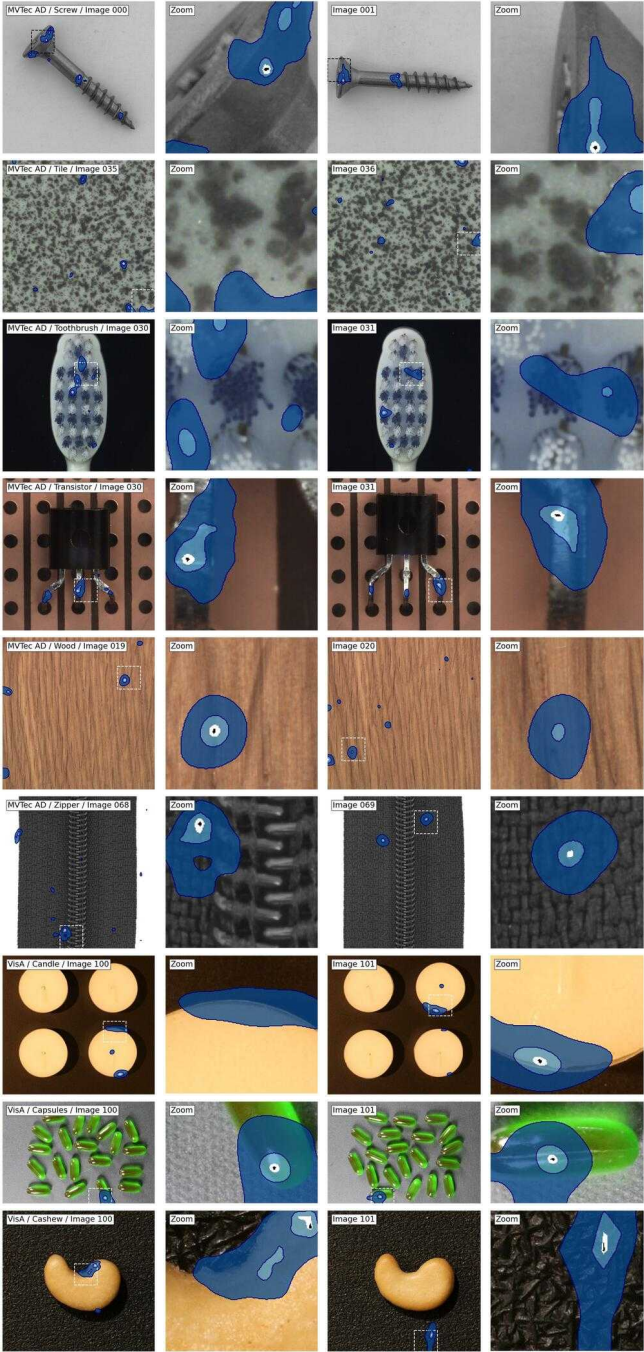
The masks are generated from the anomaly score maps produced by a randomly picked model from our benchmark. The different masks in a single image are generated from the same anomaly score map (*i.e.* same model), but different samples may have masks from different models.

Inside AUPIMO’s integration bounds ( $10^{-5} \sim 10^{-4}$ , *i.e.* between black and white in Fig. 7), FP regions become barely visible at the image scale and generally irrelevant compared to the objects’ structures.

Disclaimer: the *Shared* FPR used in Per-Image Overlap (PIMO) is the *average* Image FPR across all normal images, so it is not to be confused with the Image FPR of a single image. This visual intuition should be understood as an average behavior, not as a strict rule.









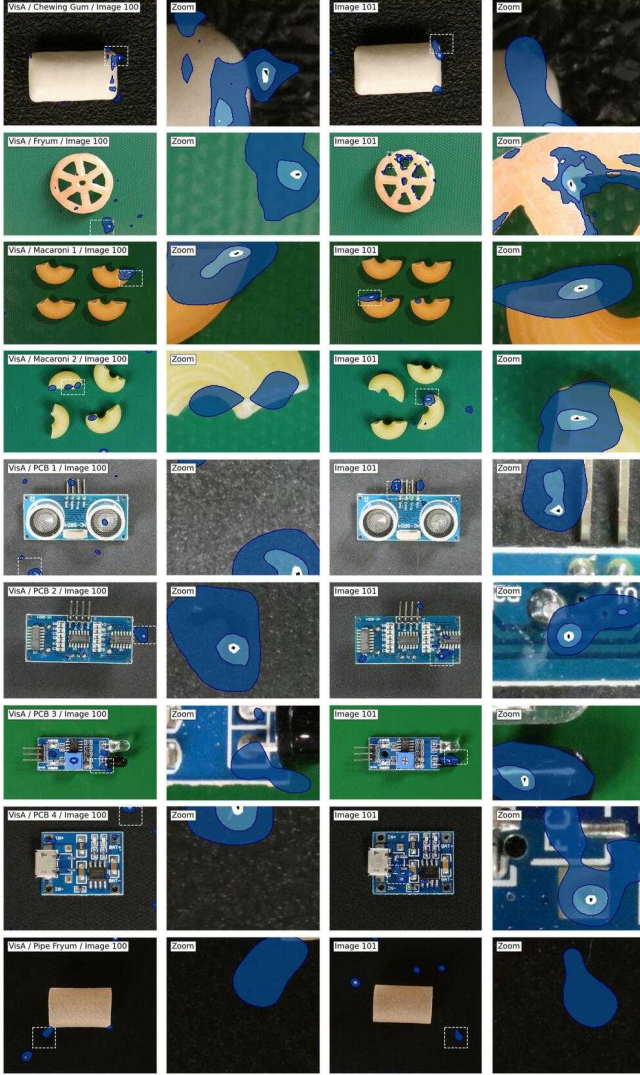


Figure 7: Visual intuition of Image False Positive Rate (ImFPR) levels on normal images. Images are normal samples from the datasets in MVTECAD and VisA. Each color corresponds to a predicted mask at a given ImFPR level: darker blue is  $10^{-2}$ , lighter blue is  $10^{-3}$ , white is  $10^{-4}$ , and black is  $10^{-5}$ .

## B Anomaly size

Fig. 8 shows the distributions of the relative region size in ground truth annotations in each dataset from MVTec AD and VisA. Reminder: relative size is the number of pixels in a maximally connected component divided by the number of pixels in the image. Lower and upper whiskers are set with maximum size to 1.5 inter-quartile range (IQR), and fliers (outliers) are shown as gray dots. The gray-shaded span is AUPIMO’s integration range, and the vertical gray line represents the relative size of a single pixel at resolution  $256 \times 256$  (input size seen by the models in our experiments).

**MVTec AD** Fig. 8 shows that the size of the anomalies in MVTec AD are generally between  $10^{-3}$  and  $10^{-1}$ . Few cases are as small  $10^{-4}$ . Given this distribution, the AUPIMO scores from our experiments can be interpreted as a (near) FP-free recall. Since (almost) none of the anomalies are as small as the FPR integration range, any prediction with relative size above the integration range is a True Positive (TP). Conversely, one could dismiss any prediction with relative size below the integration range.

**VisA** The anomalies in VisA are largely biased towards small regions of relative sizes as small as  $\sim 10^{-6}$  (*i.e.* a single pixel at resolution  $1000 \times 1000$ ). They are so numerous that the actual anomalous regions show as outliers in Fig. 8.

**Tiny regions** Let “tiny” refer to connected components of relative size smaller than  $\frac{1}{256^2}$ , which corresponds to a single pixel at resolution  $256 \times 256$ . In other words, an actual anomaly this small would be seen as a single pixel by the models in our experiments or simply not seen at all. Fig. 9 displays several examples of tiny regions in VisA with zoomed-in views on the right. These regions are meaningless: as Fig. 9 shows, they are often 1-pixel (or “very few”-pixel) regions. They are often near the surroundings of an actual anomaly (e.g. Fryum/Image 048). Extreme cases where completely isolated regions with insignificant size also occur (e.g. Chewing Gum/Image 068 and Macaroni 2/Image 067).

**How often and how small are these tiny regions?** Tab. 2 shows statistics about the absolute sizes (at original resolution) and the number of tiny regions per image in each dataset from VisA. The right-most plot in Fig. 8 shows VisA’s anomalous region size distribution when discarding the tiny regions.

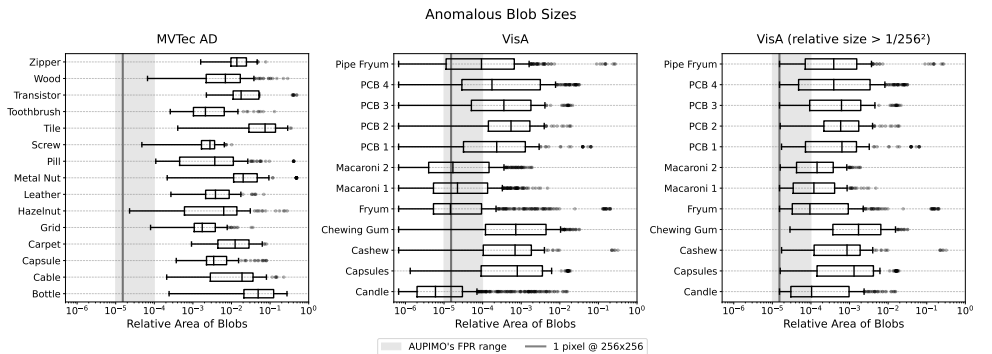


Figure 8: Distribution of relative size of anomalous regions.

Table 2: Statistics from tiny blobs in VisA [28].

(a) Sizes.				(b) Number of regions per image.			
Reg Size (abs) Category	1 - 9	10 - 19	20 - 29	Nb Reg/Img Category	1 - 5	6+	Total
Candle	358	98	20	Candle	5	18	23
Capsules	8	7	3	Capsules	6	1	7
Cashew	10	0	1	Cashew	5	0	5
Chewing Gum	39	1	0	Chewing Gum	6	1	7
Fryum	158	96	22	Fryum	22	13	35
Macaroni 1	114	52	14	Macaroni 1	27	10	37
Macaroni 2	123	54	6	Macaroni 2	21	8	29
PCB 1	19	20	9	PCB 1	10	2	12
PCB 2	11	8	4	PCB 2	10	1	11
PCB 3	20	11	0	PCB 3	8	1	9
PCB 4	32	19	12	PCB 4	10	5	15
Pipe Fryum	44	34	9	Pipe Fryum	17	3	20

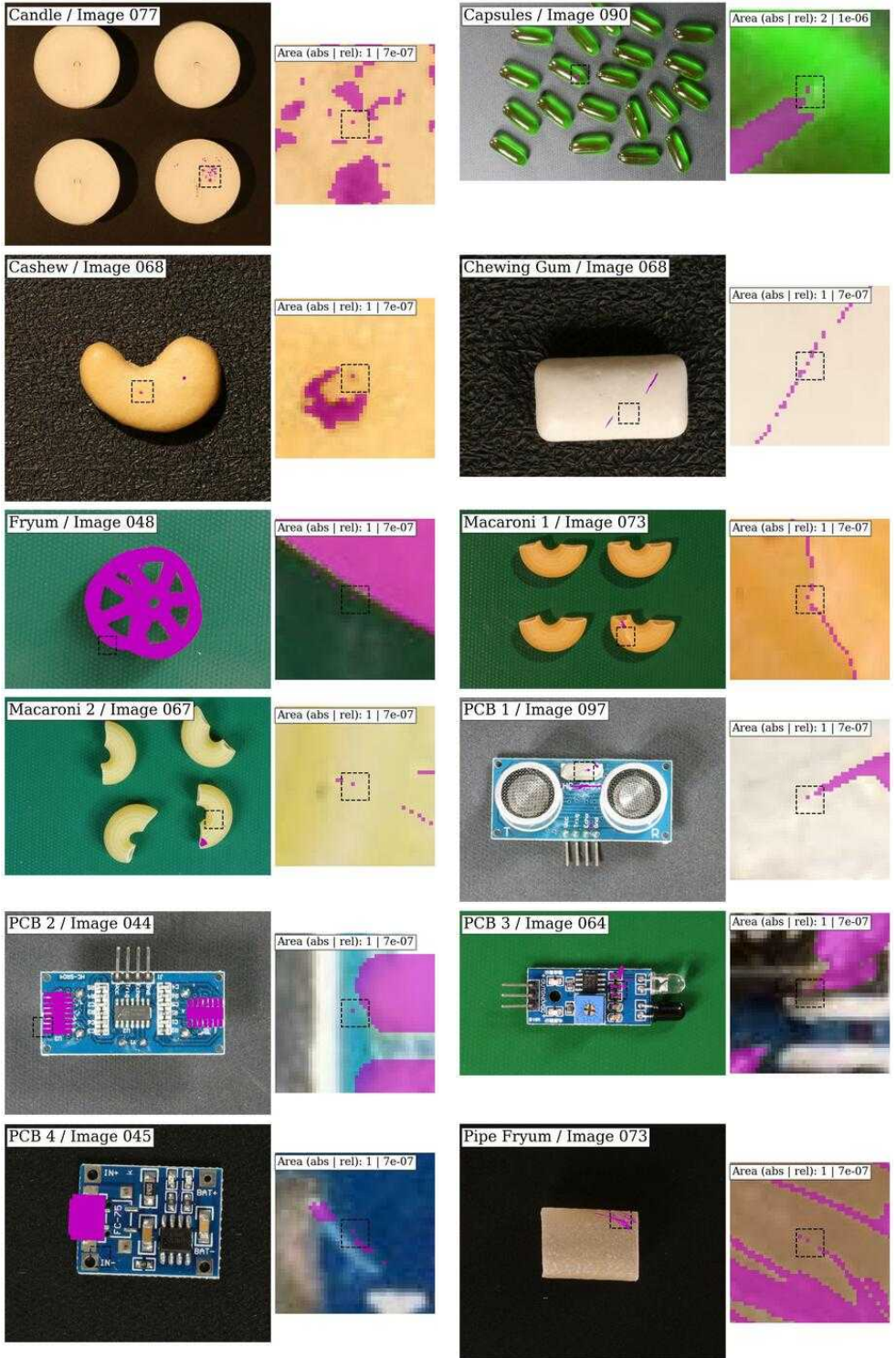


Figure 9: Tiny anomalous regions in VisA.

## C Additional results

### C.1 Ablation study

Tab. 3 showcases the use of statistical tests in an ablation study of EfficientAD [10] on the dataset MVTEC AD / Capsule. The Wilcoxon signed-rank test [13, 14] is used to assess the consistency of performance gain given by different components of the model. The null hypothesis  $H_0$  is that two models  $A$  and  $B$  are equivalent (average ranks tend to equal), and the alternative hypothesis  $H_1$  is that one of the two models (say,  $A$ ) is *more often* better than  $B$ . No assumption is made about the scores distributions making it robust to outliers [13, 14]. Interpretation: high confidence ( $C = 1 - \text{p-value}$ ) to reject the null hypothesis (*i.e.* low p-value) means that  $A$  *consistently* outperforms  $B$ .

Table 3: Ablation study (use-case of statistical tests). Layout and model configurations based on Tab. 4 in [10]. At each row a component is added to the model above starting with Patch Description Network (PDN) at top and resulting in EfficientAD at the bottom.  $C$  refers to the confidence to reject the null hypothesis ( $1 - \text{p-value}$ ); higher means more confidence on the improvement by adding the new component. Each component generally shows significant improvements, but the bottom right cell is an exception. Pretraining penalty causes a score drop, and the low confidence on the alternative hypothesis confirms that the drop is consistent across images.

Avg. AUPIMO (Diff. [%]; $C$ [%])	EfficientAD-S	EfficientAD-M
PDN	$\sim 0$	$\sim 0$
→ map normalization	22 (+22; 100)	23 (+23; 100)
→ hard feature loss	57 (+35; 100)	59 (+36; 100)
→ pretraining penalty	64 (+7; 100)	57 (-2; 0.02)

### C.2 Does AUPIMO correlate with AUROC and AUPRO?

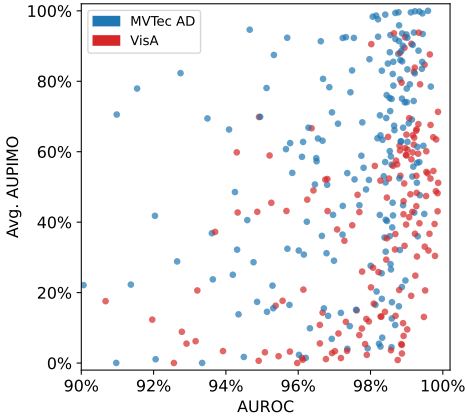
Fig. 10 shows scatter plots of AUROC and AUPRO vs. (cross-image) average AUPIMO. All models and datasets in the benchmark confounded. Notice that the scales of the axes are different for each metric. Both plots seem to show a positive correlation, but one metric is not enough to imply the other. High levels of AUROC and AUPRO do not guarantee high levels of AUPIMO. Conversely, high levels of AUPIMO *tend* to imply higher levels of AUPRO and AUROC (notice the slightly triangular shape of the point clouds).

### C.3 Video

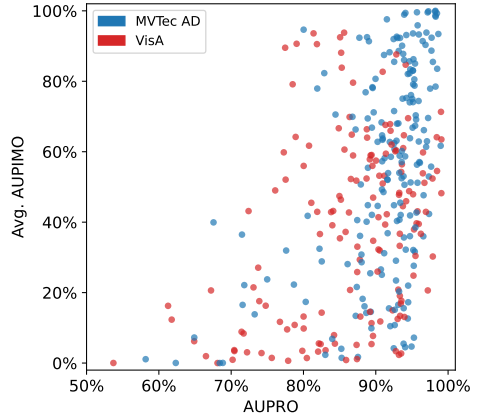
In this section we present how AUPIMO can be used in video applications. It must be stressed that this is not a full-fledged video AUPIMO application, but rather a proof of concept. The UCSD Pedestrian dataset [15] was used to illustrate this concept because it has been widely used and cited in the literature, but other datasets like A Day on Campus (ADOC) [16] and Street Scene [17] would also be relevant to this discussion.

A PatchCore [18] model was trained on the normal videos from UCSD Pedestrian dataset at every 2 frames. The model was evaluated with the same procedure than our experiments by ignoring the temporal dimension of the videos and treating all the frames from all the





(a) AUPIMO vs. AUROC



(b) AUPIMO vs. AUPRO

Figure 10: Scatter plots of AUPIMO vs. {AUROC, AUPRO}

videos as a single dataset. In Fig. 11 we show the AUPIMO scores for each frame in the test videos along the time axis (referenced by the frame index). A selection of frames from the video Test006 are shown in Fig. 12.

Notice how AUPIMO’s validation works in practice: the normal frame (175) does not have any visible FP region – *i.e.* anomaly score values above the threshold  $t_L$ , corresponding to the lowest FPR level  $L$  used in AUPIMO. Frame 61 shows an example case where the image-scoped has limitations: the AUPIMO score is around 50% because there are two independent anomalous regions in the frame; one of them is well detected by the model, but the other is ignored.. A better modelization for this case would require a more complete annotation where each instance of anomaly is labeled separately, which is not the case in the UCSD Pedestrian dataset.

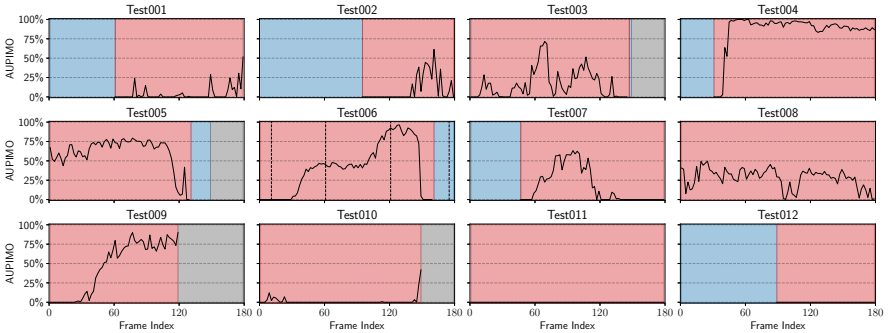


Figure 11: Time vs. AUPIMO in test videos from the UCSD Pedestrian dataset. The x-axis is the frame index in each video and the y-axis is the AUPIMO score at that frame. Blue zones indicate the frame is normal, red zones indicate the frame has an anomaly, and gray zones indicate there is no frame. Vertical dashed lines in "Test006" correspond to the frames shown in Fig. 12.

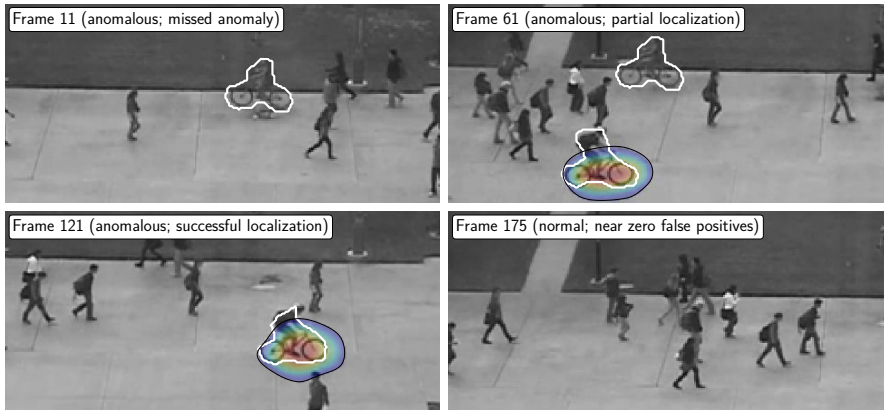


Figure 12: Frames from the video Test006. White contours indicate the ground truth anomalous regions. Black contours correspond to the level sets in each anomaly score map  $\mathbf{a}$  at  $t_L$ , where  $F_{sh}(t_L) = L$ . Anomaly scores above below  $t_L$  are not shown and above are colored using the JET colormap with local maxima in red and  $t_L$  in blue.

## C.4 Precision vs. Intersection over Union

Since AUPIMO only concerns recall, our analysis lacks a discussion about the segmentation quality. In this section we aim to mitigate this shortcoming by extending our validation-evaluation framework. Two candidate metrics are considered: the image-scoped precision and the image-scoped Intersection over Union (IoU). As detailed in the next paragraphs, the precision is not suitable for our purposes, so the IoU is chosen to build a Shared FPR-based curve and an AUC score like PIMO and AUPIMO respectively. The anomaly score maps in this section are from PatchCore in the dataset MVTec AD / Metal Nut. We made this restricted choice to simplify the discussion, but similar results are obtained for the other datasets and models.

Fig. 13 shows the precision as a function of binarization thresholds in five images (note: not indexed by  $F_{sh}$  like PIMO). The level sets of the anomaly score maps at three thresholds along these curves are shown in black superimposed on the images, which can be compared to the contour from the ground truth annotations in white. The precision curves are not smooth, and optimizing this metric does not correspond to improving the visual aspect of the segmentation. It can be seen that optimizing for precision is not a viable option, as the segmentations tend to have a recall-disaster behavior as the precision increases.

The threshold-vs-precision curves show a breakpoint phenomenon where increasing the threshold generally increases the precision but dramatically decreases the recall at some point. For instance, in image 11 the breakpoint is between 60% and 62% precision; *i.e.* somewhere between their respective contour lines the segmentation switches from being too big to being too small (recall drops from 84% to 6%). In image 67, on the other hand, the breakpoint is between 95% and 98% precision (recall drops from 75% to 8% respectively). Image 102 shows an extreme case of this, where the segmentation is reduced to a nearly invisible region as the precision increases from 60% to 63% (recall drops from 91% to almost 0%).

The IoU curves in Fig. 14 (built in the same way as Fig. 13 described above) are smoother, generally show a global maximum, and the level sets at near-maximum-IoU are more visually stable. As the IoU accounts for a balance between precision and recall, it is a more suitable metric for our purposes.



Fig. 15 shows the Shared FPR vs. IoU curve, which is analogous to the PIMO curve. From this curve, the AUC score is computed like AUPIMO using the same integration bounds (blue area in Fig. 15).

The cross-image average AUC scores were added to the results in our benchmark in Appendix D. Since the paper already contains a large number of figures, we decided to not include the distributions of the IoU scores in the paper, but this promising metric deserves in-depth analysis in future work.

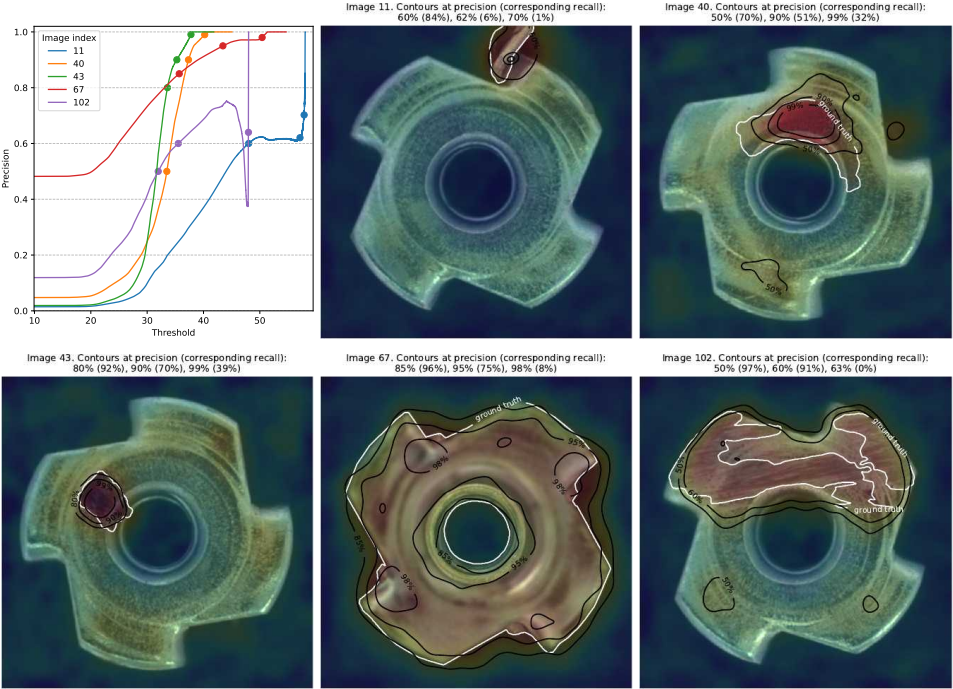


Figure 13: Precision curves and contours at different points along the curves.

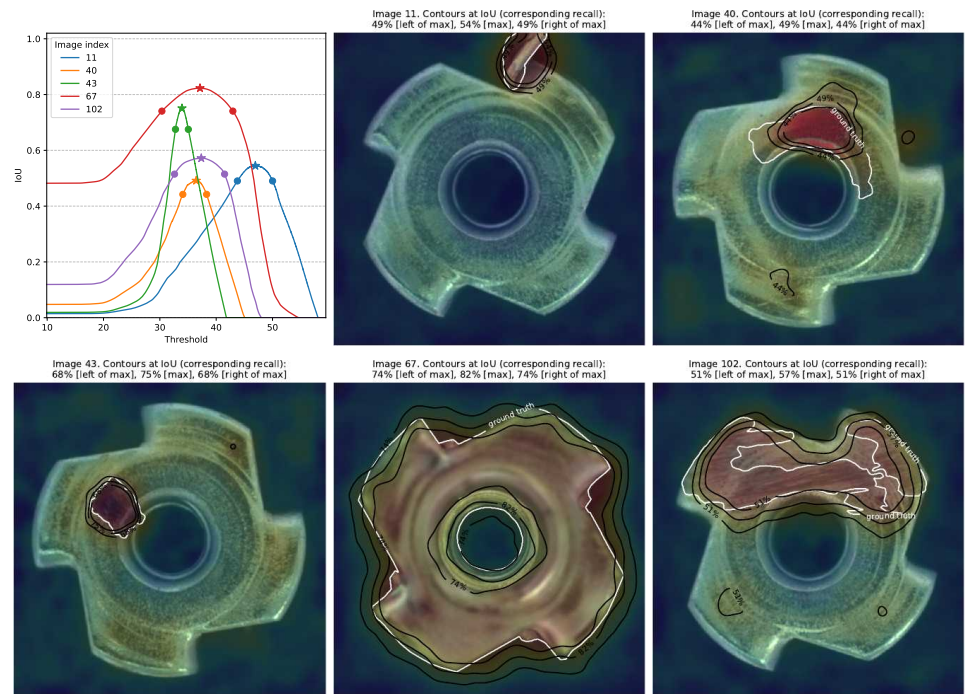


Figure 14: Intersection over union curves and contours at different points along the curves.

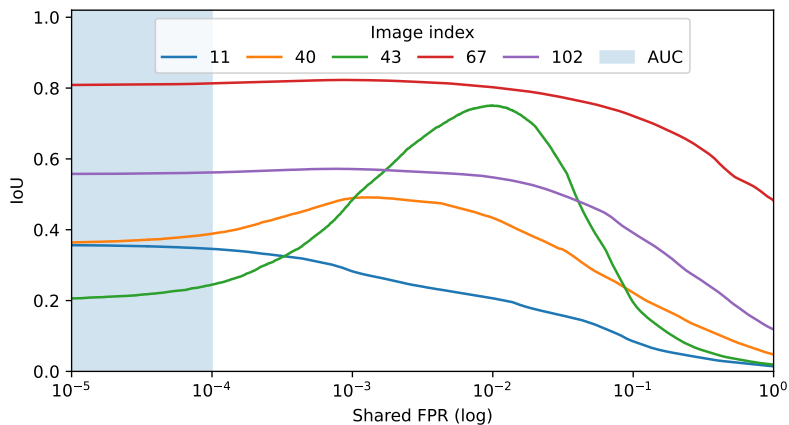


Figure 15: Shared FPR vs. IoU curve.

## D Benchmark

In this section we provide additional details about our experiments and results omitted from the main text for brevity. The following paragraphs provide discuss and detail the evaluation guidelines in our experiments and define a standard format to publish AUPIMO scores.

**Full resolution** Many models typically downsample input images, which conveniently reduces computational costs. However, for a fair and model agnostic evaluation, it is important to use the original resolution as it impacts the decision-making when choosing the most suitable model for a use-case. If a small anomaly is missed due to downsampling, it is desirable to penalize this, while rewarding models that can handle higher resolution. As [2] pointed out, downsampling ground truth masks creates artifacts, leading to inconsistent results across papers. While AUPRO’s computational cost is high at full resolution – especially on CPU – AUPIMO is orders of magnitude faster (see our results in the paper). Our recommendation is to apply bilinear interpolation to upsample anomaly score maps and evaluate at the original resolution in each image.

**No crop** Center crop has been used to leverage the center alignment of the objects depicted in MVTec AD and VisA. However, this is a prior knowledge, hence we do not apply crop.

**Sample selection** To avoid biases from cherry-picking qualitative samples, we propose a systematic selection procedure. Select the images whose AUPIMO are closest to the statistics in a boxplot: mean, first/second/third quartiles, and low/high whiskers set with maximum size of 1.5IQR (inter-quartile range). We applied this procedure to select the samples shown in Appendix D. Note that this is applicable to any per-instance score.

**Score publication** We recommend to publish AUPIMO scores for all images. A standard format is specified below. The field `paths` is optional but recommended. For standard datasets like MVTec AD and VisA, it is a list of paths to the images in the test set with the path truncated to the dataset root directory. The field `num_threshs` is the effective number of thresholds used to compute the AUC, which differs from the number of thresholds used to compute the PIMO curve because only a portion of the curve is used to compute the AUPIMO score.

It is advised to report score distributions (*e.g.* as boxplots and histograms) when possible for a more comprehensive evaluation. All the scores from our experiments are available in this format at [github.com/jpcbertoldo/aupimo](https://github.com/jpcbertoldo/aupimo).

```
{
  "shared_fpr_metric": "mean_perimage_fpr",
  "fpr_lower_bound": 0.00001,
  "fpr_upper_bound": 0.0001,
  "num_threshs": 300,
  "thresh_lower_bound": 0.3342,
  "thresh_upper_bound": 1.1588,
  "aupimos": [0.72107, 0.02415, 0.98991],
  "paths": [
    "MVTec/bottle/test/broken_large/000.png",
    "MVTec/bottle/test/broken_large/001.png",
    "MVTec/bottle/test/broken_large/002.png",
  ]
}
```

## D.1 Models

Appendix D.1 lists the models in the benchmark and provides details on the implementation sources and hyperparameters.

We trained and evaluated 13 models from 8 papers listed in Tab. 4. For some models we considered two backbones and selected the (generally) best out of the two to show in the main text of the paper (see column Tab. 4).

We used the following implementations with the same hyperparameters reported in the papers:

- `anomalib` [10] ([github.com/openvinotoolkit/anomalib](https://github.com/openvinotoolkit/anomalib)<sup>7</sup>) for PaDiM [8], PatchCore [22], and FastFlow [26];
- [github.com/gasharper/PyramidFlow](https://github.com/gasharper/PyramidFlow) for PyramidFlow [14];
- [github.com/donaldrr/simplenet](https://github.com/donaldrr/simplenet) for SimpleNet [15];
- [github.com/tientrandinh/revisiting-reverse-distillation](https://github.com/tientrandinh/revisiting-reverse-distillation) for RevDist++ [25];
- [github.com/mtailanian/uflow](https://github.com/mtailanian/uflow) for UFlow [24];
- [github.com/nelson1425/EfficientAD](https://github.com/nelson1425/EfficientAD) for EfficientAD [9].

The non-official implementations are the ones from `anomalib` and EfficientAD.

Model	Publication	Backbone	Family	Paper	Implem.
PaDiM	ICPR 21	ResNet18	probability density	✓	<code>anomalib</code>
PaDiM	ICPR 21	WideResNet50	probability density	–	<code>anomalib</code>
PatchCore	CVPR 22	WideResNet50	memory bank	–	<code>anomalib</code>
PatchCore	CVPR 22	WideResNet101	memory bank	✓	<code>anomalib</code>
SimpleNet	CVPR 23	WideResNet50	reconstruction	✓	official
PyramidFlow	CVPR 23	ResNet18	normalizing flow	–	official
PyramidFlow	CVPR 23	–	normalizing flow	✓	official
RevDist++	CVPR 23	WideResNet50	student-teacher	✓	official
FastFlow	arXiv (21)	WideResNet50	normalizing flow	–	<code>anomalib</code>
FastFlow	arXiv (21)	Cait M48	normalizing flow	✓	<code>anomalib</code>
EfficientAD-S	arXiv (23)	WideResNet101	student-teacher	–	unofficial
EfficientAD-M	arXiv (23)	WideResNet101	student-teacher	✓	unofficial
UFlow	arXiv (23)	–	normalizing flow	✓	official

Table 4: Models. Years were abbreviated to the last two digits.

<sup>7</sup>Commit 09ad1d4b1e8f634b72f788314275d3aea33815dd.

## D.2 Cross-dataset analysis

In this section, the model performances are summarized across all the datasets in MVTec AD and VisA (all confounded) according to

1. AUROC (Fig. 16),
2. AUPRO (Fig. 17),
3. average AUPIMO (Fig. 18),
4. 33<sup>rd</sup> percentile AUPIMO (Fig. 19),
5. average image-wise rank according to AUPIMO scores (Fig. 20).

**Scores** In Fig. 16, Fig. 17, Fig. 18, and Fig. 19, each point represents the score in the test set or an AUPIMO statistic (average and 33<sup>rd</sup> percentile) across the images in the test set. Diamonds are averages across datasets (both collections confounded) or across models. Notice the difference in the X-axis scales.

**Percentile 33 score** While the average AUPIMO is a useful indicator, we propose the use of the 33<sup>rd</sup> percentile of AUPIMO scores, denoted  $P_{33}$ , for a more rigorous, worst-case evaluation. A  $P_{33}$  score of value  $V$  indicates that two thirds of the images in the test set have an AUPIMO score of *at least*  $V$ . Otherwise stated, a  $P_{33}$  score of value  $V$  indicates that one third of the images in the test set have an AUPIMO score of *at most*  $V$ .

**Average ranks** Fig. 20 shows the average image ranks according to AUPIMO as points and the average across datasets as diamonds. At each image from a given dataset, ranks are assigned to the models (“which model best detects this specific image?”), and the average is taken across all images from the same dataset. The range of rank values is from 1 (best) to number of models (worst).

**Summary table** Tab. 5 summarizes the average scores across datasets within each dataset collection (MVTec AD and VisA) and across all datasets (both collections confounded).

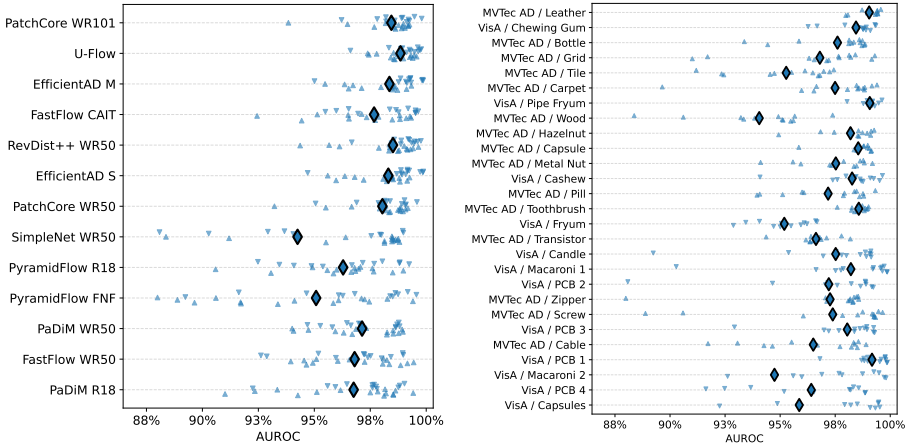


Figure 16: AUROC

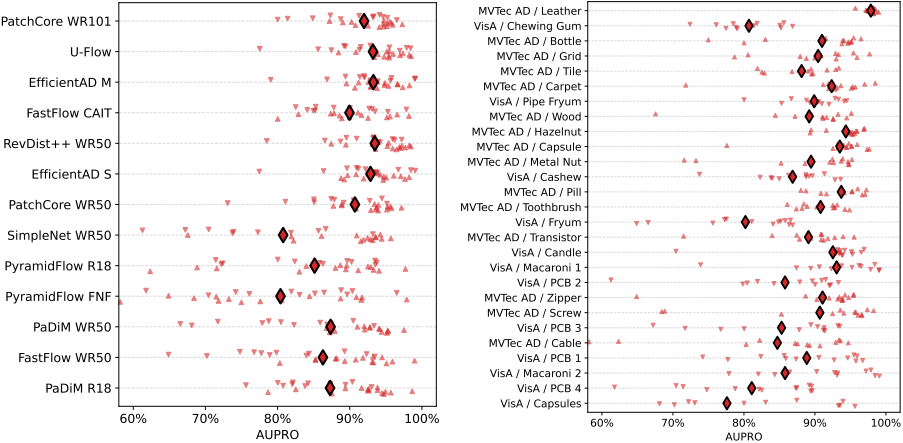


Figure 17: AUPRO

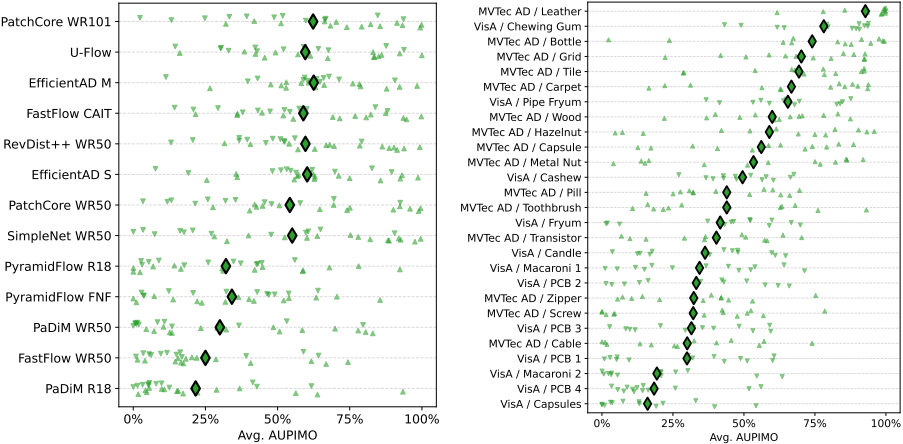


Figure 18: Average AUPIMO

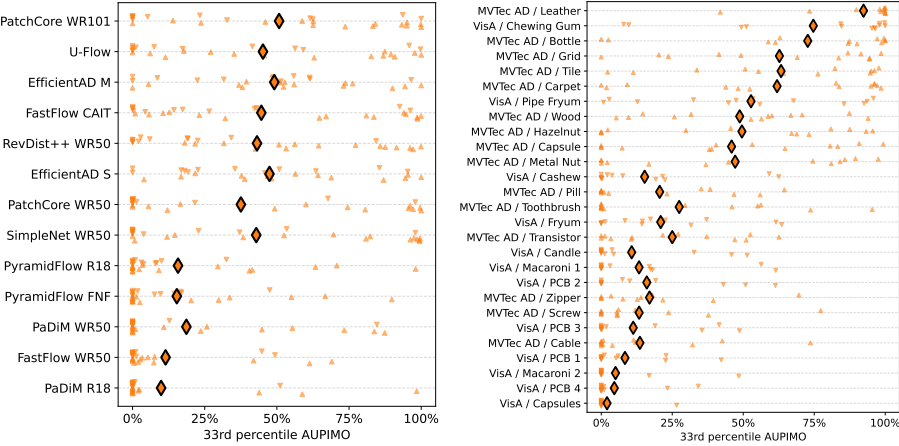


Figure 19:  $P_{33}$  AUPIMO

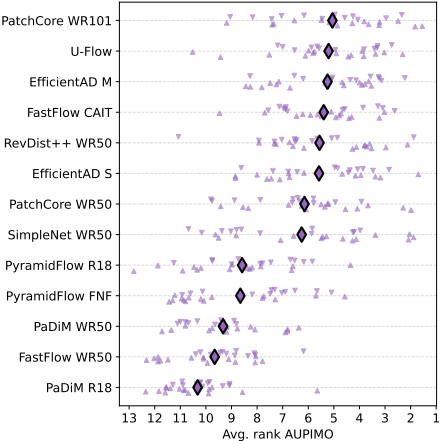


Figure 20: Average rank according to AUPIMO



Model	Dataset Collection	AUROC	AUPRO	AUPIMO	Avg.	P <sub>33</sub>	Avg. Rank
PaDiM R18	MVTec AD	96.62	91.58		25.75	14.34	10.5
PaDiM R18	VisA	97.22	81.87		16.42	4.33	10.1
PaDiM R18	All	96.89	87.27		21.61	9.89	10.3
FastFlow WR50	MVTec AD	97.01	90.87		28.49	14.15	10.3
FastFlow WR50	VisA	96.83	80.54		20.65	8.03	8.9
FastFlow WR50	All	96.93	86.28		25.00	11.43	9.7
PaDiM WR50	MVTec AD	97.19	92.57		40.14	27.06	8.9
PaDiM WR50	VisA	97.32	80.81		17.34	8.12	9.9
PaDiM WR50	All	97.25	87.35		30.01	18.64	9.3
PyramidFlow FNF	MVTec AD	94.21	79.10		36.26	19.94	9.4
PyramidFlow FNF	VisA	96.62	82.03		31.55	9.56	7.8
PyramidFlow FNF	All	95.28	80.40		34.17	15.33	8.7
PyramidFlow R18	MVTec AD	96.36	85.81		36.32	23.91	9.0
PyramidFlow R18	VisA	96.53	84.27		26.84	5.55	8.1
PyramidFlow R18	All	96.44	85.13		32.11	15.75	8.6
SimpleNet WR50	MVTec AD	97.13	89.48		71.39	62.78	5.3
SimpleNet WR50	VisA	91.17	69.88		34.66	17.93	7.4
SimpleNet WR50	All	94.48	80.77		55.07	42.84	6.3
PatchCore WR50	MVTec AD	98.01	93.13		67.21	54.95	5.6
PatchCore WR50	VisA	98.26	87.69		38.02	15.74	6.9
PatchCore WR50	All	98.12	90.72		54.24	37.53	6.1
EfficientAD S	MVTec AD	97.96	93.65		64.76	55.16	5.9
EfficientAD S	VisA	98.89	91.90		54.62	37.78	5.2
EfficientAD S	All	98.37	92.87		60.25	47.44	5.6
RevDist++ WR50	MVTec AD	98.23	95.03		71.93	64.93	4.9
RevDist++ WR50	VisA	99.00	91.53		44.30	15.85	6.3
RevDist++ WR50	All	98.57	93.48		59.65	43.11	5.6
FastFlow CAIT	MVTec AD	97.37	90.44		66.79	57.83	5.4
FastFlow CAIT	VisA	98.25	89.37		49.10	28.09	5.4
FastFlow CAIT	All	97.76	89.96		58.93	44.61	5.4
EfficientAD M	MVTec AD	97.96	94.10		66.08	55.97	5.8
EfficientAD M	VisA	99.00	92.25		58.06	40.52	4.6
EfficientAD M	All	98.42	93.28		62.52	49.10	5.2
U-Flow	MVTec AD	98.74	94.89		66.07	56.07	5.4
U-Flow	VisA	99.09	91.14		51.48	31.54	4.9
U-Flow	All	98.89	93.22		59.58	45.17	5.2
PatchCore WR101	MVTec AD	98.35	93.53		73.19	66.12	4.7
PatchCore WR101	VisA	98.70	90.06		48.72	31.58	5.5
PatchCore WR101	All	98.51	91.99		62.31	50.77	5.1

Table 5: Model averages. Scores are in percentages. Ranks range from 1 (best) to number of models (worst).

### D.3 Per-model analyses

Fig. 21 shows that current anomaly localization models still are not capable of cracking the datasets from MVTec AD and VisA. Fig. 21b shows the AUPIMO distributions of PatchCore WR101, the model with best cross-dataset average. Even though it is the overall best, it still has a long tail of low AUPIMO scores on several datasets like Grid and Wood, or in some cases it practically fails to detect any anomaly at all, like in Capsules and Macaroni 2. Fig. 21b shows the AUPIMO distributions of the best model per dataset. Even if a user would be willing to select a model per dataset, there is no clear winner, and most datasets from VisA show challenging images that are not detected.

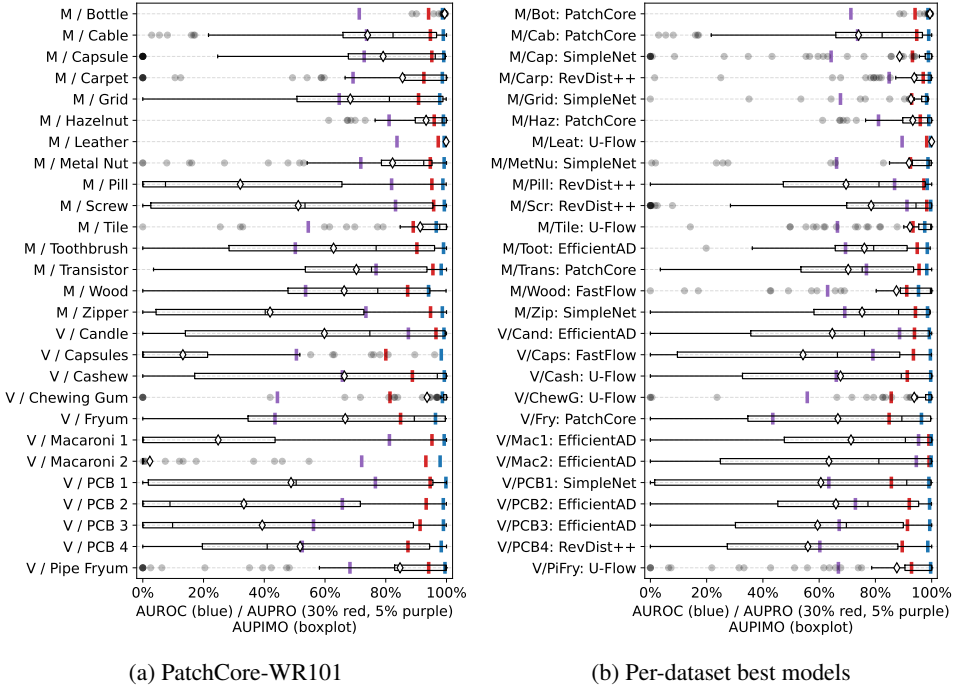


Figure 21: AUPIMO distributions for PatchCore-WR101 (left) and per-dataset best models (right).

## D.4 Per-dataset analyses

The following figures are detailed results from the benchmark of all the datasets from MVTec AD or VisA.

- |   |  |
|---|--|
| 1. Fig. <a href="#">22</a> : MVTec AD / Bottle      | 15. Fig. <a href="#">36</a> : MVTec AD / Zipper  |
| 2. Fig. <a href="#">23</a> : MVTec AD / Cable       | 16. Fig. <a href="#">37</a> : VisA / Candle      |
| 3. Fig. <a href="#">24</a> : MVTec AD / Capsule     | 17. Fig. <a href="#">38</a> : VisA / Capsules    |
| 4. Fig. <a href="#">25</a> : MVTec AD / Carpet      | 18. Fig. <a href="#">39</a> : VisA / Cashew      |
| 5. Fig. <a href="#">26</a> : MVTec AD / Grid        | 19. Fig. <a href="#">40</a> : VisA / Chewing Gum |
| 6. Fig. <a href="#">27</a> : MVTec AD / Hazelnut    | 20. Fig. <a href="#">41</a> : VisA / Fryum       |
| 7. Fig. <a href="#">28</a> : MVTec AD / Leather     | 21. Fig. <a href="#">42</a> : VisA / Macaroni 1  |
| 8. Fig. <a href="#">29</a> : MVTec AD / Metal Nut   | 22. Fig. <a href="#">43</a> : VisA / Macaroni 2  |
| 9. Fig. <a href="#">30</a> : MVTec AD / Pill        | 23. Fig. <a href="#">44</a> : VisA / PCB 1       |
| 10. Fig. <a href="#">31</a> : MVTec AD / Screw      | 24. Fig. <a href="#">45</a> : VisA / PCB 2       |
| 11. Fig. <a href="#">32</a> : MVTec AD / Tile       | 25. Fig. <a href="#">46</a> : VisA / PCB 3       |
| 12. Fig. <a href="#">33</a> : MVTec AD / Toothbrush | 26. Fig. <a href="#">47</a> : VisA / PCB 4       |
| 13. Fig. <a href="#">34</a> : MVTec AD / Transistor | 27. Fig. <a href="#">48</a> : VisA / Pipe Fryum  |
| 14. Fig. <a href="#">35</a> : MVTec AD / Wood       |  |

Each figure contains the following elements:

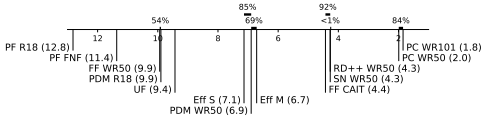
1. a plot with one model per row containing:
  - (a) the AUROC score as a blue vertical line;
  - (b) the AUPRO score as a red vertical line;
  - (c) a boxplot of AUPIMO scores;
    - i. lower and upper whiskers set with maximum size to 1.5 inter-quartile range (IQR);
    - ii. the mean is displayed as a white diamond;
    - iii. fliers are displayed as gray dots;
2. a diagram of (image-wise) average rank according to AUPIMO scores; lower is better; 1 means that the model has the best AUPIMO score at all images;
3. a table comprising two parts:
  - (a) the upper part, in bold, comprises:
    - i. the AUROC scores (in blue);
    - ii. the AUPRO scores (in red);
    - iii. the average and standard deviation AUPIMO score (in black);

- iv. the 33<sup>rd</sup> percentile AUPIMO score (in black);
  - v. the values in parentheses are the ranks of the models according to the respective score metric in each row;
- (b) the lower part shows the results of pairwise Wilcoxon signed rank tests using AUPIMO scores; each cell shows the confidence to reject the null hypothesis  $C = 1 - p$  (where  $p$  is the p-value) assuming that the row model is better than the column model as alternative hypothesis; confidence values below 95% (*i.e.* “low confidence”) are highlighted in bold;
4. PIMO curves and heatmap samples from the model with best average AUPIMO rank;
- (a) samples are selected according to the recommendations from the paragraph “Sample selection”;
  - (b) the (2-pixel wide, outer) contour of the ground truth mask is shown in white.
  - (c) heatmaps are colored according to the color scheme described below;

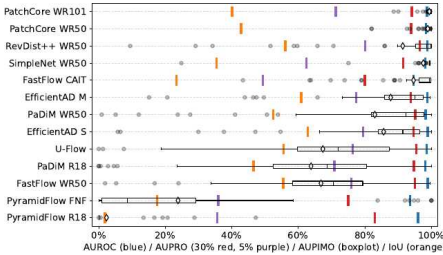
**Heatmaps coloring scheme** The input images are superimposed by their respective anomaly score map **a**. Coloring rules are linked to the thresholds in AUPIMO’s integration bounds: transparent is for scores below the lowest threshold, blues are for scores between the lowest and the highest thresholds, and reds are for scores above the highest threshold. Darker blue/red tones mean higher scores. The coloring strategy links the heatmaps to the validation-evaluation framework employed in AUPIMO. Transparent heatmap zones are never accounted in the metric because the validation requirement is not respected. Blue zones visually express the average recall measured by the integration in AUPIMO. Additionally, red zones show the model’s local behavior (per-image normalization) within the *valid* score range (*i.e.* scores above the threshold given by the Shared FPR lower bound).

	PF R18	PF FNF	FF WR50	PDM R18	UF	Eff S	PDM WR50	Eff M	FF CAIT	SN WR50	RD++ WR50	PC WR50	PC WR101
AUROC	98.0% (11)	93.0% (13)	98.9% (1)	98.2% (10)	98.7% (6)	98.9% (2)	98.3% (8)	98.8% (4)	94.7% (12)	98.2% (9)	98.8% (3)	98.4% (7)	98.7% (5)
AUPRO	83.0% (11)	75.0% (13)	95.3% (1)	94.7% (10)	95.4% (12)	94.6% (6)	95.1% (8)	93.8% (9)	86.0% (12)	91.5% (10)	96.5% (1)	93.4% (8)	94.1% (7)
AUPRO 5%	95.8% (11)	85.9% (13)	95.8% (1)	95.8% (10)	95.8% (12)	95.8% (6)	95.8% (8)	95.8% (9)	95.8% (10)	95.8% (10)	95.8% (1)	95.8% (8)	95.8% (7)
Avg. AUPIMO	2.3% (13)	23.8% (12)	66.8% (10)	63.8% (11)	67.4% (9)	85.7% (7)	83.0% (8)	87.8% (6)	94.7% (4)	97.6% (3)	91.4% (5)	98.9% (2)	99.4% (1)
Std. AUPIMO	7.9%	11.3%	13.8%	18.6%	25.3%	20.0%	24.3%	18.2%	10.8%	9.8%	18.3%	1.4%	1.9%
P33 AUPIMO	0.0% (13)	2.5% (12)	61.3% (10)	58.8% (11)	62.9% (9)	86.9% (8)	87.4% (7)	90.0% (6)	98.7% (4)	99.5% (3)	97.7% (5)	100.0% (2)	100.0% (1)
Avg. Rank	12.8	11.4	9.9	9.8	9.4	7.1	6.7	6.7	4.4	4.3	4.3	2.0	1.8
Avg. Iou	13.0% (13)	17.3% (12)	55.5% (5)	46.4% (7)	55.5% (4)	82.8% (1)	82.9% (1)	60.8% (2)	23.4% (11)	35.4% (10)	56.1% (1)	42.8% (18)	40.1% (19)
PC WR101 (1.8)	100%	100%	100%	100%	100%	100%	100%	100%	100%	100%	100%	100%	100%
PC WR50 (2.0)	100%	100%	100%	100%	100%	100%	100%	100%	100%	100%	100%	100%	100%
RD++ WR50 (4.3)	100%	100%	100%	100%	100%	100%	100%	100%	100%	100%	100%	100%	100%
SN WR50 (4.3)	100%	100%	100%	100%	100%	100%	100%	100%	100%	100%	100%	100%	100%
FF CAIT (4.4)	100%	100%	100%	100%	100%	100%	100%	100%	100%	100%	100%	100%	100%
Eff M (6.7)	100%	100%	100%	100%	100%	100%	100%	100%	100%	100%	100%	100%	100%
PDM WR50 (6.9)	100%	100%	100%	100%	100%	100%	100%	100%	100%	100%	100%	100%	100%
Eff S (7.1)	100%	100%	100%	100%	100%	100%	100%	100%	100%	100%	100%	100%	100%
PDM R18 (9.9)	100%	100%	100%	100%	100%	100%	100%	100%	100%	100%	100%	100%	100%
UF (9.4)	100%	100%	100%	100%	100%	100%	100%	100%	100%	100%	100%	100%	100%
FF WR50 (18.9)	100%	100%	100%	100%	100%	100%	100%	100%	100%	100%	100%	100%	100%
PF FNF (11.4)	100%	100%	100%	100%	100%	100%	100%	100%	100%	100%	100%	100%	100%

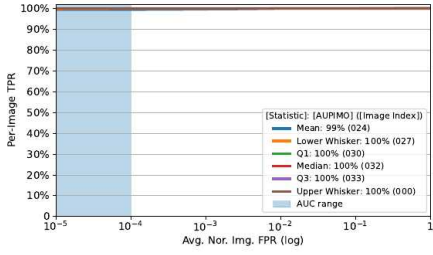
(a) Statistics and pairwise statistical tests.



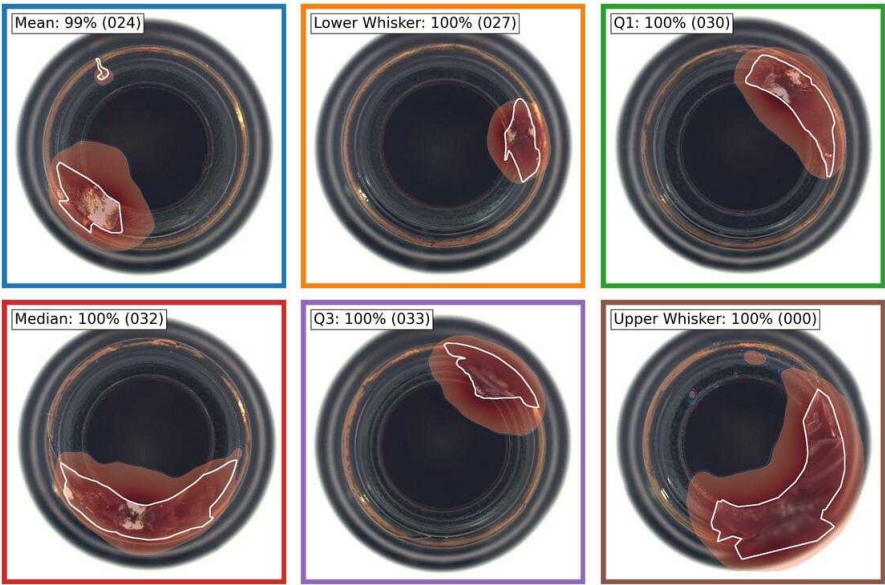
(b) Average rank diagram.



(c) Score distributions.



(d) PIMO curves.

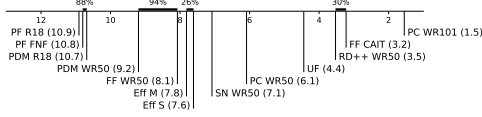


(e) Heatmaps. Images selected according to AUPIMO's statistics. Statistic and image index annotated on upper left corner.

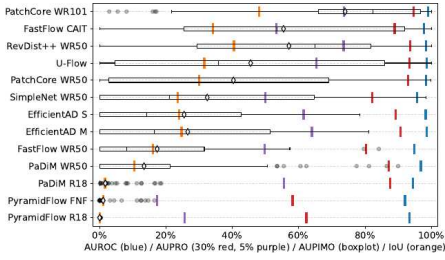
Figure 22: Benchmark on MVTec AD / Bottle. PIMO curves and heatmaps are from PatchCore WR101. 083 images (020 normal, 063 anomalous).

	PF R18	PF FNF	PDM R18	PDM WR50	FF WR50	Eff M	Eff S	SN WR50	PC WR50	UF	RD++ WR50	FF CAIT	PC WR101
AUROC	93.3% (12)	92.1% (13)	94.5% (11)	95.8% (8)	94.9% (10)	98.6% (3)	98.3% (6)	95.7% (9)	98.3% (3)	98.8% (2)	98.4% (5)	97.8% (7)	98.9% (1)
AUPRO	82.3% (12)	86.2% (11)	87.5% (10)	87.4% (9)	86.5% (11)	90.7% (5)	89.2% (10)	89.2% (10)	92.4% (4)	92.4% (3)	93.4% (2)	88.9% (17)	94.7% (12)
AUPRO 5%	25.7% (10)	3.4% (11)	4.3%	4.3%	4.3%	61.9% (4)	61.5% (1)	61.5% (1)	77.6% (2)	77.6% (2)	77.6% (2)	51.3% (11)	77.7% (11)
Avg. AUPIMO	0.6% (13)	1.1% (12)	1.7% (11)	13.4% (10)	17.4% (9)	26.6% (7)	25.5% (8)	32.5% (6)	40.3% (5)	45.5% (4)	57.1% (2)	55.4% (3)	74.0% (1)
Std. AUPIMO	0.1%	3.4%	4.3%	21.1%	21.1%	18.8%	26.8%	33.3%	14.3%	18.6%	32.1%	34.3%	28.1%
P33 AUPIMO	0.0% (13)	0.0% (12)	0.0% (11)	0.0% (10)	0.5% (8)	0.0% (9)	3.9% (6)	0.7% (7)	12.1% (4)	11.4% (5)	42.6% (2)	42.6% (2)	73.7% (1)
Avg. Rank	10.9	10.8	10.7	10.2	8.1	7.8	7.8	7.1	6.1	4.4	3.5	3.2	1.5
Avg. iou	0.9% (13)	1.1% (12)	1.6% (11)	10.5% (10)	18.1% (9)	24.7% (6)	23.9% (7)	23.9% (7)	30.9% (5)	31.4% (4)	40.5% (2)	37.2% (3)	43.1% (1)
PC WR101 (1.5)	100%	100%	100%	100%	100%	100%	100%	100%	100%	100%	100%	100%	100%
FF CAIT (3.2)	100%	100%	100%	100%	100%	100%	100%	100%	100%	100%	100%	100%	100%
RD++ WR50 (3.5)	100%	100%	100%	100%	100%	100%	100%	100%	100%	100%	100%	100%	100%
UF (4.4)	100%	100%	100%	100%	100%	100%	100%	100%	100%	100%	100%	100%	100%
PC WR50 (6.1)	100%	100%	100%	100%	100%	100%	100%	100%	100%	100%	100%	100%	100%
SN WR50 (7.1)	100%	100%	100%	100%	100%	100%	100%	100%	100%	100%	100%	100%	100%
Eff S (7.6)	100%	100%	100%	100%	100%	100%	100%	100%	100%	100%	100%	100%	100%
Eff M (7.8)	100%	100%	100%	100%	100%	100%	100%	100%	100%	100%	100%	100%	100%
FF WR50 (8.1)	100%	100%	100%	100%	100%	100%	100%	100%	100%	100%	100%	100%	100%
PDM WR50 (9.2)	100%	100%	100%	100%	100%	100%	100%	100%	100%	100%	100%	100%	100%
PDM R18 (10.7)	100%	100%	100%	100%	100%	100%	100%	100%	100%	100%	100%	100%	100%
PF FNF (10.8)	100%	100%	100%	100%	100%	100%	100%	100%	100%	100%	100%	100%	100%

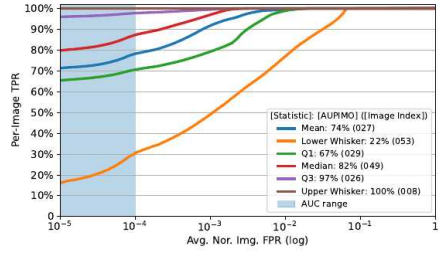
(a) Statistics and pairwise statistical tests.



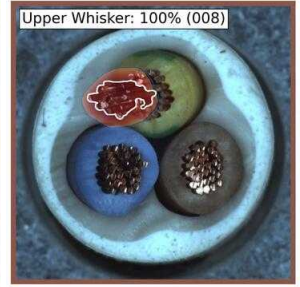
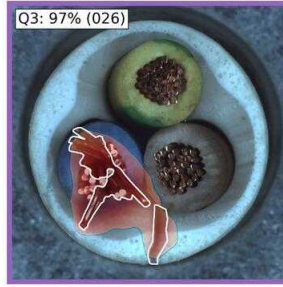
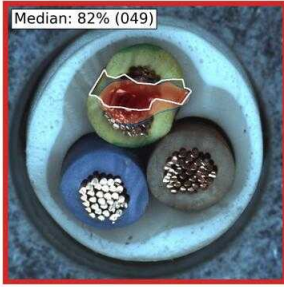
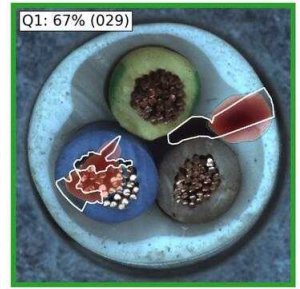
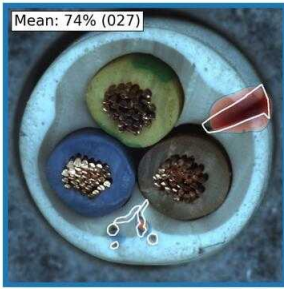
(b) Average rank diagram.



(c) Score distributions.



(d) PIMO curves.



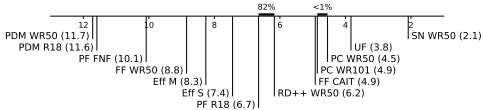
(e) Heatmaps. Images selected according to AUPIMO's statistics. Statistic and image index annotated on upper left corner. Image index annotated on upper left corner.

Figure 23: Benchmark on MVTec AD / Cable. PIMO curves and heatmaps are from PatchCore WR101. 150 images (058 normal, 092 anomalous).

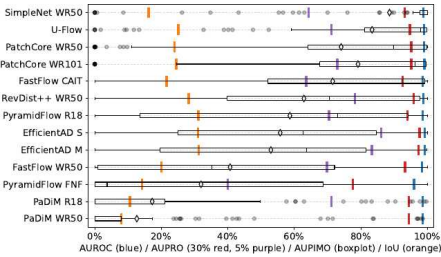


	PDM WR50	PDM R18	PF FNF	FF WR50	EFF M	EFF S	PF R18	RD++ WR50	FF CAIT	PC WR101	PC WR50	UF	SN WR50
AUROC	98.8% (9)	98.8% (8)	96.9% (13)	98.4% (12)	99.2% (2)	99.2% (3)	98.6% (10)	98.8% (7)	98.5% (11)	99.1% (3)	99.0% (5)	99.0% (8)	98.9% (6)
AUPRO	94.4% (8)	94.4% (7)	97.6% (13)	93.3% (10)	97.7% (2)	97.7% (3)	94.1% (9)	95.9% (3)	92.5% (12)	95.2% (4)	95.2% (5)	94.4% (6)	93.2% (11)
AUPRO 5%	71.3% (13)	71.3% (13)	89.9% (13)	89.8% (8)	89.1% (13)	89.1% (13)	70.4% (13)	72.3% (13)	63.3% (10)	72.9% (13)	72.9% (13)	72.9% (13)	68.1% (10)
Avg. AUPIMO	12.6% (13)	17.3% (12)	31.9% (11)	40.7% (10)	53.0% (9)	55.8% (8)	58.7% (7)	62.9% (6)	71.3% (5)	79.1% (3)	74.1% (4)	83.4% (2)	88.8% (1)
Std. AUPIMO	26.1%	28.1%	37.3%	36.1%	34.3%	32.9%	30.8%	33.0%	34.1%	31.3%	34.4%	28.1%	28.7%
P33 AUPIMO	0.0% (13)	0.0% (12)	0.0% (11)	7.4% (10)	38.0% (9)	38.9% (8)	40.5% (7)	53.2% (6)	64.7% (5)	81.3% (3)	80.6% (4)	90.8% (2)	99.3% (1)
Avg. Rank	11.7	11.6	10.1	8.8	8.3	7.4	6.7	6.2	4.9	4.9	4.3	2.1	2.1
Avg. Iou	8.0% (13)	10.4% (12)	14.2% (11)	20.1% (10)	31.3% (9)	31.0% (8)	31.5% (7)	28.2% (6)	21.6% (5)	22.5% (4)	24.9% (3)	25.1% (2)	16.2% (1)
SN WR50 (2.1)	100%	100%	100%	100%	100%	100%	100%	100%	100%	100%	100%	100%	100%
UF (3.8)	100%	100%	100%	100%	100%	100%	100%	100%	100%	100%	100%	100%	100%
PC WR101 (4.5)	100%	100%	100%	100%	100%	100%	100%	100%	100%	100%	100%	100%	100%
PC WR50 (4.9)	100%	100%	100%	100%	100%	100%	100%	100%	100%	100%	100%	100%	100%
FF CAIT (4.9)	100%	100%	100%	100%	100%	100%	100%	100%	100%	100%	100%	100%	100%
RD++ WR50 (6.2)	100%	100%	100%	100%	100%	100%	100%	100%	100%	100%	100%	100%	100%
PF R18 (6.7)	100%	100%	100%	100%	100%	100%	100%	100%	100%	100%	100%	100%	100%
EFF S (7.4)	100%	100%	100%	100%	100%	100%	100%	100%	100%	100%	100%	100%	100%
EFF M (8.3)	100%	100%	100%	100%	100%	100%	100%	100%	100%	100%	100%	100%	100%
PF FNF (10.1)	100%	100%	100%	100%	100%	100%	100%	100%	100%	100%	100%	100%	100%
PDM R18 (11.6)	98%	100%	100%	100%	100%	100%	100%	100%	100%	100%	100%	100%	100%

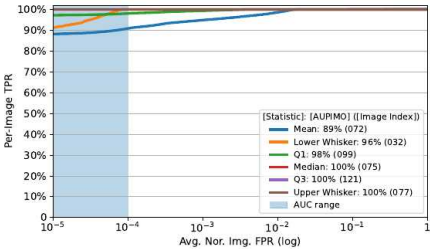
(a) Statistics and pairwise statistical tests.



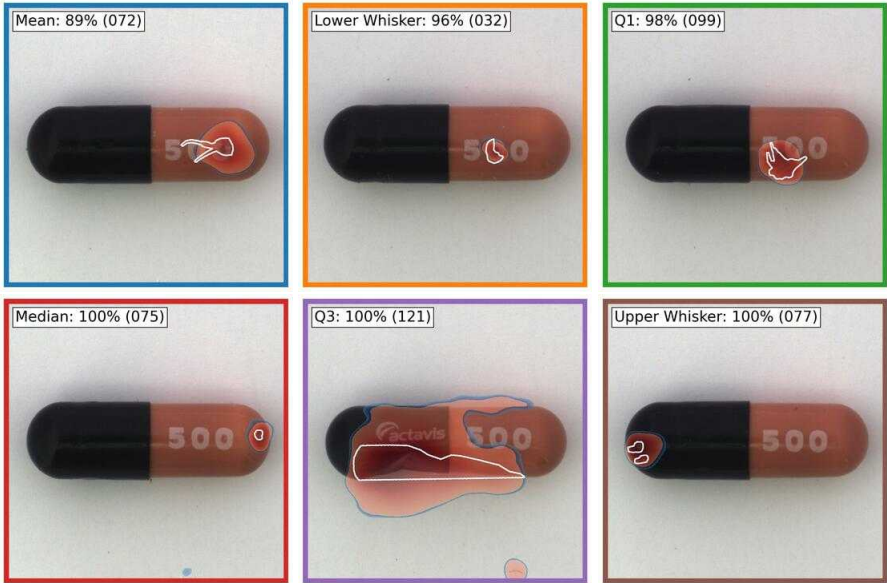
(b) Average rank diagram.



(c) Score distributions.



(d) PIMO curves.

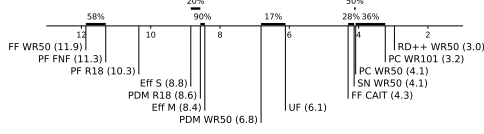


(e) Heatmaps. Images selected according to AUPIMO's statistics. Statistic and image index annotated on upper left corner.

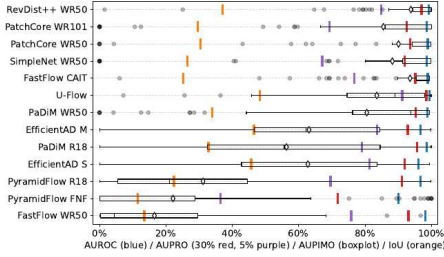
Figure 24: Benchmark on MVTEC AD / Capsule. PIMO curves and heatmaps are from SimpleNet WR50. 132 images (023 normal, 109 anomalous).

	FF WR50	PF FNF	PF R18	Eff S	PDM R18	Eff M	PDM WR50	UF	FF CAIT	SN WR50	PC WR50	PS WR101	RD++ WR50
AUDROC	98.1% (19)	90.1% (13)	98.8% (19)	98.1% (12)	98.6% (7)	96.7% (13)	98.8% (5)	99.4% (1)	98.9% (8)	98.5% (8)	98.9% (3)	98.6% (6)	99.2% (2)
AUPRO	93.1% (17)	71.8% (13)	91.2% (12)	91.9% (10)	95.7% (12)	92.9% (8)	95.3% (4)	98.5% (1)	95.1% (9)	91.4% (11)	93.6% (6)	92.5% (9)	97.0% (2)
AUPRO 5%	79.8% (17)	36.4% (13)	89.5% (12)	81.3% (13)	93.6% (13)	81.6% (8)	91.3% (1)	97.5% (1)	76.3% (10)	57.5% (10)	87.5% (6)	85.2% (9)	94.9% (2)
Avg. AUPIMO	16.3% (13)	22.1% (12)	31.2% (11)	62.8% (9)	56.3% (10)	63.1% (8)	80.5% (7)	83.6% (6)	93.6% (2)	88.2% (4)	90.1% (3)	85.5% (5)	93.8% (1)
Std. AUPIMO	12.7%	15.1%	32.6%	29.1%	33.1%	25.1%	28.3%	18.4%	13.9%	26.1%	21.9%	28.4%	14.4%
P33 AUPIMO	1.9% (12)	0.0% (13)	9.1% (11)	48.2% (9)	43.9% (10)	52.3% (8)	83.8% (6)	82.7% (7)	98.6% (1)	96.2% (3)	97.2% (2)	95.0% (5)	96.1% (4)
Avg. Rank	11.9	11.9	10.3	6.8	8.6	8.4	6.8	6.1	4.3	4.1	4.1	3.2	3.0
Avg. iou	13.1% (12)	21.6% (12)	22.2% (11)	45.7% (9)	32.8% (6)	46.3% (2)	33.9% (3)	50.7% (1)	25.7% (11)	26.9% (9)	30.4% (7)	23.6% (8)	37.0% (1)
RD++ WR50 (3.0)	100%	100%	100%	100%	100%	100%	100%	100%	100%	82%	89%	86%	100%
PC WR101 (3.1)	100%	100%	100%	100%	100%	100%	100%	100%	100%	4%	18%	100%	
PC WR50 (4.1)	100%	100%	100%	100%	100%	100%	100%	100%	100%	93%	91%	37%	
SN WR50 (4.1)	100%	100%	100%	100%	100%	100%	100%	100%	100%	28%			
FF CAIT (4.3)	100%	100%	100%	100%	100%	100%	100%	100%	100%				
UF (6.1)	100%	100%	100%	100%	100%	100%	100%	100%					
PDM WR50 (6.8)	100%	100%	100%	100%	100%	100%							
Eff M (8.4)	100%	100%	100%	100%	100%								
PDM R18 (8.6)	100%	100%	100%	100%									
Eff S (8.8)	100%	100%	100%										
PF R18 (10.3)	100%	100%											
PF FNF (11.3)	59%												

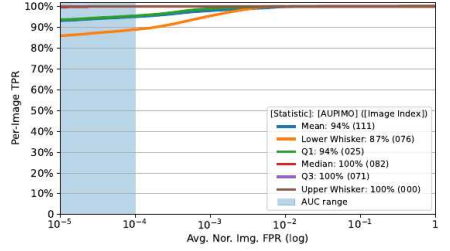
(a) Statistics and pairwise statistical tests.



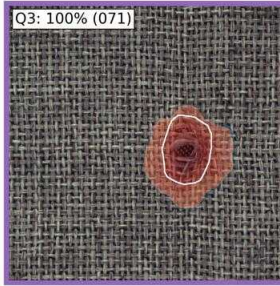
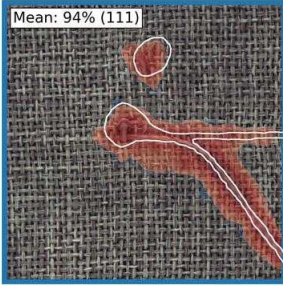
(b) Average rank diagram.



(c) Score distributions.



(d) PIMO curves.

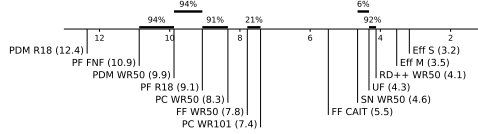


(e) Heatmaps. Images selected according to AUPIMO's statistics. Statistic and image index annotated on upper left corner.

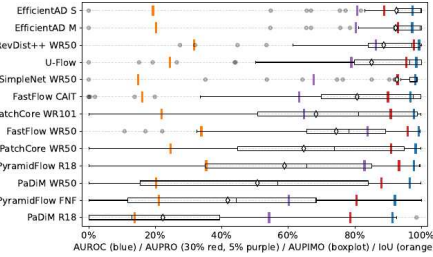
Figure 25: Benchmark on MVTec AD / Carpet. PIMO curves and heatmaps are from RevDist++ WR50. 117 images (028 normal, 089 anomalous).

	PDM R18	PF FNF	PDM WR50	PF R18	PC WR50	FF WR50	PC WR101	FF CAIT	SN WR50	UF	RD++ WR50	Eff M	Eff S
AUROC	91.4% (13)	92.0% (12)	96.5% (11)	97.7% (7)	98.3% (4)	99.2% (2)	97.8% (6)	96.3% (10)	98.2% (5)	98.5% (3)	99.3% (1)	97.2% (9)	97.8% (8)
AUPRO	78.7% (13)	80.4% (12)	87.9% (11)	89.3% (4)	90.9% (7)	95.9% (2)	90.0% (8)	90.0% (9)	92.9% (6)	95.4% (3)	97.7% (1)	93.0% (5)	88.4% (10)
AUPRO 5%	51.5% (11)	50.5% (10)	57.9% (11)	58.3% (8)	59.9% (12)	64.9% (4)	64.9% (10)	63.3% (9)	67.4% (6)	75.4% (3)	80.3% (1)	69.4% (4)	60.4% (11)
Avg. AUPIMO	22.3% (13)	41.8% (12)	50.7% (11)	58.9% (10)	64.6% (9)	74.4% (7)	68.3% (8)	80.7% (6)	92.7% (1)	85.0% (5)	88.7% (4)	92.3% (3)	94.5% (2)
Std. AUPIMO	28.0%	31.4%	33.6%	36.1%	33.3%	20.4%	18.3%	30.2%	17.0%	23.9%	17.1%	15.8%	13.6%
P33 AUPIMO	0.0% (13)	20.3% (12)	23.6% (11)	41.5% (10)	49.2% (9)	69.0% (7)	62.5% (8)	83.6% (6)	98.6% (1)	86.9% (5)	91.5% (4)	94.4% (3)	94.5% (2)
Avg. Rank	12.4	10.9	9.9	9.1	8.3	7.8	7.4	5.5	4.6	4.2	4.1	3.5	3.2
Avg. Iou	31.8% (13)	21.7% (7)	20.2% (9)	35.3% (12)	25.3% (4)	23.9% (10)	21.9% (6)	16.1% (11)	14.9% (12)	22.4% (3)	21.7% (1)	20.3% (8)	19.3% (10)
Eff S (1.2)	100%	100%	100%	100%	100%	100%	100%	100%	100%	74%	99%	97%	100%
Eff M (1.5)	100%	100%	100%	100%	100%	100%	100%	100%	100%	71%	98%	99%	100%
RD++ WR50 (4.1)	100%	100%	100%	100%	100%	100%	100%	100%	<1%	92%	90%	100%	
UF (4.3)	100%	100%	100%	100%	100%	100%	100%	100%	88%	6%			
SN WR50 (4.6)	100%	100%	100%	100%	100%	100%	100%	100%	100%	100%	100%	100%	100%
FF CAIT (5.3)	100%	100%	100%	100%	100%	100%	100%	100%	100%	100%	100%	100%	100%
PC WR101 (7.4)	100%	100%	100%	100%	100%	100%	100%	100%	100%	100%	100%	100%	100%
FF WR50 (1.8)	100%	100%	100%	100%	100%	100%	100%	100%	100%	100%	100%	100%	100%
PC WR50 (8.3)	100%	100%	100%	100%	100%	100%	100%	100%	100%	100%	100%	100%	100%
PDM WR50 (18.3)	100%	100%	100%	100%	100%	100%	100%	100%	100%	100%	100%	100%	100%
PDM WR50 (10.9)	100%	100%	100%	100%	100%	100%	100%	100%	100%	100%	100%	100%	100%

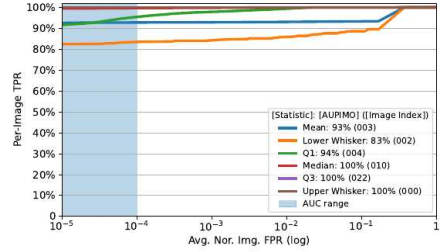
(a) Statistics and pairwise statistical tests.



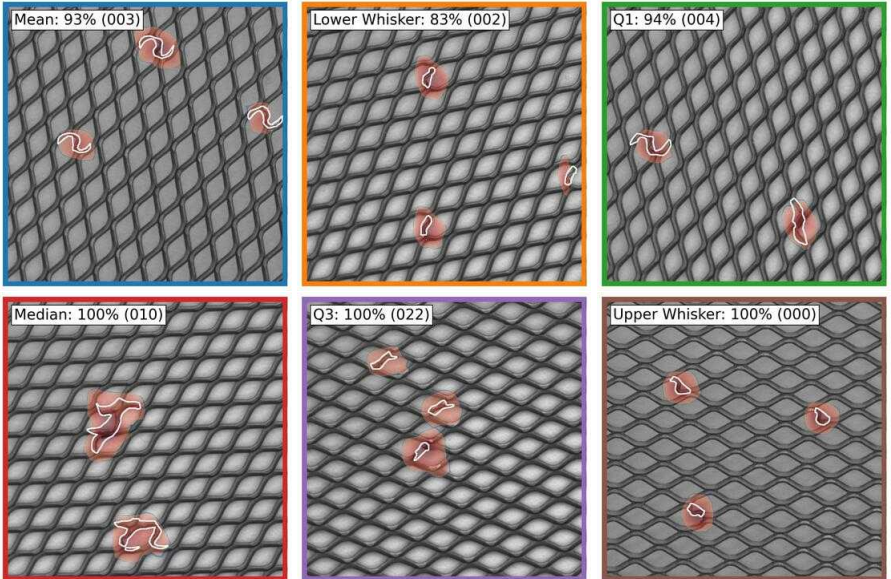
(b) Average rank diagram.



(c) Score distributions.



(d) PIMO curves.



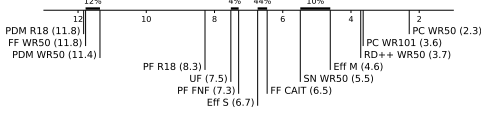
(e) Heatmaps. Images selected according to AUPIMO's statistics. Statistic and image index annotated on upper left corner.

Figure 26: Benchmark on MVTec AD / Grid. PIMO curves and heatmaps are from EfficientAD S. 078 images (021 normal, 057 anomalous).

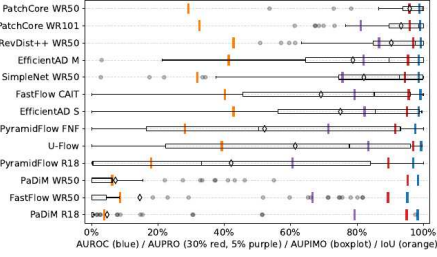


	PDM R18	FF WR50	PDM WR50	PF R18	UF	PF FNF	EFF S	FF CAIT	SN WR50	EFF M	RD++ WR50	PC WR101	PC WR50
AUROC	98.3% (10)	95.1% (13)	98.3% (9)	97.0% (12)	99.3% (1)	97.6% (13)	98.6% (8)	99.1% (3)	98.0% (7)	98.8% (6)	99.2% (2)	99.0% (4)	98.8% (5)
AUPRO	94.9% (9)	89.3% (12)	95.3% (12)	89.5% (12)	97.0% (12)	91.6% (13)	95.3% (8)	95.6% (10)	94.4% (10)	95.4% (8)	96.9% (2)	96.0% (3)	95.8% (4)
AUPRO 5%	76.3% (8)	66.4% (10)	76.3% (12)	65.5% (11)	83.4% (1)	71.4% (9)	82.3% (1)	75.8% (12)	75.8% (12)	81.3% (1)	81.3% (1)	81.3% (1)	81.3% (1)
Avg. AUPIMO	4.7% (13)	14.5% (11)	7.2% (12)	42.1% (10)	61.4% (8)	52.1% (9)	75.0% (6)	69.1% (7)	82.1% (4)	78.8% (5)	90.3% (3)	93.3% (2)	95.9% (1)
Std. AUPIMO	15.0%	28.0%	11.3%	18.9%	17.7%	17.3%	27.1%	34.1%	21.1%	25.0%	12.9%	9.7%	7.8%
P33 AUPIMO	0.0% (13)	0.0% (12)	0.0% (11)	2.3% (10)	45.6% (8)	29.8% (9)	68.8% (6)	67.0% (7)	80.9% (4)	73.1% (5)	87.5% (3)	91.3% (2)	95.6% (1)
Avg. Rank	11.8	11.8	11.4	7.5	7.5	7.3	6.7	6.5	5.5	4.6	3.7	3.6	2.3
Asp. Asp.	3.4% (13)	8.4% (11)	5.2% (12)	6.3	17.7% (10)	39.2% (5)	28.1% (9)	32.8% (11)	30.2% (12)	31.9% (9)	42.4% (2)	32.5% (3)	23.1% (1)
PC WR50 (2.3)	100%	100%	100%	100%	100%	100%	100%	100%	100%	100%	100%	100%	100%
PC WR101 (3.6)	100%	100%	100%	100%	100%	100%	100%	100%	100%	100%	100%	100%	100%
RD++ WR50 (13.7)	100%	100%	100%	100%	100%	100%	100%	100%	100%	100%	99%	100%	100%
EFF M (4.6)	100%	100%	100%	100%	100%	100%	100%	100%	100%	100%	100%	100%	100%
SN WR50 (5.5)	100%	100%	100%	100%	100%	100%	99%	100%	100%	100%	100%	100%	100%
FF CAIT (6.5)	100%	100%	100%	100%	100%	100%	45%	100%	100%	100%	100%	100%	100%
EFF S (6.7)	100%	100%	100%	100%	100%	100%	100%	100%	100%	100%	100%	100%	100%
PF FNF (7.3)	100%	100%	100%	100%	100%	100%	100%	100%	100%	100%	100%	100%	100%
UF (7.5)	100%	100%	100%	100%	100%	100%	100%	100%	100%	100%	100%	100%	100%
PF R18 (8.3)	100%	100%	100%	100%	100%	100%	100%	100%	100%	100%	100%	100%	100%
PDM WR50 (11.4)	99%	13%											
FF WR50 (11.8)	99%												

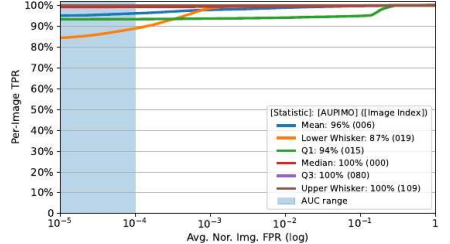
(a) Statistics and pairwise statistical tests.



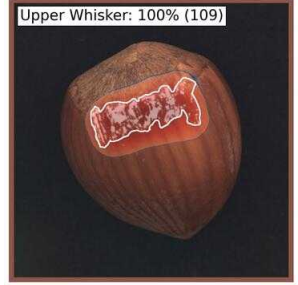
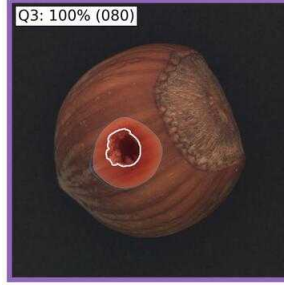
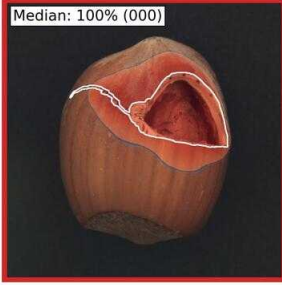
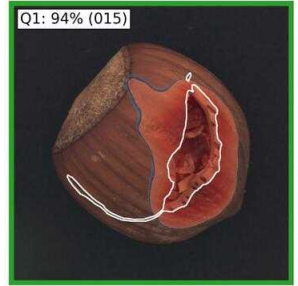
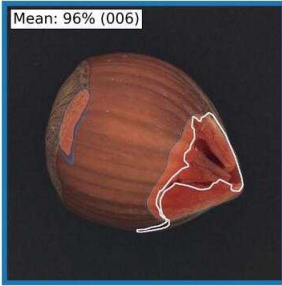
(b) Average rank diagram.



(c) Score distributions.



(d) PIMO curves.

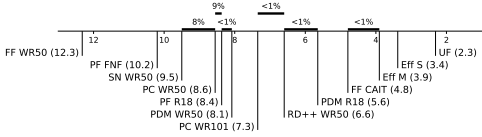


(e) Heatmaps. Images selected according to AUPIMO's statistics. Statistic and image index annotated on upper left corner.

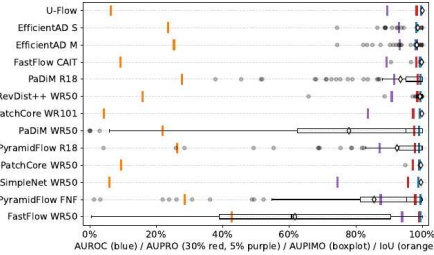
Figure 27: Benchmark on MVTec AD / Hazelnut. PIMO curves and heatmaps are from PatchCore WR50. 110 images (040 normal, 070 anomalous).

	FF WR50	PF FNF	SN WR50	PC WR50	PF R18	PDM WR50	PC WR101	RD++ WR50	PDM R18	FF CAIT	Eff M	Eff S	UF
AUROC	99.3% (2)	99.4% (5)	98.8% (11)	99.1% (8)	99.0% (9)	99.0% (10)	99.2% (7)	99.4% (4)	99.4% (13)	99.4% (6)	98.1% (18)	98.2% (12)	99.8% (1)
AUPRO	99.0% (1)	97.9% (8)	95.7% (13)	97.2% (12)	97.7% (9)	97.5% (10)	97.3% (11)	98.5% (3)	98.7% (17)	98.2% (17)	98.3% (14)	98.2% (10)	98.2% (5)
AUPRO 5%	99.0% (1)	97.9% (8)	95.7% (13)	97.2% (12)	97.7% (9)	97.5% (10)	97.3% (11)	98.5% (3)	98.7% (17)	98.2% (17)	98.3% (14)	98.2% (10)	98.2% (5)
Avg. AUPIMO	61.7% (13)	85.5% (11)	99.6% (4)	99.8% (5)	92.4% (10)	77.9% (12)	99.9% (2)	99.3% (6)	93.4% (9)	99.8% (3)	98.3% (8)	98.7% (7)	100.0% (1)
Std. AUPIMO	29.7%	21.0%	0.0%	0.5%	16.8%	30.3%	0.0%	1.7%	13.1%	1.0%	4.4%	4.0%	0.0%
P33 AUPIMO	41.9% (13)	89.8% (11)	99.6% (8)	99.6% (7)	98.1% (10)	73.3% (12)	99.9% (6)	99.9% (5)	98.4% (9)	99.9% (4)	100.0% (3)	100.0% (2)	100.0% (1)
Avg. Rank	12.3	10.2	9.5	8.4	8.4	8.1	7.3	6.6	5.6	4.8	3.9	3.4	2.3
Avg. Iou	52.2% (11)	28.7% (12)	5.9% (12)	9.4% (9)	25.3% (4)	21.0% (12)	4.2% (11)	15.9% (8)	27.8% (13)	9.2% (10)	23.3% (16)	6.3% (11)	
UF (2.3)	100%	100%	100%	100%	100%	100%	100%	100%	100%	100%	95%	100%	100%
FF CAIT (4.8)	100%	100%	100%	100%	100%	100%	100%	100%	100%	100%	100%	100%	100%
Eff M (3.9)	100%	100%	100%	100%	100%	100%	100%	100%	100%	100%	100%	100%	100%
Eff S (3.4)	100%	100%	100%	100%	100%	100%	100%	100%	100%	100%	100%	100%	100%
PDM R18 (5.6)	100%	100%	100%	100%	100%	100%	100%	100%	100%	100%	100%	100%	100%
RD++ WR50 (6.6)	100%	100%	100%	100%	100%	100%	100%	100%	100%	100%	100%	100%	100%
PC WR101 (7.3)	100%	100%	100%	100%	100%	100%	100%	100%	100%	100%	100%	100%	100%
PDM WR50 (8.1)	100%	100%	100%	100%	100%	100%	100%	100%	100%	100%	100%	100%	100%
PF R18 (8.4)	100%	100%	100%	100%	100%	100%	100%	100%	100%	100%	100%	100%	100%
PC WR50 (9.5)	100%	100%	100%	100%	100%	100%	100%	100%	100%	100%	100%	100%	100%
SN WR50 (10.2)	100%	100%	100%	100%	100%	100%	100%	100%	100%	100%	100%	100%	100%
FF FNF (10.2)	100%	100%	100%	100%	100%	100%	100%	100%	100%	100%	100%	100%	100%

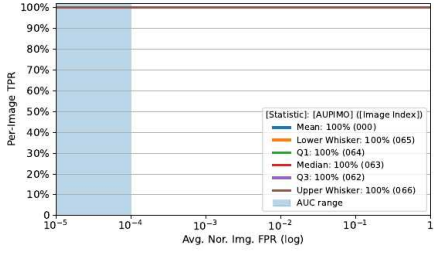
(a) Statistics and pairwise statistical tests.



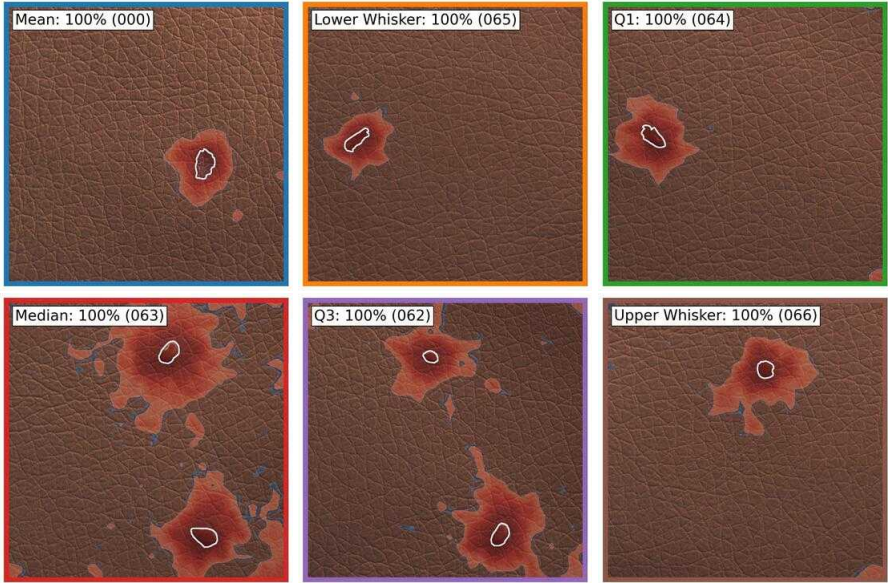
(b) Average rank diagram.



(c) Score distributions.



(d) PIMO curves.

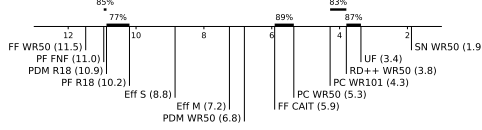


(e) Heatmaps. Images selected according to AUPIMO's statistics. Statistic and image index annotated on upper left corner.

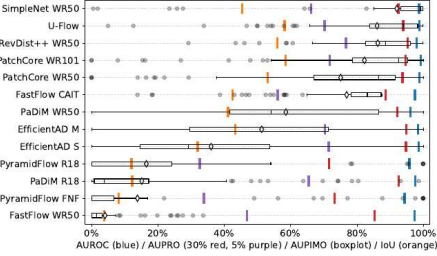
Figure 28: Benchmark on MVTec AD / Leather. PIMO curves and heatmaps are from U-Flow. 124 images (032 normal, 092 anomalous).

	FF WR50	PF FNF	PDM R18	PF R18	Eff S	Eff M	PDM WR50	FF CAIT	PC WR50	PC WR101	RD++ WR50	UF	SN WR50
AUDROC	97.4% (10)	94.3% (13)	97.6% (8)	95.8% (12)	98.5% (5)	98.4% (6)	96.1% (11)	97.4% (9)	98.9% (2)	99.2% (1)	98.0% (7)	98.8% (3)	98.7% (4)
AUPRO	85.2% (11)	73.2% (12)	82.6% (12)	71.6% (13)	94.7% (3)	94.8% (2)	92.1% (9)	88.6% (10)	93.7% (6)	94.7% (4)	95.2% (1)	93.9% (1)	92.5% (8)
AUPRO 5%	46.8% (9)	33.9% (10)	45.5% (11)	31.5% (11)	71.5% (4)	70.4% (4)	56.1% (10)	56.1% (10)	61.3% (7)	61.3% (7)	61.3% (7)	61.3% (7)	56.3% (10)
Avg. AUPIMO	4.1% (13)	13.8% (12)	15.1% (11)	16.5% (10)	36.0% (9)	51.3% (8)	58.6% (7)	76.9% (5)	75.1% (6)	82.2% (4)	86.3% (2)	86.0% (3)	92.0% (1)
Std. AUPIMO	7.5%	28.3%	21.3%	21.9%	28.6%	28.2%	28.3%	16.3%	25.1%	22.9%	11.5%	19.1%	18.4%
P33 AUPIMO	0.1% (13)	0.0% (13)	2.1% (10)	0.0% (12)	16.8% (9)	36.9% (8)	44.8% (7)	81.0% (5)	74.5% (6)	84.1% (4)	85.8% (3)	89.5% (2)	97.5% (1)
Avg. Rank	11.3	11.0	10.9	10.2	8.8	7.2	6.8	5.9	5.3	4.3	3.8	3.4	1.9
Avg. iou	3.2% (13)	8.1% (12)	12.2% (10)	12.2% (11)	32.0% (9)	43.4% (8)	51.1% (7)	82.2% (5)	81.1% (6)	88.1% (4)	91.1% (3)	91.1% (2)	95.2% (1)
SN WR50 (1.9)	100%	100%	100%	100%	100%	100%	100%	100%	100%	100%	100%	100%	100%
UF (1.4)	100%	100%	100%	100%	100%	100%	100%	100%	100%	100%	100%	100%	100%
RD++ WR50 (1.8)	100%	100%	100%	100%	100%	100%	100%	100%	100%	100%	84%	87%	100%
PC WR101 (4.3)	100%	100%	100%	100%	100%	100%	100%	100%	100%	100%	100%	100%	100%
PC WR50 (5.3)	100%	100%	100%	100%	100%	100%	100%	100%	100%	100%	100%	100%	100%
FF CAIT (5.9)	100%	100%	100%	100%	100%	100%	100%	100%	89%	100%	100%	100%	100%
PDM WR50 (6.8)	100%	100%	100%	100%	100%	100%	100%	100%	100%	100%	100%	100%	100%
PF R18 (10.9)	100%	100%	100%	100%	100%	100%	100%	100%	100%	100%	100%	100%	100%
PF FNF (11.0)	100%	100%	100%	100%	100%	100%	100%	100%	100%	100%	100%	100%	100%

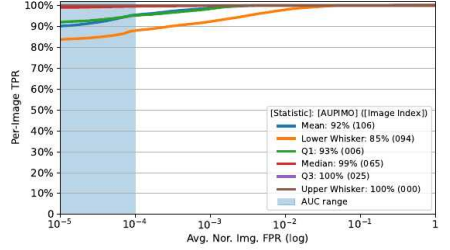
(a) Statistics and pairwise statistical tests.



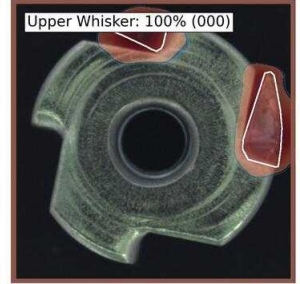
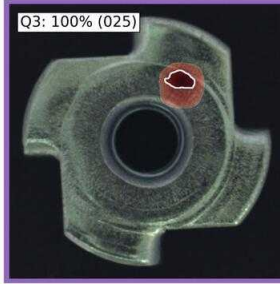
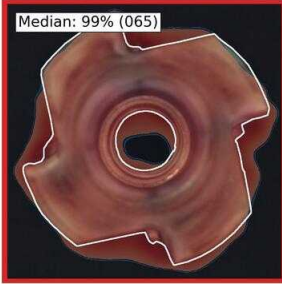
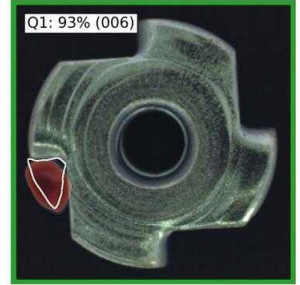
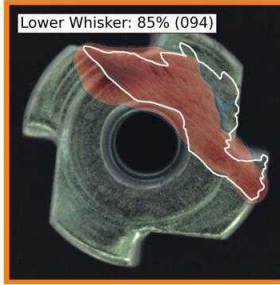
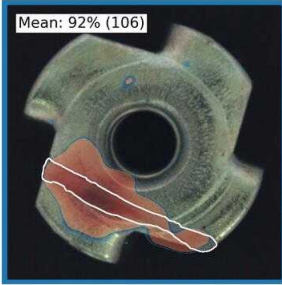
(b) Average rank diagram.



(c) Score distributions.



(d) PIMO curves.



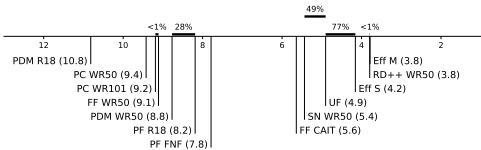
(e) Heatmaps. Images selected according to AUPIMO's statistics. Statistic and image index annotated on upper left corner.

Figure 29: Benchmark on MVTec AD / Metal Nut. PIMO curves and heatmaps are from SimpleNet WR50. 115 images (022 normal, 093 anomalous).

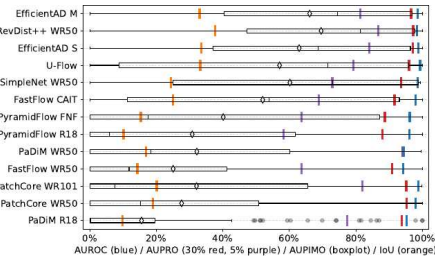


	PDM R18	PC WR50	PC WR101	FF WR50	PDM WR50	PF R18	PF FNF	FF CAIT	SN WR50	UF	Eff S	RD++ WR50	Eff M
AUROC	95.3% (11)	98.0% (7)	98.0% (8)	94.2% (13)	94.3% (12)	96.2% (10)	96.2% (9)	98.0% (8)	99.3% (5)	99.4% (1)	98.8% (2)	98.4% (6)	98.7% (4)
AUPRO	93.3% (8)	95.5% (8)	95.2% (8)	90.0% (11)	94.1% (17)	88.0% (13)	88.7% (12)	91.6% (10)	93.6% (9)	96.0% (4)	97.1% (2)	97.2% (3)	96.7% (3)
AUPRO 5%	97.4% (9)	91.0% (1)	91.3% (1)	83.6% (10)	93.3% (11)	83.3% (11)	85.3% (10)	88.3% (8)	92.9% (5)	94.0% (3)	95.0% (1)	95.1% (4)	94.3% (4)
Avg. AUPIMO	15.6% (13)	27.6% (11)	32.1% (8)	25.1% (12)	32.2% (8)	30.8% (10)	40.1% (7)	52.0% (6)	60.2% (4)	57.1% (5)	63.0% (3)	68.6% (1)	66.1% (2)
Std. AUPIMO	25.6%	31.0%	37.4%	36.1%	34.3%	40.4%	42.3%	39.0%	38.6%	39.3%	33.9%	32.6%	31.3%
P33 AUPIMO	0.0% (13)	0.0% (12)	0.0% (11)	2.6% (7)	1.0% (8)	0.0% (9)	0.0% (10)	23.1% (6)	38.4% (4)	35.2% (5)	46.7% (3)	64.5% (1)	56.0% (2)
Avg. Rank	10.8	9.4	9.2	9.1	8.8	8.2	7.8	5.4	3.4	4.9	4.2	3.8	3.8
Avg. Iou	53.9% (13)	18.3% (8)	20.1% (7)	14.4% (11)	17.0% (9)	10.3% (12)	15.4% (10)	25.0% (6)	24.4% (6)	31.3% (3)	31.5% (2)	37.7% (1)	33.2% (4)
Eff M (3.8)	100%	100%	100%	100%	100%	100%	100%	100%	96%	98%	100%	<1%	
RD++ WR50 (3.8)	100%	100%	100%	100%	100%	100%	100%	100%	100%	100%	100%	100%	
UF (4.9)	100%	100%	100%	100%	100%	100%	100%	100%	100%	100%	100%	100%	
Eff S (4.2)	100%	100%	100%	100%	100%	100%	100%	100%	100%	100%	100%	100%	
SN WR50 (5.4)	100%	100%	100%	100%	100%	100%	100%	100%	83%	77%	100%		
FF CAIT (5.8)	100%	100%	100%	100%	100%	100%	100%	100%					
PF FNF (7.8)	100%	100%	99%	100%	98%	100%							
PF R18 (8.2)	100%	100%	99%	100%	98%	100%							
PDM WR50 (8.8)	100%	100%	99%	100%	99%								
FF WR50 (9.1)	100%	100%	100%	100%	100%								
PC WR101 (9.2)	100%	100%	98%										
PC WR50 (9.4)	100%	100%											

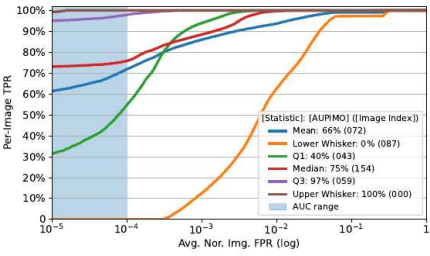
(a) Statistics and pairwise statistical tests.



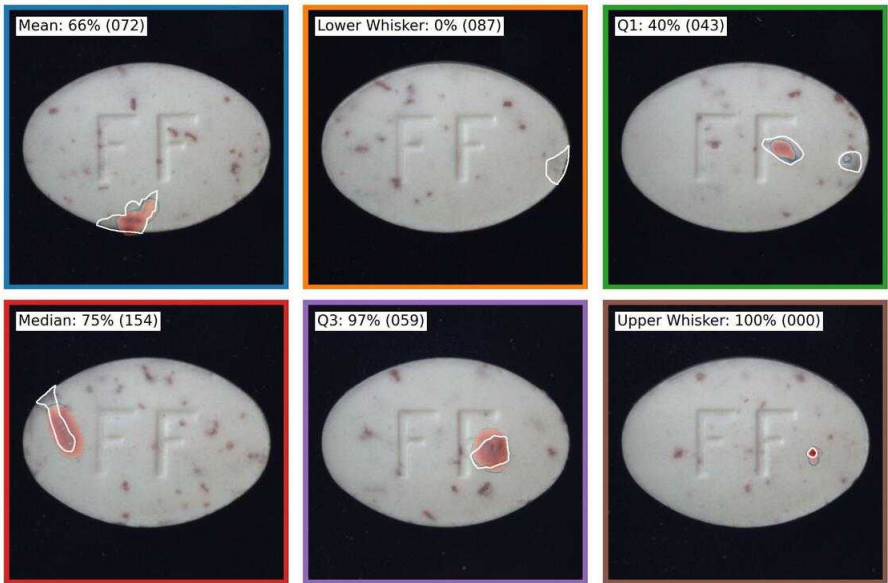
(b) Average rank diagram.



(c) Score distributions.



(d) PIMO curves.



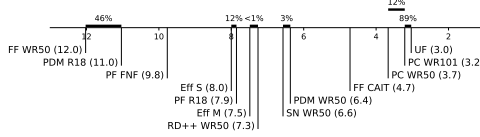
(e) Heatmaps. Images selected according to AUPIMO's statistics. Statistic and image index annotated on upper left corner.

Figure 30: Benchmark on MVTec AD / Pill. PIMO curves and heatmaps are from EfficientAD M. 167 images (026 normal, 141 anomalous).

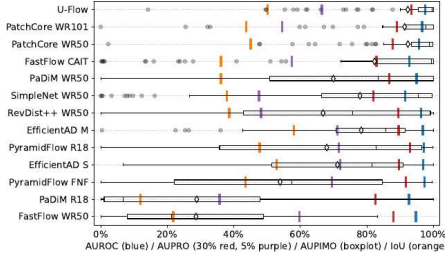


	FF WR50	PDM R18	PF FNF	Eff S	PF R18	Eff M	RD++ WR50	SN WR50	PDM WR50	FF CAIT	PC WR50	PC WR101	UF
AUROC	94.8% (19)	92.7% (12)	97.4% (2)	96.9% (4)	97.1% (3)	98.9% (5)	96.3% (7)	91.3% (13)	94.9% (9)	92.7% (11)	95.7% (8)	96.8% (6)	97.5% (1)
AUPRO	88.9% (8)	82.5% (12)	91.7% (1)	89.7% (4)	92.9% (2)	89.5% (5)	89.5% (6)	81.3% (13)	86.8% (10)	82.9% (11)	87.7% (9)	89.4% (7)	93.4% (3)
AUPRO 5%	89.5% (8)	85.7% (11)	95.5% (1)	92.4% (3)	94.8% (2)	91.5% (5)	91.8% (7)	87.5% (10)	91.3% (9)	87.3% (11)	91.3% (8)	94.5% (6)	95.5% (4)
Avg. AUPIMO	28.6% (13)	28.9% (12)	53.9% (11)	71.2% (7)	68.0% (9)	76.3% (5)	66.8% (10)	77.9% (6)	69.9% (8)	82.3% (4)	92.4% (1)	91.4% (3)	92.3% (2)
Std. AUPIMO	24.0%	27.4%	32.5%	35.7%	33.3%	20.8%	11.8%	11.5%	11.7%	11.3%	13.1%	17.8%	15.7%
P33 AUPIMO	11.3% (12)	2.2% (13)	33.6% (11)	64.3% (7)	63.4% (8)	76.3% (5)	50.7% (10)	82.3% (5)	55.4% (9)	94.7% (4)	96.2% (2)	95.1% (3)	97.8% (1)
Avg. Rank	12.8	11.0	9.8	8.8	7.9	7.5	7.3	6.8	6.4	4.7	3.7	3.2	3.0
Avg. Iou	21.8% (12)	12.5% (13)	43.3% (7)	52.8% (12)	47.8% (11)	58.1% (1)	48.0% (8)	37.9% (9)	38.1% (11)	30.2% (10)	25.1% (12)	43.7% (6)	50.2% (3)
UF (3.0)	100%	100%	100%	100%	100%	100%	100%	100%	100%	100%	100%	100%	
PC WR101 (3.7)	100%	100%	100%	100%	100%	100%	100%	100%	100%	100%	100%	100%	
PC WR50 (1.1)	100%	100%	100%	100%	100%	100%	100%	100%	100%	100%	100%	100%	
FF CAIT (4.7)	100%	100%	100%	100%	100%	100%	100%	100%	100%	100%	100%	100%	
RevDist++ WR50 (6.4)	100%	100%	100%	100%	100%	100%	100%	100%	100%	100%	100%	100%	
SN WR50 (6.6)	100%	100%	100%	100%	100%	100%	100%	100%	100%	100%	100%	100%	
RD++ WR50 (7.3)	100%	100%	100%	100%	100%	100%	100%	100%	100%	100%	100%	100%	
Eff M (7.5)	100%	100%	100%	100%	100%	100%	100%	100%	100%	100%	100%	100%	
PF R18 (7.8)	100%	100%	100%	100%	100%	100%	100%	100%	100%	100%	100%	100%	
Eff S (8.0)	100%	100%	100%	100%	100%	100%	100%	100%	100%	100%	100%	100%	
PF FNF (9.8)	100%	100%	100%	100%	100%	100%	100%	100%	100%	100%	100%	100%	
PDM R18 (11.0)	46%												

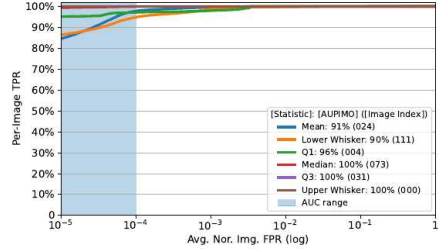
(a) Statistics and pairwise statistical tests.



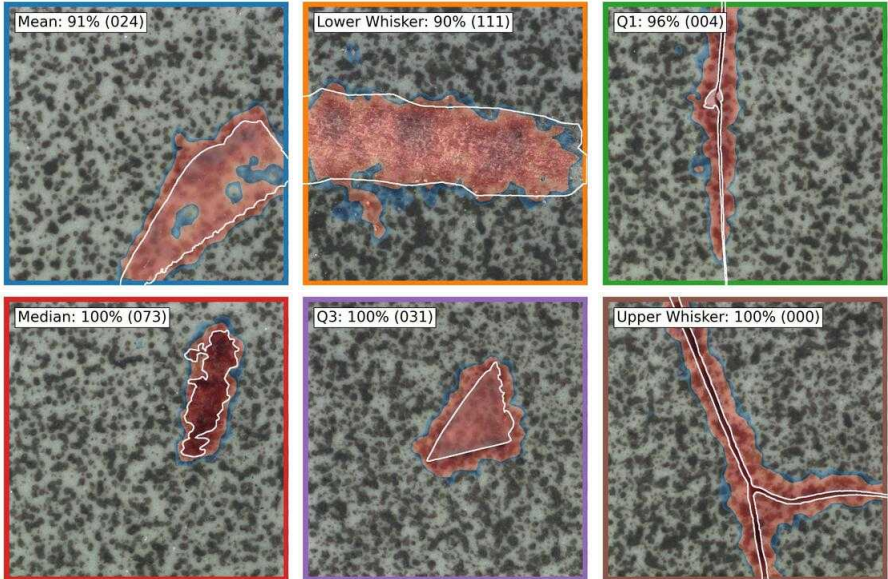
(b) Average rank diagram.



(c) Score distributions.



(d) PIMO curves.

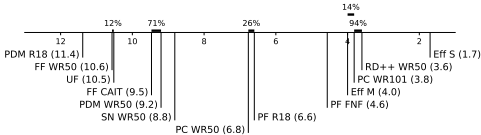


(e) Heatmaps. Images selected according to AUPIMO's statistics. Statistic and image index annotated on upper left corner.

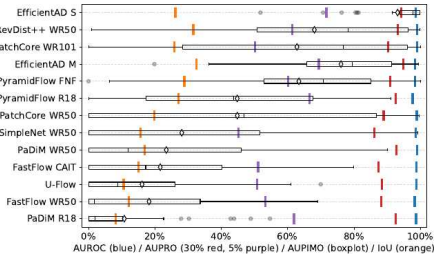
Figure 32: Benchmark on MVTec AD / Tile. PIMO curves and heatmaps are from U-Flow. 117 images (033 normal, 084 anomalous).

	PDM R18	FF WR50	UF	FF CAIT	PDM WR50	SN WR50	PC WR50	PF R18	PF FNF	Eff M	PC WR101	RD++ WR50	Eff S
AUDROC	98.7% (17)	98.3% (12)	98.8% (6)	98.3% (5)	99.0% (13)	98.6% (8)	98.9% (4)	97.7% (13)	98.3% (11)	98.4% (10)	99.4% (12)	99.1% (1)	98.6% (9)
AUPRO	92.6% (15)	86.2% (11)	86.4% (10)	87.4% (12)	92.8% (4)	86.3% (13)	86.9% (9)	82.5% (6)	90.4% (17)	94.9% (13)	90.3% (8)	93.1% (1)	94.2% (12)
AUPRO 5%	83.4% (4)	53.3% (1)	50.5% (1)	51.1% (1)	92.8% (4)	45.4% (1)	45.4% (1)	45.4% (1)	60.3% (1)	60.3% (1)	60.3% (1)	61.4% (1)	61.4% (1)
Avg. AUPIMO	10.8% (13)	18.2% (11)	18.1% (12)	21.6% (10)	23.4% (9)	28.1% (8)	44.8% (6)	44.8% (7)	83.4% (4)	76.1% (2)	62.8% (5)	68.1% (3)	93.1% (1)
Std. AUPIMO	16.4%	24.0%	21.0%	22.8%	29.2%	34.6%	41.1%	29.2%	28.9%	20.6%	36.2%	31.3%	11.0%
P33 AUPIMO	0.0% (13)	0.0% (12)	0.0% (11)	0.9% (7)	0.0% (10)	0.0% (9)	0.0% (8)	29.6% (6)	55.0% (4)	73.7% (2)	46.0% (5)	56.2% (3)	95.4% (1)
Avg. Rank	11.4	10.6	10.5	9.5	9.2	8.8	6.8	6.6	4.6	4.0	3.8	3.6	1.7
Avg. Iou	8.2% (13)	12.1% (11)	10.6% (12)	15.1% (10)	16.9% (8)	15.4% (9)	15.9% (7)	27.1% (1)	28.9% (1)	32.9% (1)	25.0% (6)	31.4% (2)	24.2% (1)
Eff S (1.7)	100%	100%	100%	100%	100%	100%	100%	100%	100%	100%	100%	100%	100%
RD++ WR50 (3.6)	100%	100%	100%	100%	100%	100%	100%	100%	100%	100%	100%	100%	100%
PC WR101 (3.8)	100%	100%	100%	100%	100%	100%	100%	100%	99%	55%	14%	95%	100%
Eff M (4.0)	100%	100%	100%	100%	100%	100%	100%	100%	100%	100%	100%	100%	100%
PF FNF (4.6)	100%	100%	100%	100%	100%	100%	99%	100%	100%	99%	100%	100%	100%
PF R18 (6.6)	100%	100%	100%	100%	100%	100%	96%	27%	100%	100%	100%	100%	100%
PC WR50 (6.8)	100%	100%	100%	100%	100%	100%	100%	100%	100%	100%	100%	100%	100%
SN WR50 (8.8)	100%	100%	100%	100%	100%	100%	100%	100%	100%	100%	100%	100%	100%
PDM WR50 (9.2)	100%	100%	100%	72%	92%	100%	100%	100%	100%	100%	100%	100%	100%
UF (10.5)	98%	12%	98%										
FF WR50 (10.6)	100%												

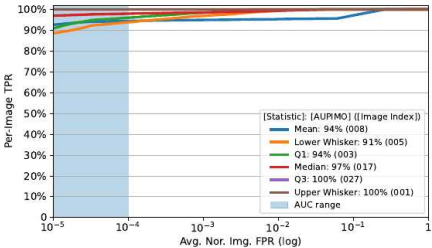
(a) Statistics and pairwise statistical tests.



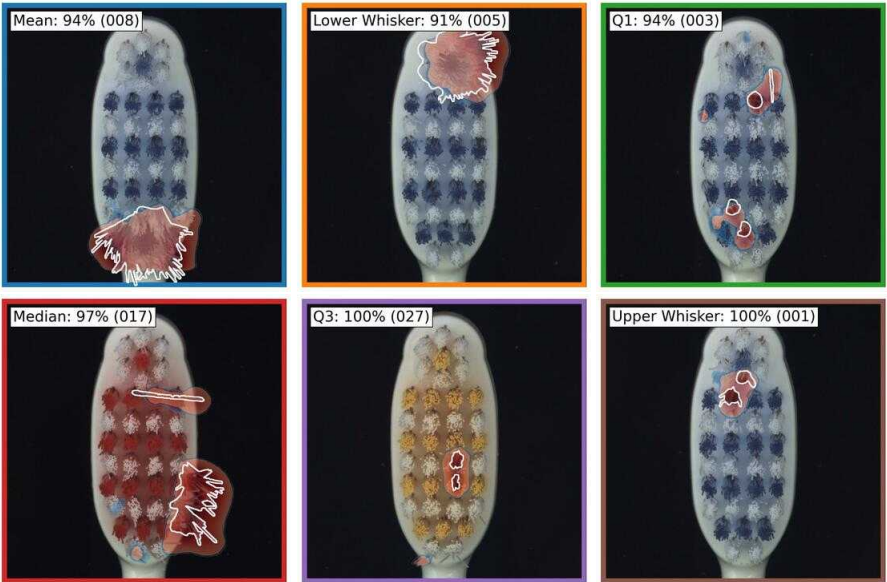
(b) Average rank diagram.



(c) Score distributions.



(d) PIMO curves.



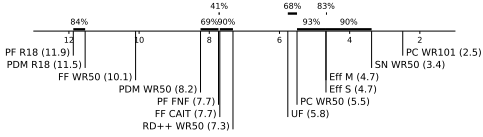
(e) Heatmaps. Images selected according to AUPIMO's statistics. Statistic and image index annotated on upper left corner.

Figure 33: Benchmark on MVTec AD / Toothbrush. PIMO curves and heatmaps are from EfficientAD S. 042 images (012 normal, 030 anomalous).

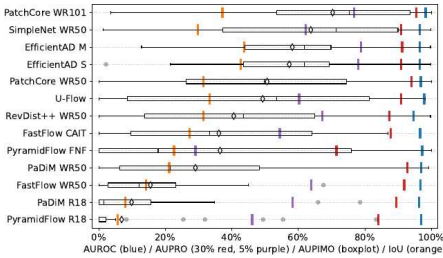


	PF R18	PDM R18	FF WR50	PDM WR50	PF FNF	FF CAIT	RD++ WR50	UF	PC WR50	Eff S	Eff M	SN WR50	PC WR101
AUROC	86.3% (3)	86.3% (13)	86.7% (7)	87.0% (4)	87.2% (3)	88.7% (8)	94.6% (13)	97.9% (2)	96.8% (6)	96.5% (10)	96.5% (11)	96.3% (9)	98.3% (1)
AUPRO	84.0% (12)	89.4% (9)	91.8% (6)	92.8% (1)	71.3% (11)	87.8% (10)	87.4% (11)	90.9% (8)	94.0% (2)	90.9% (12)	91.2% (15)	91.0% (10)	95.5% (1)
AUPIMO 5%	85.3% (10)	88.1% (11)	91.3% (5)	92.8% (1)	71.3% (11)	87.8% (10)	87.4% (11)	90.9% (8)	94.0% (2)	90.9% (12)	91.2% (15)	91.0% (10)	95.5% (1)
Avg. AUPIMO	8.9% (13)	9.9% (12)	15.3% (11)	28.1% (10)	36.3% (8)	36.1% (8)	40.6% (7)	49.3% (6)	50.6% (5)	57.3% (4)	58.2% (3)	63.8% (2)	70.3% (1)
Std. AUPIMO	17.6%	17.2%	15.5%	18.4%	39.3%	39.0%	27.7%	15.0%	28.7%	20.8%	18.2%	10.7%	23.9%
P33 AUPIMO	0.0% (13)	0.0% (12)	3.4% (10)	10.8% (8)	1.3% (11)	10.6% (6)	21.7% (7)	27.1% (6)	37.2% (5)	47.0% (4)	51.0% (3)	52.5% (2)	62.6% (1)
Avg. Rank	11.9	10.1	8.2	7.7	7.7	7.7	5.3	3.3	3.3	2.7	2.7	2.7	2.5
Avg. Iou	57.2% (13)	60.9% (11)	14.2% (11)	21.2% (10)	22.6% (9)	27.1% (8)	31.3% (7)	33.3% (6)	31.3% (5)	32.8% (4)	4.7	29.8% (1)	37.2% (1)
PC WR101 (2.5)	100%	100%	100%	100%	100%	100%	100%	100%	100%	100%	100%	100%	
RD WR50 (2.4)	100%	100%	100%	100%	100%	100%	100%	100%	100%	100%	100%	100%	
Eff M (4.7)	100%	100%	100%	100%	100%	100%	100%	100%	100%	100%	100%	100%	
Eff S (4.7)	100%	100%	100%	100%	100%	100%	100%	100%	100%	100%	100%	100%	
PC WR50 (3.5)	100%	100%	100%	100%	100%	100%	100%	100%	100%	100%	100%	100%	
UF (5.8)	100%	100%	100%	100%	100%	100%	100%	100%	100%	100%	100%	100%	
RD++ WR50 (7.3)	100%	100%	100%	100%	100%	100%	100%	100%	100%	100%	100%	100%	
FF CAIT (7.7)	100%	100%	100%	100%	100%	100%	100%	100%	100%	100%	100%	100%	
PF FNF (7.7)	100%	100%	100%	100%	100%	100%	100%	100%	100%	100%	100%	100%	
PC WR50 (8.1)	100%	100%	100%	100%	100%	100%	100%	100%	100%	100%	100%	100%	
FF WR50 (10.1)	100%	100%	100%	100%	100%	100%	100%	100%	100%	100%	100%	100%	
PDM R18 (11.5)	85%												

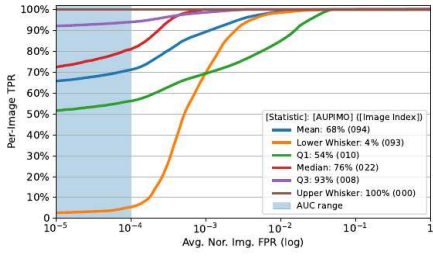
(a) Statistics and pairwise statistical tests.



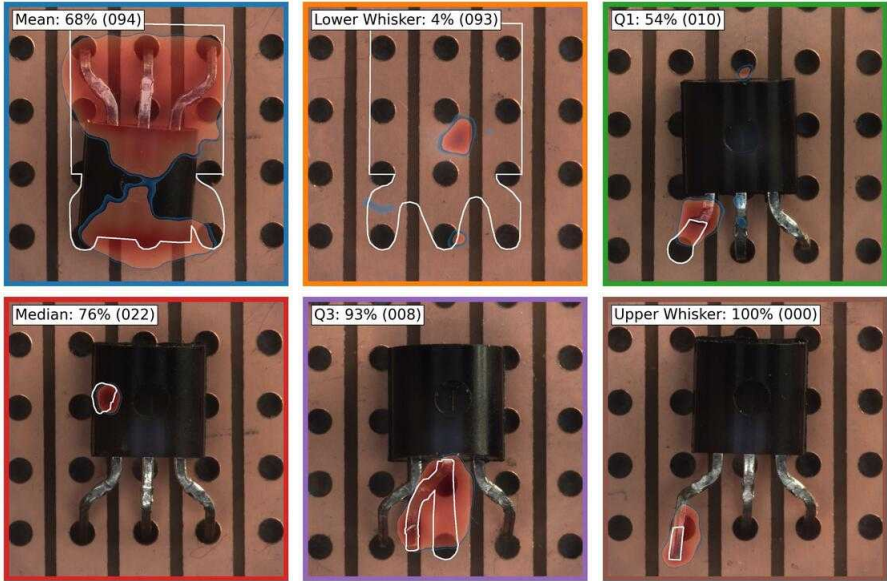
(b) Average rank diagram.



(c) Score distributions.



(d) PIMO curves.

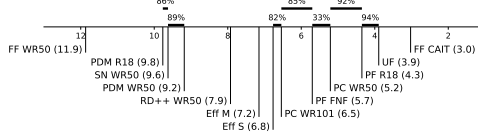


(e) Heatmaps. Images selected according to AUPIMO's statistics. Statistic and image index annotated on upper left corner.

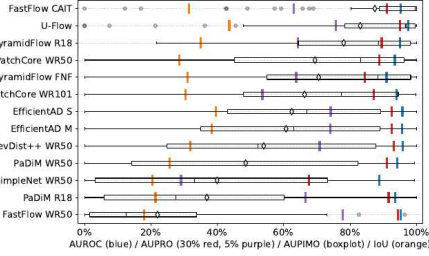
Figure 34: Benchmark on MVTec AD / Transistor. PIMO curves and heatmaps are from PatchCore WR101. 100 images (060 normal, 040 anomalous).

	FF WR50	PDM R18	SN WR50	PDM WR50	RD++ WR50	Eff M	Eff S	PC WR101	PF FNF	PC WR50	PF R18	UF	FF CAIT
AUDROC	95.3% (6)	93.6% (10)	88.8% (13)	94.3% (8)	95.8% (2)	95.7% (4)	95.8% (3)	94.1% (9)	91.0% (12)	93.3% (11)	95.1% (7)	97.5% (1)	95.3% (5)
AUPRO	94.5% (2)	91.6% (6)	87.6% (13)	91.1% (8)	93.3% (3)	92.6% (4)	92.6% (5)	87.2% (11)	84.4% (12)	88.6% (10)	89.6% (9)	95.1% (1)	91.1% (7)
AUPRO 5%	77.8% (1)	65.3% (6)	52.1% (11)	75.3% (3)	74.1% (4)	74.1% (4)	74.1% (4)	51.6% (11)	43.4% (12)	64.4% (11)	75.7% (2)	97.5% (1)	71.9% (10)
Avg. AUPIMO	22.0% (13)	36.9% (12)	39.9% (11)	48.6% (10)	54.0% (9)	60.7% (8)	62.4% (7)	66.3% (6)	70.6% (4)	69.4% (5)	78.1% (3)	83.1% (2)	87.9% (1)
Std. AUPIMO	13.6%	14.4%	14.0%	14.6%	14.1%	18.7%	28.0%	32.2%	14.9%	12.3%	24.1%	26.0%	23.3%
P33 AUPIMO	5.3% (13)	9.6% (12)	14.6% (11)	25.8% (10)	31.6% (9)	52.7% (8)	56.4% (7)	58.8% (6)	66.8% (4)	60.1% (5)	70.8% (3)	87.4% (2)	94.0% (1)
Avg. Rank	11.9	9.8	9.6	9.2	7.9	7.2	6.8	5.7	3.2	4.3	3.9	3.0	3.0
Avg. iou	17.7% (13)	21.4% (11)	25.5% (10)	31.2% (9)	38.4% (8)	39.8% (7)	39.8% (7)	30.6% (10)	31.1% (9)	28.3% (11)	35.0% (4)	43.4% (3)	51.2% (2)
FF CAIT (3.0)	100%	100%	100%	100%	100%	100%	100%	100%	100%	100%	100%	100%	100%
UF (1.9)	100%	100%	100%	100%	100%	100%	100%	100%	100%	100%	100%	100%	100%
PC WR101 (6.5)	100%	100%	100%	100%	100%	100%	100%	100%	100%	100%	100%	100%	100%
PC WR50 (5.2)	100%	100%	100%	100%	100%	100%	100%	100%	100%	100%	100%	100%	100%
PF R18 (4.3)	100%	100%	100%	100%	100%	100%	100%	100%	100%	100%	100%	100%	100%
PF FNF (5.7)	100%	100%	100%	100%	100%	100%	100%	100%	100%	100%	100%	100%	100%
PC WR101 (6.5)	100%	100%	100%	100%	100%	100%	100%	100%	100%	100%	100%	100%	100%
Eff S (6.8)	100%	100%	100%	100%	100%	100%	100%	100%	100%	100%	100%	100%	100%
RD++ WR50 (7.9)	100%	100%	100%	100%	100%	100%	100%	100%	100%	100%	100%	100%	100%
SN WR50 (9.6)	100%	100%	100%	100%	100%	100%	100%	100%	100%	100%	100%	100%	100%
PDM R18 (9.8)	100%	100%	100%	100%	100%	100%	100%	100%	100%	100%	100%	100%	100%

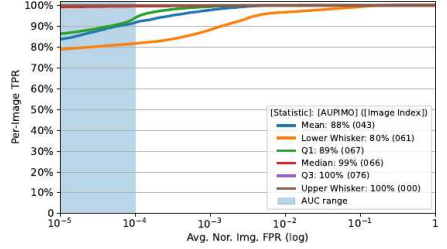
(a) Statistics and pairwise statistical tests.



(b) Average rank diagram.



(c) Score distributions.



(d) PIMO curves.



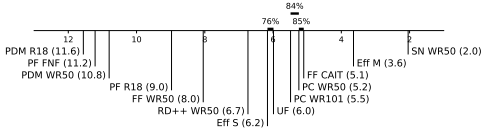
(e) Heatmaps. Images selected according to AUPIMO's statistics. Statistic and image index annotated on upper left corner.

Figure 35: Benchmark on MVTec AD / Wood. PIMO curves and heatmaps are from Fast-Flow CAIT. 079 images (019 normal, 060 anomalous).

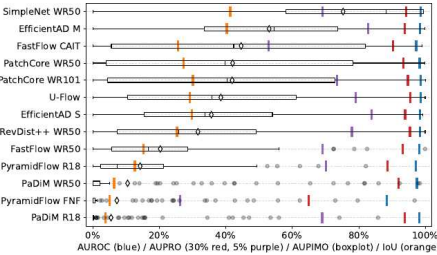


	PDM R18	PF FNF	PDM WR50	PF R18	FF WR50	RD++ WR50	Eff S	UF	PC WR101	PC WR50	FF CAT	Eff M	SN WR50
AUROC	98.2% (8)	98.3% (13)	97.4% (10)	97.2% (12)	98.2% (9)	98.4% (4)	98.4% (5)	98.6% (2)	98.4% (1)	98.3% (7)	97.2% (11)	98.4% (6)	98.5% (13)
AUPRO	93.8% (6)	94.3% (13)	92.0% (10)	88.2% (12)	93.2% (9)	93.9% (2)	93.9% (3)	95.5% (1)	94.7% (1)	93.8% (8)	90.3% (11)	93.4% (7)	94.2% (6)
AUPRO 9%	93.9% (8)	94.3% (11)	92.0% (10)	88.2% (10)	93.2% (12)	93.9% (1)	93.9% (1)	95.5% (1)	94.7% (1)	93.8% (8)	90.3% (11)	93.4% (7)	94.2% (6)
Avg. AUPIMO	5.5% (13)	7.3% (12)	10.3% (11)	14.2% (10)	20.3% (9)	31.6% (8)	35% (7)	38.5% (6)	41.9% (5)	42.0% (4)	44.6% (3)	53.0% (2)	75.3% (1)
Std. AUPIMO	14.9%	17.8%	21.5%	16.4%	18.0%	26.4%	24.4%	30.1%	31.3%	35.3%	37.4%	29.8%	10.0%
P33 AUPIMO	0.0% (13)	0.0% (11)	0.0% (11)	3.5% (10)	7.6% (9)	18.1% (4)	21.7% (3)	17.8% (5)	14.0% (7)	16.5% (6)	12.7% (8)	39.5% (2)	69.6% (1)
Avg. Rank	11.8	11.2	10.8	9.0	8.0	6.7	6.2	6.0	5.3	5.2	5.1	40.3% (2)	41.2% (1)
Avg. IQR	21.8% (13)	5.9% (12)	6.4% (11)	12.4% (10)	12.3% (9)	21.3% (8)	29.0% (4)	29.0% (5)	30.1% (1)	27.4% (6)	23.9% (7)	5.1	3.6
SN WR50 (2.0)	100%	100%	100%	100%	100%	100%	100%	100%	100%	100%	100%	100%	100%
Eff M (3.6)	100%	100%	100%	100%	100%	100%	100%	100%	100%	100%	100%	100%	100%
FF CAT (5.1)	100%	100%	100%	100%	100%	100%	100%	100%	100%	100%	100%	100%	100%
PC WR50 (5.2)	100%	100%	100%	100%	100%	100%	100%	100%	100%	100%	100%	100%	100%
PC WR101 (5.5)	100%	100%	100%	100%	100%	100%	100%	100%	100%	100%	100%	100%	100%
UF (6.0)	100%	100%	100%	100%	100%	100%	100%	100%	100%	100%	100%	100%	100%
Eff S (6.2)	100%	100%	100%	100%	100%	100%	100%	100%	100%	100%	100%	100%	100%
RD++ WR50 (6.7)	100%	100%	100%	100%	100%	100%	100%	100%	100%	100%	100%	100%	100%
FF WR50 (8.0)	100%	100%	100%	100%	100%	100%	100%	100%	100%	100%	100%	100%	100%
PF R18 (9.0)	100%	100%	100%	100%	100%	100%	100%	100%	100%	100%	100%	100%	100%
PDM WR50 (10.8)	100%	100%	100%	100%	100%	100%	100%	100%	100%	100%	100%	100%	100%
PF FNF (11.2)	100%	100%	100%	100%	100%	100%	100%	100%	100%	100%	100%	100%	100%

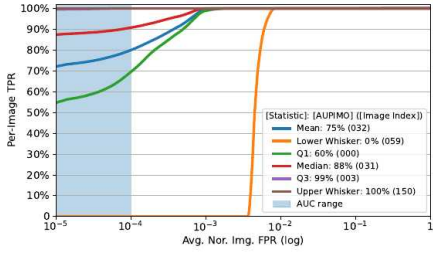
(a) Statistics and pairwise statistical tests.



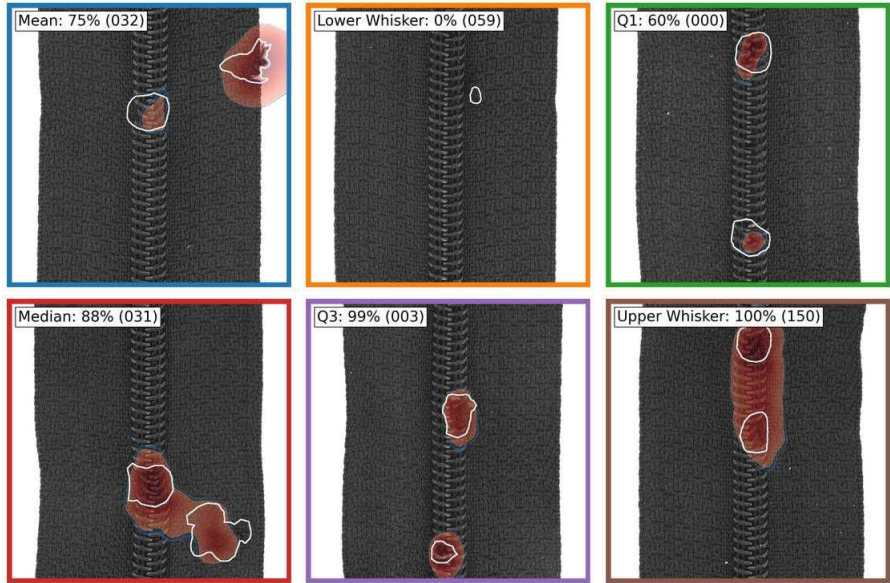
(b) Average rank diagram.



(c) Score distributions.



(d) PIMO curves.

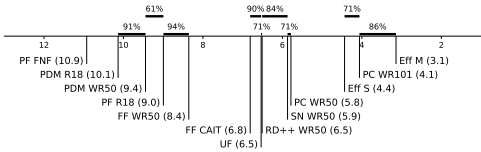


(e) Heatmaps. Images selected according to AUPIMO's statistics. Statistic and image index annotated on upper left corner.

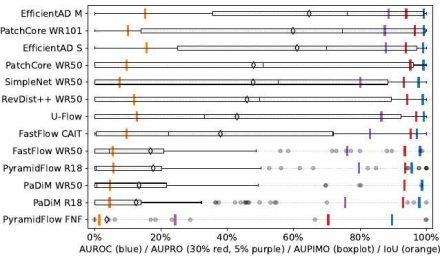
Figure 36: Benchmark on MVTec AD / Zipper. PIMO curves and heatmaps are from SimpleNet WR50. 151 images (032 normal, 119 anomalous).

	PF FNF	PDM R18	PDM WR50	FF R18	FF WR50	FF CAIT	UF	RD++ WR50	SN WR50	PC WR50	EFF S	PC WR101	EFF M
AUROC	89.7% (13)	97.9% (9)	98.7% (7)	95.4% (12)	98.1% (8)	97.1% (11)	99.2% (3)	98.9% (10)	97.6% (10)	99.1% (4)	99.9% (5)	99.2% (2)	99.2% (1)
AUPRO	76.4% (13)	93.0% (12)	93.4% (10)	92.5% (8)	93.5% (9)	95.3% (3)	96.0% (1)	94.2% (5)	93.2% (11)	95.2% (4)	93.8% (7)	96.5% (2)	93.9% (6)
AUPIMO	1.5% (13)	4.0% (12)	4.7% (11)	3.5% (10)	3.4% (10)	9.0% (7)	12.8% (1)	12.4% (4)	7.6% (10)	9.1% (6)	15.0% (1)	10.0% (3)	8.9% (2)
Avg. AUPIMO	3.7% (13)	12.5% (12)	13.4% (11)	17.7% (9)	16.9% (10)	37.9% (8)	42.9% (7)	45.9% (6)	47.8% (5)	47.9% (4)	61.0% (2)	59.8% (3)	64.7% (1)
Std. AUPIMO	15.8%	22.8%	20.8%	30.3%	25.1%	37.5%	42.4%	41.1%	41.4%	43.2%	37.4%	40.9%	36.9%
P33 AUPIMO	0.0% (13)	0.0% (12)	0.0% (11)	0.0% (10)	1.2% (6)	4.3% (4)	0.0% (8)	0.0% (7)	3.8% (5)	0.0% (9)	45.9% (2)	32.7% (3)	51.4% (1)
Avg. Rank	10.9	10.1	9.4	9.0	8.4	6.6	6.3	6.5	5.9	5.8	4.4	4.1	3.1
EFF M (13)	100%	100%	100%	100%	100%	100%	100%	100%	100%	100%	100%	100%	100%
PC WR101 (4.1)	100%	100%	100%	100%	100%	100%	100%	100%	100%	100%	100%	71%	87%
PC WR50 (5.8)	100%	100%	100%	100%	100%	100%	100%	100%	100%	100%	100%	100%	100%
SN WR50 (5.9)	100%	100%	100%	100%	100%	100%	99%	99%	99%	100%	100%	100%	100%
RD++ WR50 (6.5)	100%	100%	100%	100%	100%	99%	97%	84%	72%	100%	100%	100%	100%
UF (6.5)	100%	100%	100%	100%	100%	90%	72%						
FF CAIT (6.8)	100%	100%	100%	100%	100%								
FF WR50 (8.4)	100%	100%	97%	94%									
PF R18 (9.0)	100%	100%	90%	61%									
PDM WR50 (10.1)	100%												
PDM R18 (10.1)	100%												

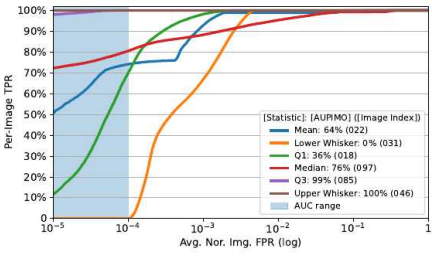
(a) Statistics and pairwise statistical tests.



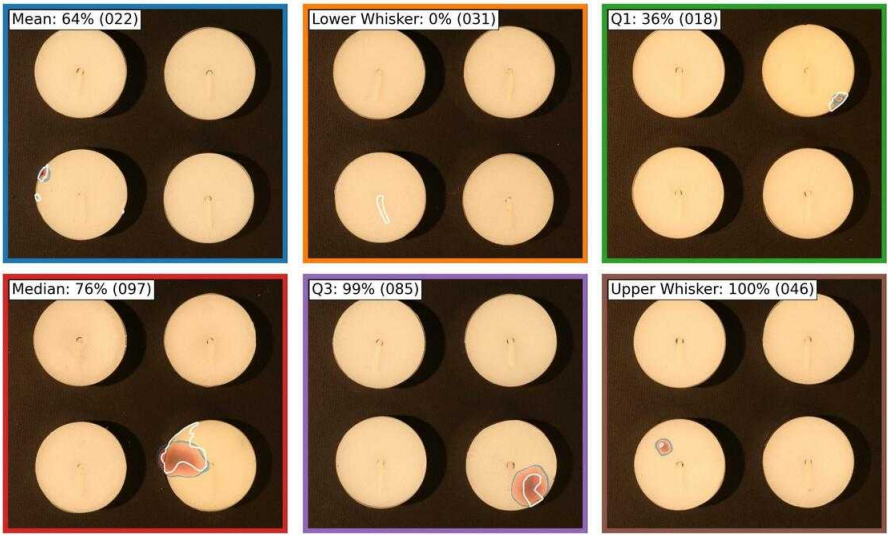
(b) Average rank diagram.



(c) Score distributions.



(d) PIMO curves.

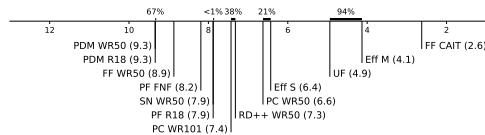


(e) Heatmaps. Images selected according to AUPIMO's statistics. Statistic and image index annotated on upper left corner.

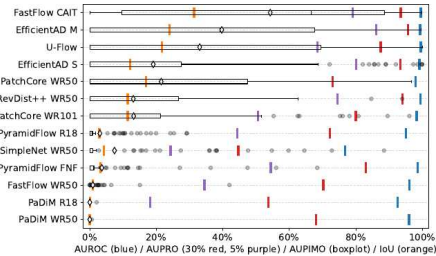
Figure 37: Benchmark on VisA / Candle. PIMO curves and heatmaps are from EfficientAD M. 200 images (100 normal, 100 anomalous).

	PCM WR50	PCM R18	FF WR50	FF FNF	SN WR50	PF R18	PC WR101	RD++ WR50	PC WR50	Eff S	UF	Eff M	FF CAIT
AUROC	99.0% (10)	92.4% (12)	96.1% (9)	96.6% (6)	76.8% (13)	95.1% (11)	98.3% (7)	99.5% (3)	99.0% (8)	99.1% (5)	99.4% (4)	99.4% (4)	99.5% (3)
AUPRO	69.1% (11)	53.7% (12)	70.2% (10)	81.1% (6)	44.6% (13)	72.2% (9)	80.0% (7)	94.0% (2)	73.1% (8)	83.3% (4)	87.5% (5)	95.4% (1)	93.5% (3)
AUPRO++	18.1% (11)	6.3% (12)	8.3% (10)	24.6% (6)	2.3% (13)	6.3% (9)	9.0% (7)	74.1% (2)	21.1% (8)	21.1% (5)	21.1% (4)	21.1% (4)	21.1% (3)
Avg. AUPIMO	0.0% (13)	0.0% (12)	0.9% (11)	3.6% (9)	7.4% (8)	3.1% (10)	13.2% (6)	13.1% (7)	21.5% (4)	19.1% (5)	33.0% (3)	39.7% (2)	54.3% (1)
Std. AUPIMO	0.1%	0.2%	4.5%	31.0%	17.4%	6.8%	24.1%	21.8%	32.0%	32.2%	39.8%	37.9%	38.2%
P13 AUPIMO	0.0% (13)	0.0% (12)	0.0% (11)	0.0% (10)	0.0% (9)	0.0% (8)	0.0% (7)	0.0% (6)	0.0% (5)	0.0% (4)	0.0% (3)	0.0% (2)	26.3% (1)
Avg. Rank	9.3	9.3	8.9	8.2	7.9	7.9	7.4	7.3	6.6	6.4	4.9	4.1	2.6
PC WR50	0.0% (13)	0.0% (12)	0.0% (11)	0.0% (10)	0.0% (9)	0.0% (8)	0.0% (7)	0.0% (6)	0.0% (5)	0.0% (4)	0.0% (3)	0.0% (2)	31.0% (1)
FF CAIT (12.8)	100%	100%	100%	100%	100%	100%	100%	100%	100%	100%	100%	100%	100%
Eff M (4.1)	100%	100%	100%	100%	100%	100%	100%	100%	100%	100%	100%	100%	100%
UF (4.9)	100%	100%	100%	100%	100%	100%	100%	100%	100%	100%	100%	100%	100%
Eff S (6.4)	100%	100%	100%	100%	100%	100%	100%	100%	100%	100%	100%	100%	100%
PC WR50 (6.6)	100%	100%	100%	100%	100%	100%	100%	100%	100%	100%	100%	100%	100%
RD++ WR50 (7.3)	100%	100%	100%	100%	100%	100%	100%	100%	100%	100%	100%	100%	100%
PC WR101 (7.4)	100%	100%	100%	100%	100%	100%	100%	100%	100%	100%	100%	100%	100%
SN WR50 (7.9)	100%	100%	100%	100%	100%	100%	100%	100%	100%	100%	100%	100%	100%
PF FNF (8.2)	100%	100%	100%	100%	100%	100%	100%	100%	100%	100%	100%	100%	100%
PF R18 (7.9)	100%	100%	100%	100%	100%	100%	100%	100%	100%	100%	100%	100%	100%
PC WR101 (7.4)	100%	100%	100%	100%	100%	100%	100%	100%	100%	100%	100%	100%	100%
SN WR50 (7.9)	100%	100%	100%	100%	100%	100%	100%	100%	100%	100%	100%	100%	100%
PF FNF (8.2)	100%	100%	100%	100%	100%	100%	100%	100%	100%	100%	100%	100%	100%
FF WR50 (8.9)	100%	100%	100%	100%	100%	100%	100%	100%	100%	100%	100%	100%	100%
PCM R18 (9.3)	100%	100%	100%	100%	100%	100%	100%	100%	100%	100%	100%	100%	100%

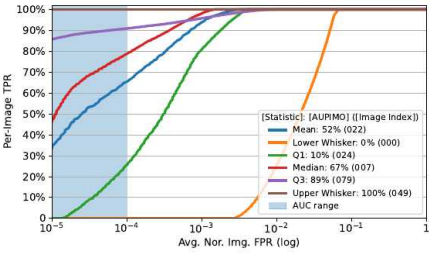
(a) Statistics and pairwise statistical tests.



(b) Average rank diagram.



(c) Score distributions.



(d) PIMO curves.



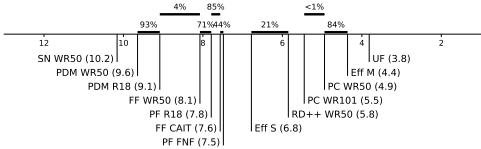
(e) Heatmaps. Images selected according to AUPIMO's statistics. Statistic and image index annotated on upper left corner.

Figure 38: Benchmark on VisA / Capsules. PIMO curves and heatmaps are from FastFlow CAIT. 160 images (060 normal, 100 anomalous).

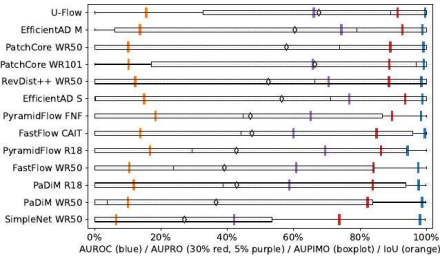


	SN WR50	PDM WR50	PDM R18	FF WR50	PF R18	FF CAIT	PF FNF	Eff S	RD++ WR50	PC WR101	PC WR50	Eff M	UF
AUROC	98.1% (10)	98.7% (7)	97.7% (11)	97.5% (12)	94.3% (13)	99.5% (2)	98.5% (5)	98.7% (6)	98.5% (8)	99.3% (3)	99.1% (4)	98.8% (5)	99.7% (1)
AUPRO	73.7% (13)	82.3% (12)	82.8% (11)	84.8% (10)	86.3% (8)	85.0% (9)	89.8% (4)	92.6% (1)	92.6% (1)	88.6% (6)	89.2% (5)	92.8% (2)	91.3% (3)
AUPRO 5%	42.2% (13)	82.3% (12)	82.9% (11)	80.3% (13)	85.3% (4)	85.3% (7)	89.3% (3)	92.7% (1)	92.7% (1)	85.7% (10)	85.7% (9)	92.8% (2)	91.3% (3)
Avg. AUPIMO	27.1% (13)	36.6% (12)	42.9% (9)	39.1% (11)	42.7% (10)	47.4% (7)	47.0% (8)	56.4% (5)	52.4% (6)	66.4% (2)	57.8% (4)	60.4% (3)	67.6% (1)
Std. AUPIMO	16.0%	42.9%	43.0%	40.7%	41.5%	44.1%	40.0%	42.7%	44.2%	42.6%	42.8%	43.0%	39.9%
P33 AUPIMO	0.0% (13)	0.0% (12)	0.0% (11)	0.0% (10)	3.8% (7)	0.3% (9)	7.6% (6)	19.2% (5)	2.1% (8)	62.5% (1)	21.6% (4)	22.4% (3)	59.2% (2)
Avg. Rank	10.2	9.6	9.1	6.1	7.8	7.6	7.3	6.8	5.8	4.5	4.4	4.4	3.8
Mean (P3)	6.2% (13)	10.0% (12)	11.8% (8)	10.5% (9)	16.7% (2)	17.4% (5)	10.4% (11)	24.9% (4)	12.2% (7)	10.2% (10)	10.1% (11)	12.7% (6)	12.2% (1)
UF (1.8)	100%	100%	100%	100%	100%	100%	100%	100%	100%	100%	100%	100%	100%
Eff (4.8)	100%	100%	100%	100%	100%	100%	100%	100%	100%	100%	100%	100%	100%
PC WR50 (4.3)	100%	100%	100%	100%	100%	100%	100%	100%	100%	100%	100%	100%	100%
PC WR101 (5.5)	100%	100%	100%	100%	100%	100%	100%	100%	100%	100%	100%	100%	100%
RD++ WR50 (5.3)	100%	100%	100%	100%	100%	100%	100%	100%	100%	100%	100%	100%	100%
Eff S (6.8)	100%	100%	100%	100%	100%	100%	100%	100%	100%	100%	100%	100%	100%
FF FNF (7.5)	100%	100%	100%	100%	100%	100%	100%	100%	100%	100%	100%	100%	100%
FF CAIT (7.8)	100%	100%	100%	100%	100%	100%	100%	100%	100%	100%	100%	100%	100%
PF R18 (7.8)	100%	100%	100%	100%	100%	100%	100%	100%	100%	100%	100%	100%	100%
PF WR50 (8.1)	100%	100%	100%	100%	100%	100%	100%	100%	100%	100%	100%	100%	100%
PDM R18 (9.1)	100%	100%	100%	100%	100%	100%	100%	100%	100%	100%	100%	100%	100%
PDM WR50 (9.6)	99%	94%											

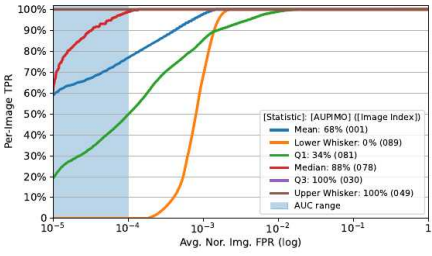
(a) Statistics and pairwise statistical tests.



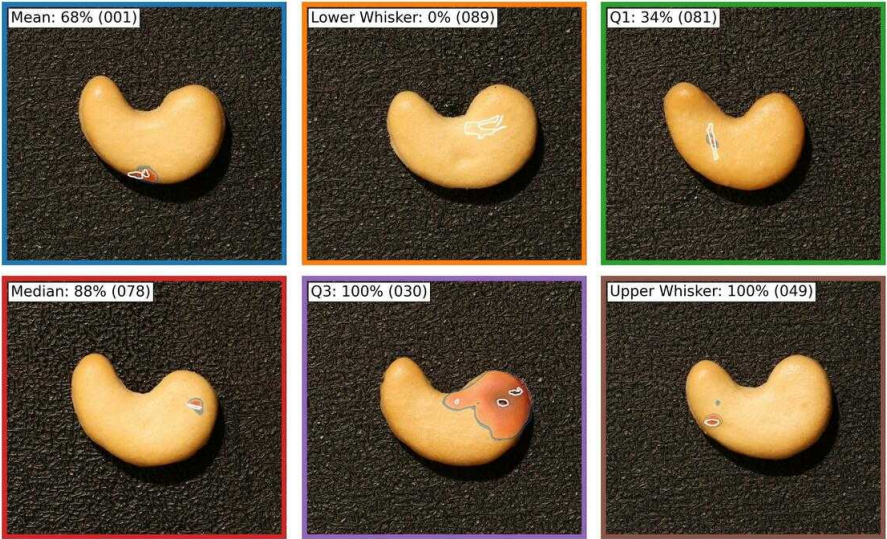
(b) Average rank diagram.



(c) Score distributions.



(d) PIMO curves.

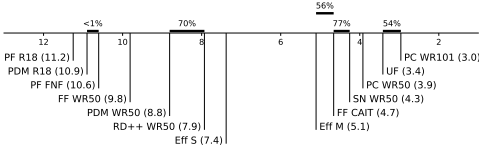


(e) Heatmaps. Images selected according to AUPIMO's statistics. Statistic and image index annotated on upper left corner.

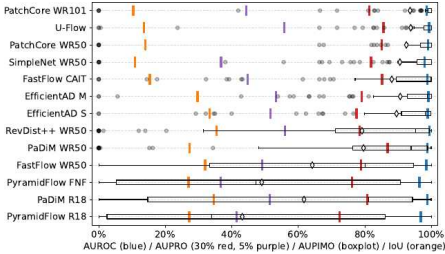
Figure 39: Benchmark on VisA / Cashew. PIMO curves and heatmaps are from U-Flow. 150 images (050 normal, 100 anomalous).

	PF R18	PDM R18	PF FNF	FF WR50	PDM WR50	RD++ WR50	Eff S	Eff M	FF CAIT	SN WR50	PC WR50	UF	PC WR101
AUROC	95.8% (112)	98.8% (8)	98.4% (113)	98.3% (10)	98.3% (8)	99.4% (11)	98.3% (1)	99.1% (12)	98.8% (7)	98.0% (11)	92.0% (4)	97.3% (12)	98.8% (8)
AUPRO	72.4% (113)	80.8% (7)	76.3% (112)	76.9% (9)	80.9% (11)	78.3% (10)	77.3% (11)	79.1% (8)	83.2% (1)	81.3% (15)	85.1% (12)	85.4% (12)	81.4% (10)
AUPRO SD	31.4% (8)	51.4% (15)	38.6% (11)	49.2% (16)	55.5% (13)	55.5% (13)	51.3% (3)	53.3% (13)	44.7% (17)	46.3% (10)	53.8% (12)	44.3% (18)	44.3% (18)
Avg. AUPIMO	81.2% (13)	81.7% (11)	49.9% (12)	64.3% (10)	79.6% (8)	79.1% (9)	89.3% (4)	90.9% (4)	88.1% (7)	90.5% (5)	92.5% (3)	93.8% (1)	93.8% (2)
Std. AUPIMO	39.2%	38.9%	40.2%	35.2%	30.3%	30.9%	20.4%	19.6%	24.0%	23.2%	22.0%	19.0%	20.6%
P31 AUPIMO	7.9% (13)	51.1% (10)	9.7% (12)	49.3% (11)	84.4% (8)	84.4% (8)	95.3% (7)	96.5% (5)	96.2% (6)	98.0% (1)	97.9% (4)	99.7% (2)	100.0% (1)
Avg. Rank	11.2	10.9	10.4	9.1	8.1	7.9	1.4	1.1	4.7	4.1	3.9	1.4	1.0
Avg. DM	27.3% (7)	34.6% (12)	27.0% (8)	32.0% (14)	27.3% (6)	35.4% (1)	31.3% (1)	29.7% (5)	15.4% (16)	10.8% (11)	14.1% (10)	13.6% (11)	10.4% (11)
PC WR101 (13.0)	100%	100%	100%	100%	100%	100%	100%	100%	100%	100%	100%	100%	100%
UF (3.4)	100%	100%	100%	100%	100%	100%	100%	100%	100%	100%	100%	100%	100%
PC WR50 (3.9)	100%	100%	100%	100%	100%	100%	100%	100%	100%	100%	100%	100%	100%
SN WR50 (4.3)	100%	100%	100%	100%	100%	100%	100%	100%	100%	100%	100%	100%	100%
FF CAIT (4.7)	100%	100%	100%	100%	100%	100%	100%	100%	100%	100%	100%	100%	100%
Eff M (5.1)	100%	100%	100%	100%	100%	100%	100%	100%	100%	100%	100%	100%	100%
Eff S (1.4)	100%	100%	100%	100%	100%	100%	100%	100%	100%	100%	100%	100%	100%
RD++ WR50 (7.9)	100%	100%	100%	100%	100%	100%	100%	100%	100%	100%	100%	100%	100%
PDM WR50 (8.8)	100%	100%	100%	100%	100%	100%	100%	100%	100%	100%	100%	100%	100%
FF WR50 (9.8)	100%	100%	100%	100%	100%	100%	100%	100%	100%	100%	100%	100%	100%
PF FNF (10.6)	100%	100%	100%	100%	100%	100%	100%	100%	100%	100%	100%	100%	100%
PDM R18 (10.9)	100%	100%	100%	100%	100%	100%	100%	100%	100%	100%	100%	100%	100%

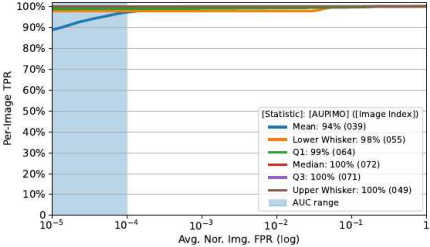
(a) Statistics and pairwise statistical tests.



(b) Average rank diagram.



(c) Score distributions.



(d) PIMO curves.

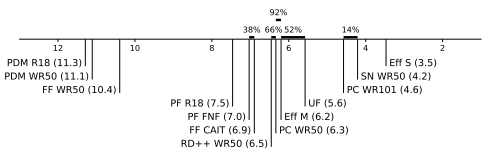


(e) Heatmaps. Images selected according to AUPIMO's statistics. Statistic and image index annotated on upper left corner.

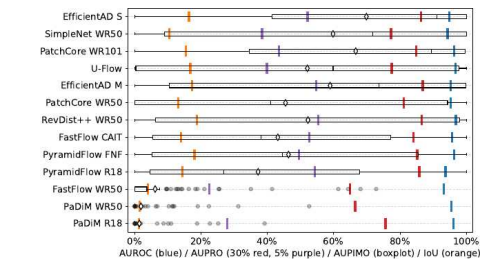
Figure 40: Benchmark on VisA / Chewing Gum. PIMO curves and heatmaps are from PatchCore WR101. 150 images (050 normal, 100 anomalous).

	PDM R18	PDM WR50	FF WR50	PF R18	PF FNF	FF CAIT	RD++ WR50	PC WR50	EFM	UF	PC WR101	SN WR50	EFF S
AUROC	86.3% (1)	85.5% (7)	81.2% (13)	83.7% (12)	86.2% (4)	85.7% (6)	86.8% (1)	85.1% (8)	85.2% (9)	86.7% (2)	86.4% (3)	84.3% (11)	84.9% (10)
AUPRO	72.6% (11)	69.5% (12)	61.9% (13)	65.3% (8)	65.2% (10)	64.1% (7)	69.6% (2)	61.1% (10)	66.5% (1)	77.3% (3)	84.9% (6)	77.3% (10)	86.4% (1)
AUPRO %	27.9% (10)		22.5% (11)	24.3% (9)	29.5% (6)	22.6% (4)	25.4% (1)	21.4% (11)	24.7% (2)	39.9% (8)	43.5% (7)	38.4% (9)	52.2% (5)
Avg. AUPIMO	1.5% (13)	2.0% (12)	6.2% (11)	37.2% (10)	46.4% (7)	41.2% (9)	52.3% (5)	45.5% (8)	58.9% (4)	32.1% (6)	66.7% (2)	59.8% (3)	69.9% (1)
Std. AUPIMO	5.4%	7.0%	14.5%	34.9%	32.2%	16.4%	40.1%	42.0%	41.2%	41.4%	40.0%	40.9%	36.6%
P33 AUPIMO	6.0% (13)	6.0% (12)	6.0% (11)	8.4% (9)	14.5% (7)	14.3% (8)	22.6% (5)	1.4% (10)	31.6% (4)	17.4% (6)	61.5% (2)	37.1% (3)	63.5% (1)
Avg. Rank	11	11.1	10.4	7.5	7.9	6.9	6.3	6.2	5.5	4.5	4.2	4.2	2.5
Avg. IoU	1.2% (13)	1.6% (12)	2.0% (11)	14.5% (7)	18.1% (2)	14.0% (8)	18.6% (1)	13.1% (9)	17.4% (3)	16.5% (4)	35.5% (6)	10.4% (10)	16.4% (5)
EFF S (3.3)	100%	100%	100%	100%	100%	100%	100%	100%	100%	100%	53%	97%	
SN WR50 (4.2)	100%	100%	100%	100%	100%	100%	100%	100%	100%	100%	100%	33%	
PC WR101 (4.8)	100%	100%	100%	100%	100%	100%	100%	100%	100%	100%	100%		
UF (5.6)	100%	100%	100%	100%	100%	100%	100%	100%	100%	100%			
EF M (6.2)	100%	100%	100%	100%	100%	100%	100%	100%	100%	100%			
PC WR50 (6.3)	100%	100%	100%	98%	70%	94%	66%	96%	92%	52%	100%		
RD++ WR50 (6.5)	100%	100%	100%	100%	100%	100%	97%	96%	92%	100%			
FF CAIT (6.9)	100%	100%	100%	98%	39%	98%							
PF FNF (7.0)	100%	100%	100%	100%									
PF R18 (7.5)	100%	100%	100%										
FF WR50 (10.4)	100%	100%											
PDM WR50 (11.1)	100%												

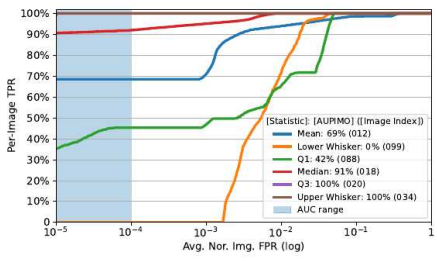
(a) Statistics and pairwise statistical tests.



(b) Average rank diagram.



(c) Score distributions.



(d) PIMO curves.



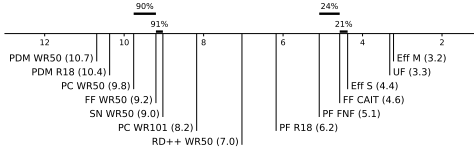
(e) Heatmaps. Images selected according to AUPIMO's statistics. Statistic and image index annotated on upper left corner.

Figure 41: Benchmark on VisA / Fryum. PIMO curves and heatmaps are from EfficientAD S. 150 images (050 normal, 100 anomalous).

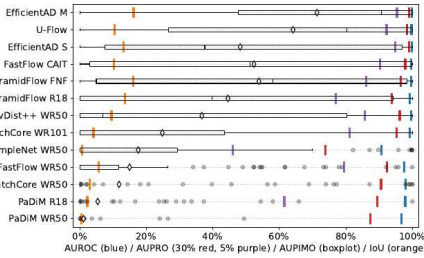


	PDM WR50	PDM R18	PC WR50	FF WR50	SN WR50	PC WR101	RD++ WR50	PF R18	PF FNF	PF CAIT	EFF S	UF	EFF M
AUROC	95.8% (12)	97.3% (10)	98.0% (9)	97.6% (11)	99.7% (1)	99.3% (8)	99.6% (3)	99.3% (7)	99.6% (6)	99.7% (4)	99.9% (2)	99.7% (5)	99.9% (1)
AUPRO	87.2% (11)	89.4% (11)	90.4% (10)	92.3% (9)	92.6% (13)	95.2% (7)	96.4% (6)	93.7% (8)	96.5% (5)	97.8% (4)	99.1% (1)	98.4% (3)	99.8% (2)
ASPRO S	61.5% (18)	61.5% (18)	61.5% (18)	65.4% (16)	45.9% (13)	81.3% (7)	85.9% (6)	77.9% (8)	85.1% (5)	88.3% (4)	84.8% (2)	87.3% (3)	95.3% (1)
Ans. AUPIMO	1.1% (13)	5.4% (12)	11.8% (11)	15.0% (10)	17.6% (9)	24.8% (8)	16.7% (7)	44.5% (6)	53.9% (5)	52.4% (4)	48.2% (3)	44.3% (2)	71.3% (1)
Std. AUPIMO	6.0%	15.7%	27.8%	27.2%	30.8%	39.6%	42.0%	41.9%	42.1%	41.9%	40.3%	39.3%	34.7%
P33 AUPIMO	0.0% (13)	0.0% (12)	0.0% (11)	0.0% (10)	0.0% (9)	0.0% (8)	0.0% (7)	3.1% (6)	16.9% (5)	17.4% (4)	18.1% (3)	56.3% (2)	61.5% (1)
Arg. Rank	10.7	10.4	9.8	9.2	8.9	8.2	7.0	6.2	5.1	4.6	4.4	3.3	3.2
Avg. ICM	0.5% (13)	2.2% (11)	3.0% (10)	5.7% (8)	0.7% (12)	4.1% (9)	9.5% (7)	13.6% (6)	16.1% (5)	10.3% (4)	13.1% (3)	10.4% (2)	16.2% (1)
EFF M (3.2)	100%	100%	100%	100%	100%	100%	100%	100%	100%	100%	100%	99%	
UF (3.3)	100%	100%	100%	100%	100%	100%	100%	100%	100%	100%	100%	100%	
EFF S (4.4)	100%	100%	100%	100%	100%	100%	100%	99%	97%	3%			
PF CAIT (4.6)	100%	100%	100%	100%	100%	100%	100%	97%		25%	21%		
PF FNF (5.1)	100%	100%	100%	100%	100%	100%	100%	100%					
PF R18 (6.2)	100%	100%	100%	100%	100%	100%	99%						
RD++ WR50 (7.0)	100%	100%	100%	100%	100%	100%							
PC WR101 (8.2)	100%	100%	100%	100%	97%								
SN WR50 (9.0)	100%	100%	100%	91%									
FF WR50 (9.2)	100%	100%	100%										
PC WR50 (9.8)	100%	100%	100%										
PDM R18 (10.4)	100%	99%											

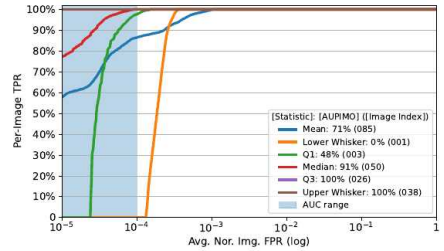
(a) Statistics and pairwise statistical tests.



(b) Average rank diagram.



(c) Score distributions.



(d) PIMO curves.

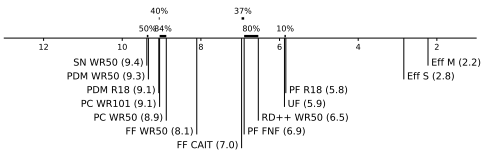


(e) Heatmaps. Images selected according to AUPIMO's statistics. Statistic and image index annotated on upper left corner.

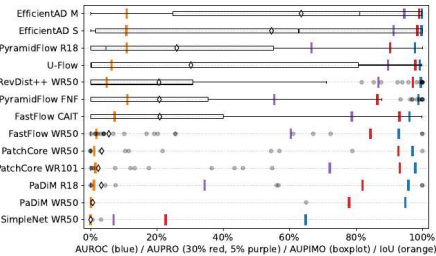
Figure 42: Benchmark on VisA / Macaroni 1. PIMO curves and heatmaps are from EfficientAD M. 200 images (100 normal, 100 anomalous).

	SN WR50	PDM WR50	PDM R18	PC WR101	PC WR50	FF WR50	FF CAIT	PF FNF	RD++ WR50	UF	PF R18	Eff S	Eff M
AUTROC	84.9% (13)	84.9% (11)	85.8% (10)	87.9% (8)	87.9% (8)	82.9% (12)	86.1% (9)	86.4% (8)	89.3% (3)	89.3% (4)	87.8% (7)	90.7% (2)	90.9% (1)
AUPRO	22.8% (13)	22.9% (12)	22.0% (11)	23.3% (9)	22.8% (7)	24.8% (10)	23.3% (6)	26.4% (8)	27.2% (5)	27.2% (5)	28.2% (6)	28.5% (2)	28.5% (1)
AUPRO std	7.9% (11)	7.9% (11)	18.3% (10)	7.3% (8)	7.3% (8)	60.4% (18)	78.7% (15)	55.4% (20)	86.2% (4)	88.0% (3)	66.4% (7)	91.9% (1)	94.5% (1)
Avg. AUPIMO	0.0% (13)	0.0% (12)	2.3% (10)	2.3% (11)	2.4% (9)	18.2%	20.8% (1)	20.7% (6)	20.8% (5)	20.8% (3)	26.0% (4)	34.5% (2)	63.5% (1)
Std. AUPIMO	0.3%	6.3%	15.9%	8.2%	14.8%	18.2%	31.7%	34.8%	34.3%	34.3%	34.0%	42.8%	39.3%
P33 AUPIMO	0.0% (13)	0.0% (12)	0.0% (11)	0.0% (10)	0.0% (9)	0.0% (8)	0.0% (7)	0.0% (6)	0.0% (5)	0.0% (4)	0.0% (3)	16.9% (2)	48.4% (1)
Avg. Rank	9.4	9.1	9.1	9.1	8.9	8.1	7.0	6.9	6.5	6.5	5.4	2.8	2.2
Avg. IoU	0.0% (13)	0.1% (12)	1.0% (11)	1.4% (9)	1.1% (10)	1.7% (8)	7.2% (5)	11.1% (1)	4.9% (7)	6.3% (6)	10.8% (3)	10.8% (4)	10.9% (2)
Eff M (2.2)	100%	100%	100%	100%	100%	100%	100%	100%	100%	100%	100%	100%	100%
Eff S (2.8)	100%	100%	100%	100%	100%	100%	100%	100%	100%	100%	100%	100%	100%
PF R18 (5.8)	100%	100%	100%	100%	100%	100%	100%	96%	98%	88%	10%		
UF (5.9)	100%	100%	100%	100%	100%	100%	100%	100%	100%	100%			
RD++ WR50 (6.5)	100%	100%	100%	100%	100%	100%	63%	81%					
PF FNF (6.9)	100%	100%	100%	100%	100%	100%	37%						
PC WR101 (9.1)	100%	100%	100%	100%	100%	100%							
PC WR50 (8.9)	100%	100%	100%	100%	100%	100%							
FF WR50 (8.1)	100%	100%	98%	99%	99%								
FF CAIT (7.0)	100%	100%	100%	100%	100%								
PC WR101 (9.1)	100%	97%	46%	84%									
PDM R18 (9.1)	95%	95%											
PDM WR50 (9.5)	50%												

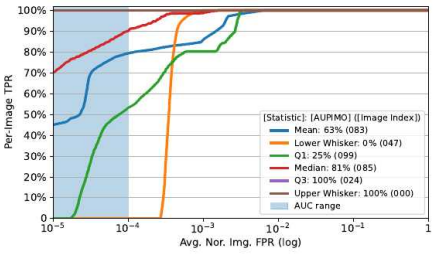
(a) Statistics and pairwise statistical tests.



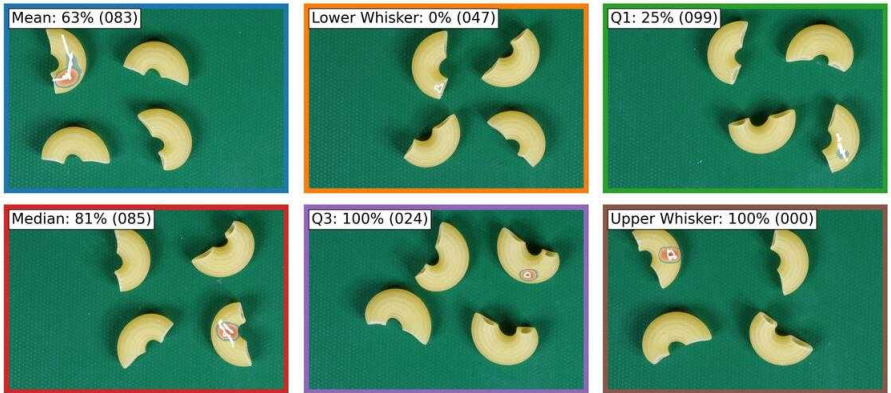
(b) Average rank diagram.



(c) Score distributions.



(d) PIMO curves.

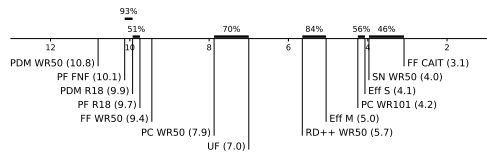


(e) Heatmaps. Images selected according to AUPIMO's statistics. Statistic and image index annotated on upper left corner.

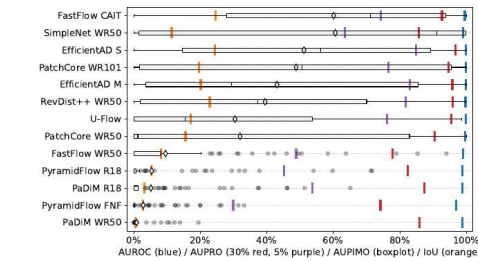
Figure 43: Benchmark on VisA / Macaroni 2. PIMO curves and heatmaps are from EfficientAD M. 200 images (100 normal, 100 anomalous).

	PDM WR50	PF FNF	PDM R18	PF R18	FF WR50	PC WR50	UF	RD++ WR50	Eff M	PC WR101	Eff S	SN WR50	FF CAIT
AUROC	98.8% (12)	98.9% (13)	98.9% (10)	98.8% (11)	99.0% (9)	99.6% (6)	99.8% (4)	99.8% (5)	99.9% (2)	99.8% (3)	99.9% (1)	99.9% (8)	99.5% (7)
AUPRO 9%	85.9% (10)	74.2% (13)	87.3% (8)	82.8% (11)	77.7% (12)	90.6% (7)	95.5% (4)	95.9% (2)	95.5% (3)	94.6% (1)	86.7% (1)	85.7% (10)	92.7% (6)
Avg. AUPIMO	8.9% (13)	2.8% (12)	5.2% (11)	5.4% (10)	8.6% (9)	32.0% (7)	10.4% (8)	39.5% (6)	43.1% (5)	48.8% (4)	51.2% (3)	60.6% (1)	60.1% (2)
Std. AUPIMO	1.1%	6.0%	12.3%	14.4%	19.3%	40.4%	14.3%	15.1%	16.9%	42.3%	36.9%	41.7%	15.9%
P33 AUPIMO	0.0% (13)	0.0% (12)	0.0% (11)	0.0% (10)	0.0% (9)	0.0% (8)	1.1% (7)	5.9% (5)	8.6% (4)	5.2% (3)	22.7% (1)	22.9% (2)	42.2% (1)
Avg. Rank	10.8	10.1	9.9	9.7	9.4	7.9	7.8	5.7	5.0	4.2	3.1	3.1	3.1
Avg. Iou	94.6% (13)	2.9% (12)	3.2% (11)	5.4% (10)	8.2% (9)	15.5% (7)	17.7% (8)	22.9% (6)	20.1% (4)	37.6% (5)	4.1	11.4% (8)	24.2% (1)
FF CAIT (3.1)	100%	100%	100%	100%	100%	100%	100%	100%	100%	100%	100%	46%	
SN WR50 (4.0)	100%	100%	100%	100%	100%	100%	100%	100%	100%	100%	100%		
Eff S (4.1)	100%	100%	100%	100%	100%	100%	100%	100%	100%	100%	57%		
PC WR101 (4.2)	100%	100%	100%	100%	100%	100%	100%	100%	100%	100%			
UF (7.0)	100%	100%	100%	100%	100%	100%	100%	100%	100%	100%			
RD++ WR50 (5.7)	100%	100%	100%	100%	100%	99%	100%	85%					
PC WR50 (7.9)	100%	100%	100%	100%	100%	70%							
FF WR50 (8.4)	100%	100%	100%	100%	100%								
PF R18 (9.3)	100%	100%	98%	100%	100%								
PDM R18 (9.9)	100%	93%	81%										
PF FNF (10.1)	99%												

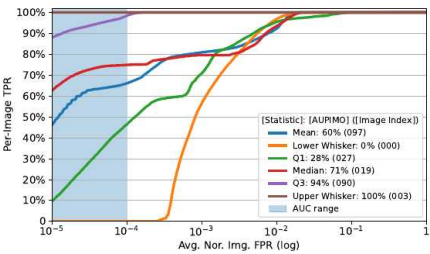
(a) Statistics and pairwise statistical tests.



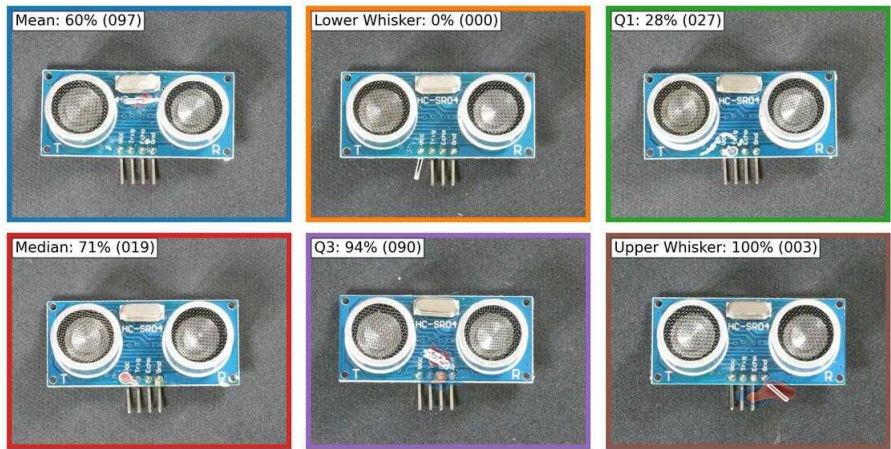
(b) Average rank diagram.



(c) Score distributions.



(d) PIMO curves.

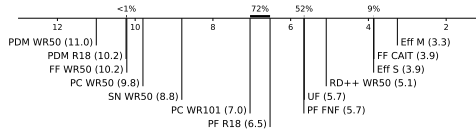


(e) Heatmaps. Images selected according to AUPIMO's statistics. Statistic and image index annotated on upper left corner.

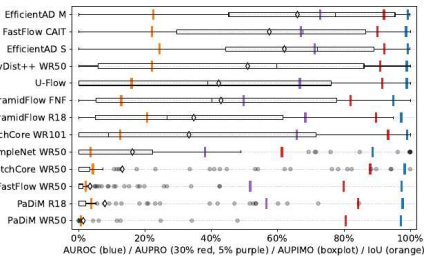
Figure 44: Benchmark on VisA / PCB 1. PIMO curves and heatmaps are from FastFlow CAIT. 200 images (100 normal, 100 anomalous).

	PC W/RSO	PC R18	PF F50	PC W/RSO	SN W/RSO	PC W/RSO	PF R18	PF FFF	UF	RD + W/RSO	EFF 25	FF CAT	EFF 1
AURIC	97.2m (13)	97.3m (8)	97.4m (9)	98.3m (7)	98.6m (3)	98.9m (3)	97.1m (10)	94.9m (12)	94.9m (12)	98.9m (4)	99.2m (2)	98.7m (4)	99.3m (1)
AURIC	98.3m (11)	98.4m (10)	98.5m (12)	97.9m (12)	97.9m (12)	97.9m (12)	99.6m (1)	91.9m (14)	91.9m (14)	91.6m (16)	92.3m (12)	90.9m (6)	92.0m (5)
AURIC 95%	95.7m (13)	95.8m (12)	95.8m (12)	96.2m (10)	96.2m (10)	96.2m (10)	98.6m (13)	49.7m (13)	66.7m (13)	71.8m (12)	67.6m (14)	67.6m (14)	72.6m (11)
AURIC 90%	94.9m (13)	95.1m (12)	95.1m (12)	94.2m (10)	94.2m (10)	94.2m (10)	97.9m (13)	47.9m (13)	64.7m (13)	69.8m (12)	65.8m (14)	65.8m (14)	70.8m (11)
AURIC 85%	94.2m (13)	94.4m (12)	94.4m (12)	93.5m (10)	93.5m (10)	93.5m (10)	97.2m (13)	46.2m (13)	63.2m (13)	68.2m (12)	65.2m (14)	65.2m (14)	70.2m (11)
AURIC 80%	93.5m (13)	93.7m (12)	93.7m (12)	92.8m (10)	92.8m (10)	92.8m (10)	96.5m (13)	44.5m (13)	61.5m (13)	66.5m (12)	64.5m (14)	64.5m (14)	69.5m (11)
AURIC 75%	92.8m (13)	93.0m (12)	93.0m (12)	92.1m (10)	92.1m (10)	92.1m (10)	95.8m (13)	42.8m (13)	59.8m (13)	64.8m (12)	63.8m (14)	63.8m (14)	68.8m (11)
AURIC 70%	92.1m (13)	92.3m (12)	92.3m (12)	91.4m (10)	91.4m (10)	91.4m (10)	95.1m (13)	41.1m (13)	58.1m (13)	63.1m (12)	63.1m (14)	63.1m (14)	68.1m (11)
AURIC 65%	91.4m (13)	91.6m (12)	91.6m (12)	90.7m (10)	90.7m (10)	90.7m (10)	94.4m (13)	39.4m (13)	56.4m (13)	61.4m (12)	61.4m (14)	61.4m (14)	67.4m (11)
AURIC 60%	90.7m (13)	90.9m (12)	90.9m (12)	90.0m (10)	90.0m (10)	90.0m (10)	93.7m (13)	37.7m (13)	54.7m (13)	59.7m (12)	59.7m (14)	59.7m (14)	66.7m (11)
AURIC 55%	90.0m (13)	90.2m (12)	90.2m (12)	89.3m (10)	89.3m (10)	89.3m (10)	93.0m (13)	36.0m (13)	53.0m (13)	58.0m (12)	58.0m (14)	58.0m (14)	66.0m (11)
AURIC 50%	89.3m (13)	89.5m (12)	89.5m (12)	88.6m (10)	88.6m (10)	88.6m (10)	92.3m (13)	34.3m (13)	51.3m (13)	56.3m (12)	56.3m (14)	56.3m (14)	65.3m (11)
AURIC 45%	88.6m (13)	88.8m (12)	88.8m (12)	87.9m (10)	87.9m (10)	87.9m (10)	91.6m (13)	32.6m (13)	49.6m (13)	54.6m (12)	54.6m (14)	54.6m (14)	64.6m (11)
AURIC 40%	87.9m (13)	88.1m (12)	88.1m (12)	87.2m (10)	87.2m (10)	87.2m (10)	90.9m (13)	30.9m (13)	47.9m (13)	52.9m (12)	52.9m (14)	52.9m (14)	63.9m (11)
AURIC 35%	87.2m (13)	87.4m (12)	87.4m (12)	86.5m (10)	86.5m (10)	86.5m (10)	90.2m (13)	29.2m (13)	46.2m (13)	51.2m (12)	51.2m (14)	51.2m (14)	63.2m (11)
AURIC 30%	86.5m (13)	86.7m (12)	86.7m (12)	85.8m (10)	85.8m (10)	85.8m (10)	89.5m (13)	27.5m (13)	44.5m (13)	49.5m (12)	49.5m (14)	49.5m (14)	62.5m (11)
AURIC 25%	85.8m (13)	86.0m (12)	86.0m (12)	85.1m (10)	85.1m (10)	85.1m (10)	88.8m (13)	25.8m (13)	42.8m (13)	47.8m (12)	47.8m (14)	47.8m (14)	61.8m (11)
AURIC 20%	85.1m (13)	85.3m (12)	85.3m (12)	84.4m (10)	84.4m (10)	84.4m (10)	88.1m (13)	24.1m (13)	41.1m (13)	46.1m (12)	46.1m (14)	46.1m (14)	61.1m (11)
AURIC 15%	84.4m (13)	84.6m (12)	84.6m (12)	83.7m (10)	83.7m (10)	83.7m (10)	87.4m (13)	22.4m (13)	39.4m (13)	44.4m (12)	44.4m (14)	44.4m (14)	60.4m (11)
AURIC 10%	83.7m (13)	83.9m (12)	83.9m (12)	83.0m (10)	83.0m (10)	83.0m (10)	86.7m (13)	20.7m (13)	37.7m (13)	42.7m (12)	42.7m (14)	42.7m (14)	59.7m (11)
AURIC 5%	83.0m (13)	83.2m (12)	83.2m (12)	82.3m (10)	82.3m (10)	82.3m (10)	86.0m (13)	19.0m (13)	36.0m (13)	41.0m (12)	41.0m (14)	41.0m (14)	59.0m (11)
AURIC 0%	82.3m (13)	82.5m (12)	82.5m (12)	81.6m (10)	81.6m (10)	81.6m (10)	85.3m (13)	17.3m (13)	34.3m (13)	39.3m (12)	39.3m (14)	39.3m (14)	58.3m (11)
AURIC 90%	94.9m (13)	95.1m (12)	95.1m (12)	94.2m (10)	94.2m (10)	94.2m (10)	97.9m (13)	47.9m (13)	64.7m (13)	69.8m (12)	65.8m (14)	65.8m (14)	70.8m (11)
AURIC 85%	94.2m (13)	94.4m (12)	94.4m (12)	93.5m (10)	93.5m (10)	93.5m (10)	97.2m (13)	46.2m (13)	63.2m (13)	68.2m (12)	65.2m (14)	65.2m (14)	70.2m (11)
AURIC 80%	93.5m (13)	93.7m (12)	93.7m (12)	92.8m (10)	92.8m (10)	92.8m (10)	96.5m (13)	44.5m (13)	61.5m (13)	66.5m (12)	64.5m (14)	64.5m (14)	69.5m (11)
AURIC 75%	92.8m (13)	93.0m (12)	93.0m (12)	92.1m (10)	92.1m (10)	92.1m (10)	95.8m (13)	42.8m (13)	59.8m (13)	64.8m (12)	63.8m (14)	63.8m (14)	68.8m (11)
AURIC 70%	92.1m (13)	92.3m (12)	92.3m (12)	91.4m (10)	91.4m (10)	91.4m (10)	95.1m (13)	41.1m (13)	58.1m (13)	63.1m (12)	63.1m (14)	63.1m (14)	68.1m (11)
AURIC 65%	91.4m (13)	91.6m (12)	91.6m (12)	90.7m (10)	90.7m (10)	90.7m (10)	94.4m (13)	39.4m (13)	56.4m (13)	61.4m (12)	61.4m (14)	61.4m (14)	67.4m (11)
AURIC 60%	90.7m (13)	90.9m (12)	90.9m (12)	90.0m (10)	90.0m (10)	90.0m (10)	93.7m (13)	37.7m (13)	54.7m (13)	59.7m (12)	59.7m (14)	59.7m (14)	66.7m (11)
AURIC 55%	90.0m (13)	90.2m (12)	90.2m (12)	89.3m (10)	89.3m (10)	89.3m (10)	93.0m (13)	36.0m (13)	53.0m (13)	58.0m (12)	58.0m (14)	58.0m (14)	66.0m (11)
AURIC 50%	89.3m (13)	89.5m (12)	89.5m (12)	88.6m (10)	88.6m (10)	88.6m (10)	92.3m (13)	34.3m (13)	51.3m (13)	56.3m (12)	56.3m (14)	56.3m (14)	65.3m (11)
AURIC 45%	88.6m (13)	88.8m (12)	88.8m (12)	87.9m (10)	87.9m (10)	87.9m (10)	91.6m (13)	32.6m (13)	49.6m (13)	54.6m (12)	54.6m (14)	54.6m (14)	64.6m (11)
AURIC 40%	87.9m (13)	88.1m (12)	88.1m (12)	87.2m (10)	87.2m (10)	87.2m (10)	90.9m (13)	30.9m (13)	47.9m (13)	52.9m (12)	52.9m (14)	52.9m (14)	63.9m (11)
AURIC 35%	87.2m (13)	87.4m (12)	87.4m (12)	86.5m (10)	86.5m (10)	86.5m (10)	90.2m (13)	29.2m (13)	46.2m (13)	51.2m (12)	51.2m (14)	51.2m (14)	63.2m (11)
AURIC 30%	86.5m (13)	86.7m (12)	86.7m (12)	85.8m (10)	85.8m (10)	85.8m (10)	89.5m (13)	27.5m (13)	44.5m (13)	49.5m (12)	49.5m (14)	49.5m (14)	62.5m (11)
AURIC 25%	85.8m (13)	86.0m (12)	86.0m (12)	85.1m (10)	85.1m (10)	85.1m (10)	88.8m (13)	25.8m (13)	42.8m (13)	47.8m (12)	47.8m (14)	47.8m (14)	61.8m (11)
AURIC 20%	85.1m (13)	85.3m (12)	85.3m (12)	84.4m (10)	84.4m (10)	84.4m (10)	88.1m (13)	24.1m (13)	41.1m (13)	46.1m (12)	46.1m (14)	46.1m (14)	61.1m (11)
AURIC 15%	84.4m (13)	84.6m (12)	84.6m (12)	83.7m (10)	83.7m (10)	83.7m (10)	87.4m (13)	22.4m (13)	39.4m (13)	44.4m (12)	44.4m (14)	44.4m (14)	60.4m (11)
AURIC 10%	83.7m (13)	83.9m (12)	83.9m (12)	83.0m (10)	83.0m (10)	83.0m (10)	86.7m (13)	20.7m (13)	37.7m (13)	42.7m (12)	42.7m (14)	42.7m (14)	59.7m (11)
AURIC 5%	83.0m (13)	83.2m (12)	83.2m (12)	82.3m (10)	82.3m (10)	82.3m (10)	86.0m (13)	19.0m (13)	36.0m (13)	41.0m (12)	41.0m (14)	41.0m (14)	59.0m (11)
AURIC 0%	82.3m (13)	82.5m (12)	82.5m (12)	81.6m (10)	81.6m (10)	81.6m (10)	85.3m (13)	17.3m (13)	34.3m (13)	39.3m (12)	39.3m (14)	39.3m (14)	58.3m (11)
AURIC 90%	94.9m (13)	95.1m (12)	95.1m (12)	94.2m (10)	94.2m (10)	94.2m (10)	97.9m (13)	47.9m (13)	64.7m (13)	69.8m (12)	65.8m (14)	65.8m (14)	70.8m (11)
AURIC 85%	94.2m (13)	94.4m (12)	94.4m (12)	93.5m (10)	93.5m (10)	93.5m (10)	97.2m (13)	46.2m (13)	63.2m (13)	68.2m (12)	65.2m (14)	65.2m (14)	70.2m (11)
AURIC 80%	93.5m (13)	93.7m (12)	93.7m (12)	92.8m (10)	92.8m (10)	92.8m (10)	96.5m (13)	44.5m (13)	61.5m (13)	66.5m (12)	64.5m (14)	64.5m (14)	69.5m (11)
AURIC 75%	92.8m (13)	93.0m (12)	93.0m (12)	92.1m (10)	92.1m (10)	92.1m (10)	95.8m (13)	42.8m (13)	59.8m (13)	64.8m (12)	63.8m (14)	63.8m (14)	68.8m (11)
AURIC 70%	92.1m (13)	92.3m (12)	92.3m (12)	91.4m (10)	91.4m (10)	91.4m (10)	95.1m (13)	41.1m (13)	58.1m (13)	63.1m (12)	63.1m (14)	63.1m (14)	68.1m (11)
AURIC 65%	91.4m (13)	91.6m (12)	91.6m (12)	90.7m (10)	90.7m (10)	90.7m (10)	94.4m (13)	39.4m (13)	56.4m (13)	61.4m (12)	61.4m (14)	61.4m (14)	67.4m (11)
AURIC 60%	90.7m (13)	90.9m (12)	90.9m (12)	90.0m (10)	90.0m (10)	90.0m (10)	93.7m (13)	37.7m (13)	54.7m (13)	59.7m (12)	59.7m (14)	59.7m (14)	66.7m (11)
AURIC 55%	90.0m (13)	90.2m (12)	90.2m (12)	89.3m (10)	89.3m (10)	89.3m (10)	93.0m (13)	36.0m (13)	53.0m (13)	58.0m (12)	58.0m (14)	58.0m (14)	66.0m (11)
AURIC 50%	89.3m (13)	89.5m (12)	89.5m (12)	88.6m (10)	88.6m (10)	88.6m (10)	92.3m (13)	34.3m (13)	51.3m (13)	56.3m (12)	56.3m (14)	56.3m (14)	65.3m (11)
AURIC 45%	88.6m (13)	88.8m (12)	88.8m (12)	87.9m (10)	87.9m (10)	87.9m (10)	91.6m (13)	32.6m (13)	49.6m (13)	54.6m (12)	54.6m (14)	54.6m (14)	64.6m (11)
AURIC 40%	87.9m (13)	88.1m (12)	88.1m (12)	87.2m (10)	87.2m (10)	87.2m (10)	90.9m (13)	30.9m (13)	47.9m (13)	52.9m (12)	52.9m (14)	52.9m (14)	63.9m (11)
AURIC 35%	87.2m (13)	87.4m (12)	87.4m (12)	86.5m (10)	86.5m (10)	86.5m (10)	90.2m (13)	29.2m (13)	46.2m (13)	51.2m (12)	51.2m (14)	51.2m (14)	63.2m (11)
AURIC 30%	86.5m (13)	86.7m (12)	86.7m (12)	85.8m (10)	85.8m (10)	85.8m (10)	89.5m (13)	27.5m (13)	44.5m (13)	49.5m (12)	49.5m (14)	49.5m (14)	62.5m (11)
AURIC 25%	85.8m (13)	86.0m (12)	86.0m (12)	85.1m (10)	85.1m (10)	85.1m (10)	88.8m (13)	25.8m (13)	42.8m (13)	47.8m (12)	47.8m (14)	47.8m (14)	61.8m (11)
AURIC 20%	85.1m (13)	85.3m (12)	85.3m (12)	84.4m (10)	84.4m (10)	84.4m (10)	88.1m (13)	24.1m (13)	41.1m (13)	46.1m (12)	46.1m (14)	46.1m (14)	61.1m (11)
AURIC 15%	84.4m (13)	84.6m (12)	84.6m (12)	83.7m (10)	83.7m (10)	83.7m (10)	87.4m (13)	22.4m (13)	39.4m (13)	44.4m (12)	44.4m (14)	44.4m (14)	60.4m (11)
AURIC 10%	83.7m (13)	83.9m (12)	83.9m (12)	83.0m (10)	83.0m (10)	83.0m (10)	86.7m (13)	20.7m (13)	37.7m (13)	42.7m (12)	42.7m (14)	42.7m (14)	59.7m (11)
AURIC 5%	83.0m (13)	83.2m (12)	83.2m (12)	82.3m (10)	82.3m (10)	82.3m (10)	86.0m (13)	19.0m (13)	36.0m (13)	41.0m (12)	41.0m (14)	41.0m (14)	59.0m (11)
AURIC 0%	82.3m (13)	82.5m (12)	82.5m (12)	81.6m (10)	81.6m (10)	81.6m (10)	85.3m (13)	17.3m (13)	34.3m (13)	39.3m (12)	39.3m (14)	39.3m (14)	58.3m (11)
AURIC 90%	94.9m (13)	95.1m (12)	95.1m (12)	94.2m (10)	94.2m (10)	94.2m (10)	97.9m (13)	47.9m (13)	64.7m (13)	69.8m (12)	65.8m (14)	65.8m (14)	70.8m (11)
AURIC 85%	94.2m (13)	94.4m (12)	94.4m (12)	93.5m (10)	93.5m (10)	93.5m (10)	97.2m (13)	46.2m (13)	63.2m (13)	68.2m (12)	65.2m (14)	65.2m (14)	70.2m (11)
AURIC 80%	93.5m (13)	93.7m (12)	93.7m (12)	92.8m (10)	92.8m (10)	92.8m (10)	96.5m (13)	44.5m (13)	61.5m (13)	66.5m (12)	64.5m (14)	64.5m (14)	69.5m (11)
AURIC 75%	92.8m (13)	93.0m (12)	93.0m (12)	92.1m (10)	92.1m (10)	92.1m (10)	95.8m (13)	42.8m (13)	59.8m (13)	64.8m (12)	63.8m (14)	63.8m (14)	68.8m (11)
AURIC 70%	92.1m (13)	92.3m (12)	92.3m (12)	91.4m (10)	91.4m (10)	91.4m (10)	95.1m (13)	41.1m (13)	58.1m (13)	63.1m (12)	63.1m (14)	63.1m (14)	68.1m (11)
AURIC 65%	91.4m (13)	91.6m (12)	91.6m (12)	90.7m (10)	90.7m (10)	90.7m (10)	94.4m (13)	39.4m (13)	56.4m (13)	61.4m (12)	61.4m (14)	61.4m (14)	67.4m (11)
AURIC 60%	90.7m (13)	90.9m (12)	90.9m (12)	90.0m (10)	90.0m (10)	90.0m (10)	93.7m (13)	37.7m (13)	54.7m (13)	59.7m (12)	59.7m (14)	59.7m (14)	66.7m (11)
AURIC 55%	90.0m (1												

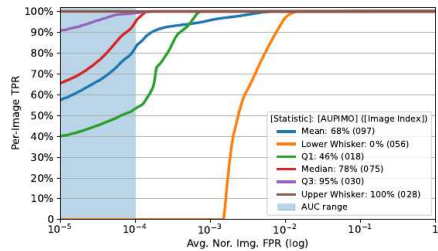
(a) Statistics and pairwise statistical tests.



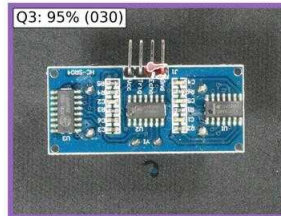
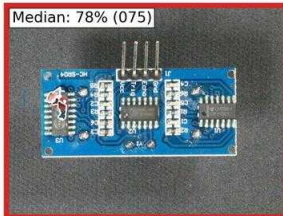
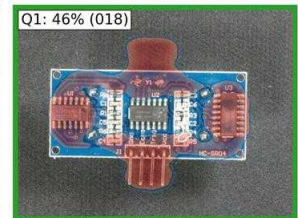
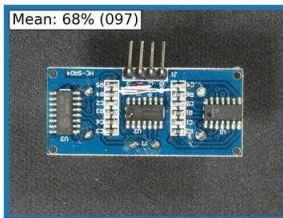
(b) Average rank diagram.



(c) Score distributions.



(d) PIMO curves.



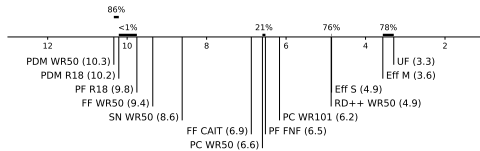
(e) Heatmaps. Images selected according to AUPIMO's statistics. Statistic and image index annotated on upper left corner.

Figure 45: Benchmark on VisA / PCB 2. PIMO curves and heatmaps are from EfficientAD M. 200 images (100 normal, 100 anomalous).

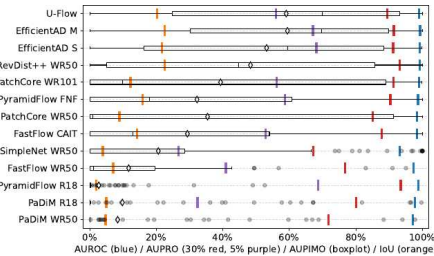


[illegible]

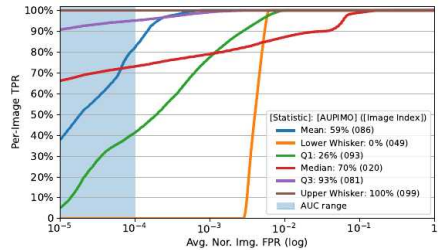
(a) Statistics and pairwise statistical tests.



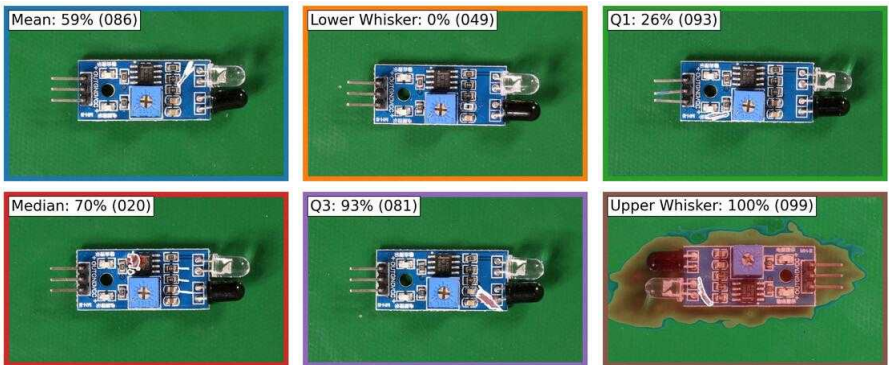
(b) Average rank diagram.



(c) Score distributions.



(d) PIMO curves.

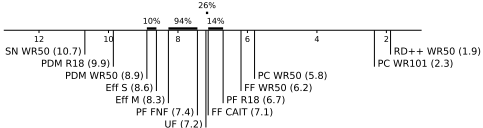


(e) Heatmaps. Images selected according to AUPIMO’s statistics. Statistic and image index annotated on upper left corner.

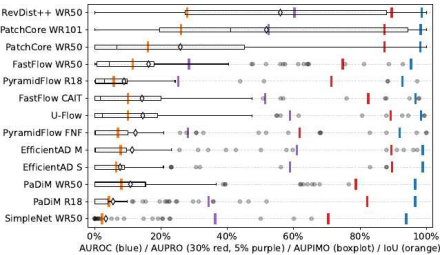
Figure 46: Benchmark on VisA / PCB 3. PIMO curves and heatmaps are from U-Flow. 201 images (101 normal, 100 anomalous).

	SN WR50	PDM R18	PDM WR50	Eff S	Eff M	PF FNF	UF	FF CAIT	PF R18	FF WR50	PC WR50	PC WR101	RD++ WR50
AUPRO	70.2% (12)	86.4% (8)	76.8% (9)	89.5% (1)	88.9% (2)	92.0% (13)	98.4% (4)	86.7% (17)	92.5% (12)	85.4% (10)	88.3% (6)	88.3% (13)	88.4% (13)
AUPRO 80%	70.2% (12)	82.4% (8)	76.8% (9)	89.5% (1)	89.4% (1)	91.8% (13)	89.2% (4)	82.5% (17)	71.4% (13)	74.8% (10)	87.4% (5)	87.3% (6)	89.5% (12)
AUPRO 90%	35.4% (17)	55.4% (8)	45.4% (10)	55.0% (13)	51.0% (13)	28.1% (18)	33.8% (14)	31.5% (16)	35.8% (13)	28.3% (19)	53.3% (13)	53.3% (13)	60.0% (12)
Avg. AUPIMO	3.4% (13)	5.4% (12)	10.8% (8)	27.7% (1)	13.3% (10)	12.3% (2)	14.5% (3)	14.3% (16)	8.9% (10)	16.3% (4)	25.8% (3)	51.8% (2)	56.0% (1)
std. AUPIMO	11.0%	11.3%	19.4%	16.6%	22.6%	24.3%	24.3%	23.8%	16.9%	23.0%	32.9%	37.6%	33.1%
P33 AUPIMO	0.0% (13)	0.0% (12)	0.0% (11)	0.0% (10)	0.0% (9)	0.0% (7)	0.0% (8)	0.0% (6)	0.9% (4)	1.0% (3)	0.3% (5)	23.3% (2)	34.2% (1)
Avg. Rank	10.7	9.9	8.9	1.6	3.3	7.4	7.2	9.1	6.7	6.2	5.1	2.1	1.9
Avg. Iou	4.2% (13)	4.4% (12)	8.1% (7)	8.5% (10)	7.9% (8)	7.1% (9)	10.1% (5)	10.1% (6)	5.8% (11)	11.5% (4)	16.2% (3)	26.1% (2)	27.0% (1)
RD++ WR50 (1.9)	100%	100%	100%	100%	100%	100%	100%	100%	100%	100%	100%	100%	99%
PC WR101 (2.3)	100%	100%	100%	100%	100%	100%	100%	100%	100%	100%	100%	100%	
PC WR50 (5.8)	100%	100%	100%	100%	100%	100%	100%	100%	100%	100%	100%	100%	
FF WR50 (6.2)	100%	100%	100%	100%	99%	100%	88%	96%	100%	100%	100%	100%	
PF R18 (6.7)	100%	100%	78%	98%	38%	62%	5%	14%	98%	100%	100%	100%	
UF (7.1)	100%	100%	100%	100%	91%	89%	27%						
FF FNF (7.4)	100%	100%	100%	100%	94%	97%							
Eff R18 (8.3)	100%	99%	58%										
Eff S (8.6)	100%	96%	11%										
PDM WR50 (8.9)	100%	100%											
PDM R18 (9.9)	99%												

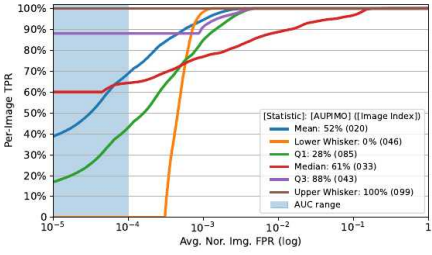
(a) Statistics and pairwise statistical tests.



(b) Average rank diagram.



(c) Score distributions.



(d) PIMO curves.

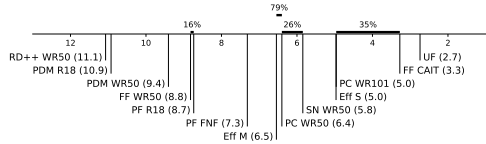


(e) Heatmaps. Images selected according to AUPIMO's statistics. Statistic and image index annotated on upper left corner.

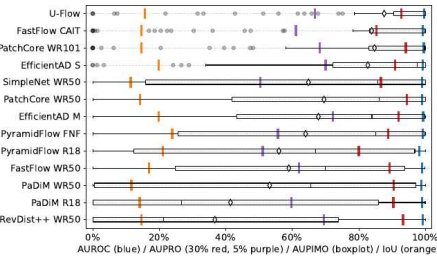
Figure 47: Benchmark on VisA / PCB 4. PIMO curves and heatmaps are from RevDist++ WR50. 201 images (101 normal, 100 anomalous).

	RD++ WR50	PDM R18	PDM WR50	FF WR50	PF R18	PF FNF	Eff M	PC WR50	SN WR50	Eff S	PC WR101	FF CAIT	UF
AUROC	99.2% (4)	99.1% (5)	98.8% (12)	99.0% (10)	98.1% (13)	99.2% (6)	99.3% (3)	99.1% (8)	99.0% (11)	99.2% (7)	99.5% (2)	99.2% (5)	99.0% (11)
AUPRO	93.3% (12)	92.4% (2)	90.5% (17)	90.3% (19)	80.0% (13)	88.8% (10)	92.0% (3)	94.3% (12)	86.3% (11)	91.0% (6)	91.1% (12)	85.3% (12)	92.0% (4)
AUPRO 5%	89.9% (13)	59.7% (8)	62.9% (16)	62.9% (16)	51.1% (10)	59.3% (8)	2.3% (1)	50.3% (11)	50.3% (11)	70.1% (12)	80.2% (4)	61.1% (17)	66.8% (15)
Avg. AUPIMO	36.7% (13)	41.4% (12)	51.2% (11)	59.0% (9)	56.0% (10)	64.0% (8)	67.8% (6)	69.5% (5)	64.9% (7)	82.7% (4)	84.7% (2)	83.9% (3)	87.6% (1)
Std. AUPIMO	37.8%	40.3%	42.3%	35.8%	39.3%	39.8%	35.4%	37.1%	41.3%	36.2%	28.1%	29.6%	25.2%
P33 AUPIMO	2.8% (12)	0.8% (13)	12.8% (11)	44.8% (9)	32.5% (10)	47.5% (8)	55.8% (6)	67.7% (5)	53.4% (7)	85.5% (4)	93.6% (2)	92.5% (3)	95.8% (1)
Avg. Rank	11.1	10.9	9.4	8.8	8.7	7.3	6.5	6.4	5.8	5.0	2.3	2.3	1.7
Avg. IoU	14.7% (8)	14.1% (11)	11.6% (12)	16.3% (5)	21.0% (2)	21.0% (2)	11.6% (13)	14.4% (10)	11.7% (11)	19.0% (3)	11.7% (11)	14.4% (9)	15.2% (6)
UF 12.7	100%	100%	100%	100%	100%	100%	100%	100%	100%	100%	91%	100%	
FF CAIT 13.8	100%	100%	100%	100%	100%	100%	100%	100%	100%	100%	96%	100%	
PC WR101 15.0	100%	100%	100%	100%	100%	100%	100%	100%	100%	100%	100%	100%	
Eff S 15.0	100%	100%	100%	100%	100%	100%	100%	100%	100%	100%	100%	100%	
SN WR50 16.8	100%	100%	100%	100%	100%	100%	91%	26%	26%	100%	100%	100%	
PC WR50 16.4	100%	100%	100%	100%	100%	100%	100%	100%	100%	100%	100%	100%	
Eff M 16.5	100%	100%	100%	100%	100%	100%	100%	100%	100%	100%	100%	100%	
PF FNF 17.3	100%	100%	100%	100%	93%								
PF R18 18.7	100%	100%	66%	16%									
FF WR50 16.8	100%	100%	100%	95%									
PDM WR50 19.4	100%	100%											
PDM R18 10.9	98%												

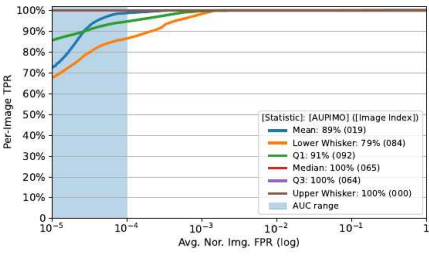
(a) Statistics and pairwise statistical tests.



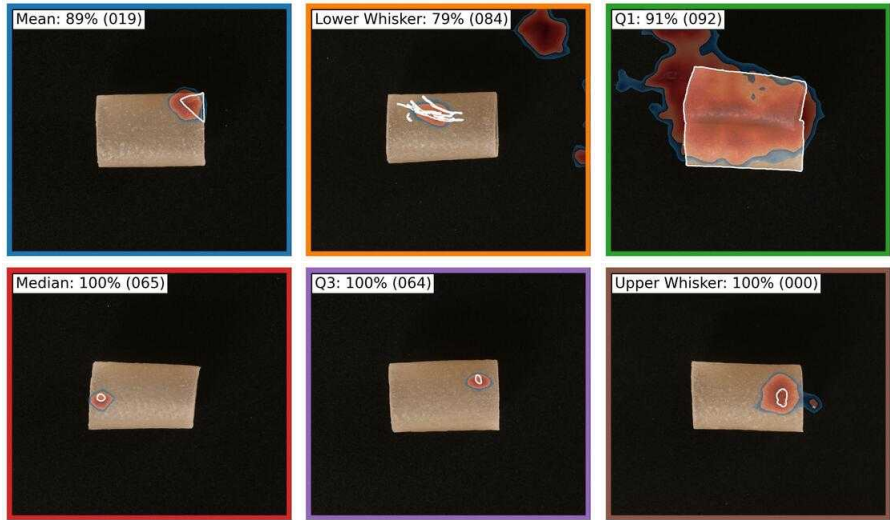
(b) Average rank diagram.



(c) Score distributions.



(d) PIMO curves.



(e) Heatmaps. Images selected according to AUPIMO’s statistics. Statistic and image index annotated on upper left corner.

Figure 48: Benchmark on VisA / Pipe Fryum. PIMO curves and heatmaps are from U-Flow. 150 images (050 normal, 100 anomalous).